Université de Montréal

Domain/Multi-Domain Protection and Provisioning in Optical Networks

par
Do Trung Kien

Département d'informatique et de recherche opérationnelle
Faculté des arts et des sciences

Thèse présentée à la Faculté des études supérieures
en vue de l'obtention du grade de Philosophiæ Doctor (Ph.D.)
en informatique

July, 2014

Université de Montréal
Faculté des études supérieures

Cette thèse intitulée:

Domain/Multi-Domain Protection and Provisioning in Optical Networks

présentée par:

Do Trung Kien

a été évaluée par un jury composé des personnes suivantes:

Bernard Gendron,	président-rapporteur
Brigitte Jaumard,	directeur de recherche
Michel Toulouse,	codirecteur
Abdelhakim Hafid,	membre du jury
Bernard Cousin,	examinateur externe
Bernard Gendron,	représentant du doyen de la FES

Thèse acceptée le: 08 July 2014

RÉSUMÉ

L'évolution récente des commutateurs de sélection de longueurs d'onde (WSS - Wavelength Selective Switch) favorise le développement du multiplexeur optique d'insertion-extraction reconfigurable (ROADM - Reconfigurable Optical Add/Drop Multiplexers) à plusieurs degrés sans orientation ni coloration, considéré comme un équipement fort prometteur pour les réseaux maillés du futur relativement au multiplexage en longueur d'onde (WDM - Wavelength Division Multiplexing). Cependant, leur propriété de commutation asymétrique complique la question de l'acheminement et de l'attribution des longueur d'ondes (RWA - Routing and Wavelength Assignment). Or la plupart des algorithmes de RWA existants ne tiennent pas compte de cette propriété d'asymétrie.

L'interruption des services causée par des défauts d'équipements sur les chemins optiques (résultat provenant de la résolution du problème RWA) a pour conséquence la perte d'une grande quantité de données. Les recherches deviennent ainsi incontournables afin d'assurer la survie fonctionnelle des réseaux optiques, à savoir, le maintien des services, en particulier en cas de pannes d'équipement. La plupart des publications antérieures portaient particulièrement sur l'utilisation d'un système de protection permettant de garantir le reroutage du trafic en cas d'un défaut d'un lien. Cependant, la conception de la protection contre le défaut d'un lien ne s'avère pas toujours suffisante en termes de survie des réseaux WDM à partir de nombreux cas des autres types de pannes devenant courant de nos jours, tels que les bris d'équipements, les pannes de deux ou trois liens, etc. En outre, il y a des défis considérables pour protéger les grands réseaux optiques multidomaines composés de réseaux associés à un domaine simple, interconnectés par des liens interdomaines, où les détails topologiques internes d'un domaine ne sont généralement pas partagés à l'extérieur.

La présente thèse a pour objectif de proposer des modèles d'optimisation de grande taille et des solutions aux problèmes mentionnés ci-dessus. Ces modèles-ci permettent de générer des solutions optimales ou quasi-optimales avec des écarts

d'optimalité mathématiquement prouvée. Pour ce faire, nous avons recours à la technique de génération de colonnes afin de résoudre les problèmes inhérents à la programmation linéaire de grande envergure.

Concernant la question de l'approvisionnement dans les réseaux optiques, nous proposons un nouveau modèle de programmation linéaire en nombres entiers (ILP - Integer Linear Programming) au problème RWA afin de maximiser le nombre de requêtes acceptées (GoS - Grade of Service). Le modèle résultant constitue celui de l'optimisation d'un ILP de grande taille, ce qui permet d'obtenir la solution exacte des instances RWA assez grandes, en supposant que tous les nœuds soient asymétriques et accompagnés d'une matrice de connectivité de commutation donnée. Ensuite, nous modifions le modèle et proposons une solution au problème RWA afin de trouver la meilleure matrice de commutation pour un nombre donné de ports et de connexions de commutation, tout en satisfaisant/maximisant la qualité d'écoulement du trafic GoS.

Relativement à la protection des réseaux d'un domaine simple, nous proposons des solutions favorisant la protection contre les pannes multiples. En effet, nous développons la protection d'un réseau d'un domaine simple contre des pannes multiples, en utilisant les p-cycles de protection avec un chemin indépendant des pannes (FIPP - Failure Independent Path Protecting) et de la protection avec un chemin dépendant des pannes (FDPP - Failure Dependent Path-Protecting). Nous proposons ensuite une nouvelle formulation en termes de modèles de flots pour les p-cycles FDPP soumis à des pannes multiples. Le nouveau modèle soulève un problème de taille, qui a un nombre exponentiel de contraintes en raison de certaines contraintes d'élimination de sous-tour. Par conséquent, afin de résoudre efficacement ce problème, on examine : (i) une décomposition hiérarchique du problème auxiliaire dans le modèle de décomposition, (ii) des heuristiques pour gérer efficacement le grand nombre de contraintes.

À propos de la protection dans les réseaux multidomaines, nous proposons des systèmes de protection contre les pannes d'un lien. Tout d'abord, un modèle d'optimisation est proposé pour un système de protection centralisée, en supposant que

la gestion du réseau soit au courant de tous les détails des topologies physiques des domaines. Nous proposons ensuite un modèle distribué de l'optimisation de la protection dans les réseaux optiques multidomaines, une formulation beaucoup plus réaliste car elle est basée sur l'hypothèse d'une gestion de réseau distribué. Ensuite, nous ajoutons une bande passante partagée afin de réduire le coût de la protection. Plus précisément, la bande passante de chaque lien intra-domaine est partagée entre les p-cycles FIPP et les p-cycles dans une première étude, puis entre les chemins pour lien/chemin de protection dans une deuxième étude. Enfin, nous recommandons des stratégies parallèles aux solutions de grands réseaux optiques multidomaines.

Les résultats de l'étude permettent d'élaborer une conception efficace d'un système de protection pour un très large réseau multidomaine (45 domaines), le plus large examiné dans la littérature, avec un système à la fois centralisé et distribué.

Mots-clés : multi-domaine, réseaux optiques de protection, système distribué, système parallèle, défauts multiples, *p*-cycles.

ABSTRACT

Recent developments in the wavelength selective switch (WSS) technology enable multi-degree reconfigurable optical add/drop multiplexers (ROADM) architectures with colorless and directionless switching, which is regarded as a very promising enabler for future reconfigurable wavelength division multiplexing (WDM) mesh networks. However, its asymmetric switching property complicates the optimal routing and wavelength assignment (RWA) problem, which is NP-hard. Most of the existing RWA algorithms do not consider such property.

Disruption of services through equipment failures on the *lightpaths* (output of RWA problem) is consequential as it involves the lost of large amounts of data. Therefore, substantial research efforts are needed to ensure the functional survivability of optical networks, i.e., the continuation of services even when equipment failures occur. Most previous publications have focused on using a protection scheme to guarantee the traffic connections in the event of single link failures. However, protection design against single link failures turns out not to be always sufficient to keep the WDM networks away from many downtime cases as other kinds of failures, such as node failures, dual link failures, triple link failures, etc., become common nowadays. Furthermore, there are challenges to protect large multi-domain optical networks which are composed of several single-domain networks, interconnected by inter-domain links, where the internal topological details of a domain are usually not shared externally.

The objective of this thesis is to propose scalable models and solution methods for the above problems. The models enable to approach large problem instances while producing optimal or near optimal solutions with mathematically proven optimality gaps. For this, we rely on the column generation technique which is suitable to solve large scale linear programming problems.

For the provisioning problem in optical networks, we propose a new ILP (Integer Linear Programming) model for RWA problem with the objective of maximizing the Grade of Service (GoS). The resulting model is a large scale optimization ILP

model, which allows the exact solution of quite large RWA instances, assuming all nodes are asymmetric and with a given switching connectivity matrix. Next, we modify the model and propose a solution for the RWA problem with the objective of finding the best switching connectivity matrix for a given number of ports and a given number of switching connections, while satisfying/maximizing the GoS.

For protection in single domain networks, we propose solutions for the protection against multiple failures. Indeed, we extent the protection of a single domain network against multiple failures, using FIPP and FDPP p-cycles. We propose a new generic flow formulation for FDPP p-cycles subject to multiple failures. Our new model ends up with a complex pricing problem, which has an exponential number of constraints due to some subtour elimination constraints. Consequently, in order to efficiently solve the pricing problem, we consider: (i) a hierarchical decomposition of the original pricing problem; (ii) heuristics in order to go around the large number of constraints in the pricing problem.

For protection in multi-domain networks, we propose protection schemes against single link failures. Firstly, we propose an optimization model for a centralized protection scheme, assuming that the network management is aware of all the details of the physical topologies of the domains. We then propose a distributed optimization model for protection in multi-domain optical networks, a much more realistic formulation as it is based on the assumption of a distributed network management. Then, we add bandwidth sharing in order to reduce the cost of protection. Bandwidth of each intra-domain link is shared among FIPP p-cycles and p-cycles in a first study, and then among paths for link/path protection in a second study. Finally, we propose parallel strategies in order to obtain solutions for very large multi-domain optical networks.

The result of this last study allows the efficent design of a protection scheme for a very large multi-domain network (45 domains), the largest one by far considered in the literature, both with a centralized and distributed scheme.

Keywords: Multi-Domain, protection optical networks, distributed scheme, parallel scheme/system, multiple failure, p-cycles.

CONTENTS

LIST OF TABLES

LIST OF FIGURES

LIST OF ACRONYMS

ATM Asynchronous Transfer Mode

AS Autonomous Systems

CG-ILP Column Generation-Integer Linear Programming

CWDM Coarse Wavelength Division Multiplexing

DLP Dedicated Link Protection

DWDM Dense Wavelength Division Multiplexing

FDPP Failure Dependent Path Protecting

FIPP Failure Independent Path Protecting

GoS Grade of Service

ILP Integer Linear Programming

IP Internet Protocol

IPC Internal Port Connection

LP Linear Programming

OADM Optical Add/Drop Multiplexer

OLT Optical Line Terminal

PP Pricing Problem

RMP Restricted Master Problem

ROADM Reconfigurable Optical Add/Drop Multiplexers

RWA Routing and Wavelength Assignment

SLP Shared Link Protection

SPP Shared Path Protection

SRLG Shared Risk Link Group

SDH Synchronous Digital Hierarchy

SONET Synchronous Optical Network

TE Traffic Engineering

WDM Wavelength Division Multiplexing

WSONs Wavelength Switched Optical Network

WSS Wavelength Selective Switch

To my great parents and wonderful wife.

ACKNOWLEDGMENTS

First and foremost, I offer my gratitude to my supervisor, Professor Brigitte Jaumard, who supported me throughout my thesis with her encouragement and knowledge. This work would not have been possible without her effort, patience and avalaibiliy during these four years, specially in the final stages.

I also would like to thank my co-supervisor Professor Michel Toulouse for the chance that I could become a PhD student at CIRRELT, Université de Montréal, Canada. I also always remember the summers in Montréal when we had chances to go out, to drink some beers together with other Vietnamese colleagues. These are always nice memories in Montréal I never forget.

My thanks also go to the rest of my committee members, Dr. Bernard Gendron, Dr. Abdelhakim Hafid and Dr. Bernard Cousin, who gave me the great help and insightful comments on my research. I thank them all for their invaluable inputs.

All my research work was financially supported by the government of Vietnam and Université de Montréal. I am extremely grateful for these supports.

I thank the Faculty of Information Technology, Hanoi National University of Education, Vietnam, where I have taught since 2004, permitted me to be absent myself for all these years to improve my professional knowledge.

The Department of Computer Science and Operations Research (DIRO) and the Interuniversity Research Centre on Enterprise Networks, Logistics and Transportation (CIRRELT) at Université de Montréal provided the support and equipment I needed to produce and complete my thesis. I thank the technical and administrative staff members for being abundantly helpful and having assisted me in numerous ways.

I thank my family on whose unconditional encouragement and love I relied throughout my entire time at the Academy.

I could not end without thanking my wife, Trang, who tirelessly supported and loved me, even when I was being unloveable. Without her I could not have made it this far.

CHAPTER 1

INTRODUCTION

1.1 Motivation and background

This research focuses on optimal design problems arising in optical networks. Wavelength division multiplexing (WDM) technology is widely used in today's optical networks. The technology uses a number of distinct wavelengths to implement separate channels. WDM network corresponds to a *wavelength routing* network where the network ensures communication through *lightpaths*. Lightpaths are optical connections carried end to end from a source node to a destination node over a wavelength on each intermediate link. At intermediate nodes in the network, the lightpaths are routed and optically switched from one link to another link. Different lightpaths in a wavelength-routing network can use the same wavelength as long as they do not share any common link. This allows the same wavelength to be reused spatially in different parts of the network. In some cases, lightpaths may be converted from one wavelength to another wavelength as well along their route [1]. Assigning a path and wavelength through the network for each lightpath is referred to as the Routing and Wavelength Assignment (RWA) problem.

The RWA problem is one of the central problems in the dimensioning and provisioning of optical WDM networks. The RWA problem can be formally stated as follows: given a WDM optical network, and a set of requested connections, the RWA problem aims at defining a set of lightpaths so as to accommodate all or most of the connections, while optimizing a given objective function. With WDM, the enormous low-loss bandwidth of optical medium can be exploited efficiently by simultaneously carrying up to a few hundred wavelengths in one fiber. The latter feature brings challenges to the RWA problem, which is a NP-hard problem [15].

Moreover, there is a new trend in optical networks to move toward Wavelength

1. We will use the terminology of Ramaswasi *et al.* [64] with respect to second generation of optical networks

Switched Optical Networks (WSONs), which have been designed to offer an all optical switching fabric with a high level of automation and efficiency, thanks to Software Defined Network tools. Therein, the Wavelength Selective Switches (WSS) represent the core switching elements with a technology enabling multi-degree Reconfigurable Optical Add/Drop Multiplexers (ROADM) architectures with colorless and directionless switching. WSON nodes are highly *asymmetric* with respect to their switching capabilities. Firstly, the *asymmetry* depends on the port size of WSS. Secondly, the selection of the switching capabilities plays another critical role in order to improve network performance, e.g., the grade of service under a given number of ports.

For this reason, future networks must consider *asymmetric nodes* when chosing a routing and wavelength assignment (RWA). Most of the RWA algorithms used today and developed so far do not consider such asymmetric nodes.

Providing resilience against failures is another important requirement for high-speed optical networks. As these networks carry increasingly more data, the amount of disruption caused by a network-related outage becomes more and more significant. A single outage can disrupt millions of users and result in millions of dollars of lost revenue to users and operators of networks [35].

A connection is often routed through many nodes in the network between its source and its destination, and there are many elements along its path that can fail. In most cases, failures are triggered by human error, such as a backhoe cutting through a fiber cable, or an operator pulling out the wrong connection or turning off the wrong switch. The next most likely failure event is the failure of active components inside network equipment, such as transmitters, receivers, or controllers. Failures can also occur due to some natural disasters, such as fires, flooding, or earthquakes.

Network failures commonly arise in the form of link failures and node failures. Links fail mostly because of fiber cuts; this is the most likely failure event. There are estimates that long-haul networks annually suffer 3 fiber cuts for every 1000 miles of fiber [64]. For a large network of 30,000 miles of fiber cable, that would be

90 cuts per year. A node failure, although likely less frequent than a link failure, can cause widespread disruption when it occurs. Examples include the fire at the Toronto central office of Bell Canada in 1999 and the obliteration, flooding, and power outages at central offices due to Hurricane Katrina in 2005 [64], or during the great east Japan earthquake on March 11, 2011, a lot of the information and communication technology (ICT) resources — telecom switching offices, optical fiber links, and so forth — were completely or partially damaged due to the tremor and the resultant tsunami [70].

Survivability is the ability for a system to remain functional after the failure of one or several of its components. Considering the consequences that failures can have in high-speed optical networks, it is critical that such systems still provide their service beyond the failure of their components. Indeed, several survivability mechanisms have been designed to protect against single link or single event failures in optical networks. However, multiple failure restorability is now becoming an issue to consider in designing today's optical networks. Multiple failures can be caused by a number of factors such as shared-risk link groups (SRLG) or simple cable cuts occurring in parallel with maintenance operations [16, 78].

There are two schemes for designing survivability mechanisms: protection and restoration. In a protection scheme, a backup route is precomputed for each potential failure during network design or at the time of connection establishment. In the event of a failure, the disrupted connections are recovered by using the reserved network resources for failure recovery. Protection schemes consume more network bandwidth but they have faster restoration time and always guarantee recovery from failure. In contrast, restoration mechanisms take action in real time which means that the backup route is computed after the failure occurrence using the residual network resources. As a result, restoration does not consume much of the network bandwidth capacities but it may fail to restore the network functionalities if the network do not have sufficient spare resources at the time of a failure event. Because of their advantages, our research focus on protection schemes.

Resources for protection can be computed with routing or after the routing is

established. Our work assumes that the working routes for the set of connection requests are defined a priori. When the protection and working networks are determined simultaneously, we have a *joint optimization problem*. In contrast, when routing is computed separately, the problem is a *non-joint optimization problem*. Joint optimization leads to more resource-efficient designs but it is a much more complex problem, solutions to even medium size problem instances cannot be computed in a reasonable amount of time. Non-joint optimization is easier to solve and is a more realistic assumption since placement of protection capacity is considered as a strategic decision whereas working routing is an operational decision [72].

Protection techniques commonly focus on single domains where it is assumed that each node of the network has a complete knowledge of the physical topology in the entire network. This assumption is not satisfied in large multi-domain optical networks which are composed of several single-domain networks, interconnected by inter-domain links. For instance, the Internet has been built-up as a decentralized set of network domains, termed as autonomous systems (AS), with each managed by its own authority and operating under its own routing policy. Due to scalability issues, delay constraints, protocol restrictions and domain management policies in multi-domain networks, the internal topological details of a domain are usually not shared externally. As a result, no node in a multi-domain network can have the complete information on the overall multi-domain network. Thus, decentralized approaches are required to model and solve the problem of providing protection in multi-domain networks, protection is more difficult in multi-domain networks than that of single domain networks.

1.2 Investigated provisioning and protection

We list the problems that have addressed in this thesis. They divide into provisioning and protection problems.

1.2.1 Provisioning problems

We study the two following RWA provisioning problems in WDM optical networks with asymmetric nodes:

- ◇ *Problem RWA_AN, i.e., RWA with asymmetric nodes.* Given a WDM optical network with asymmetric nodes (for a given set of asymmetric switch connections), and a set of requested connections, find a suitable lightpath (p, λ) for each granted connection, where a lightpath is defined by the combination of a routing path p and a wavelength λ, so that no two paths sharing a link are assigned the same wavelength. We study the objective of maximizing the number of accepted connections (or the Grade of Service (GoS)), that is equivalently minimizing the blocking rate. This objective is most relevant when there is not enough transport capacity, i.e., enough available wavelengths, to accommodate all connection requests.
- ◇ *Problem RWA_OAS, i.e., RWA with an optimized asymmetric switch matrix.* Given a WDM optical network with limited switching capabilities (i.e., number of switch connections between the ports of a node), find the (asymmetric) switching node configuration that maximizes the GoS.

1.2.2 Protection problems

With respect to protection problems, we first study the problem of *protection in optical networks against multiple failures*. Given a WDM optical network, let $\mathcal{F}$ be the set of all possible link failure sets, indexed by F. The primary routing of the requests has been done, e.g., along the shortest paths between source and destination nodes. We optimize the number of bandwidth units that need to be rerouted whenever a failure F occurs.

We next study the problem of *multi-domain protection in optical networks*. This optimization problem has two forms according to the objective function and constraints.

- ◇ *Best possible protected dimensioning*: Given a multi-domain network with ca-

pacity on each link and the set of requests. Maximize the number of protected requests while minimizing the overall cost in terms of capacity for protection.

- ◇ *Full protected dimensioning*: Capacity is provided on each link, but this problem seeks to protect all the requests. We will propose a model for this problem such that it always has a solution. To do so, we use a set of variables which estimate the amount of required additional bandwidth, if any, in order to protect all demand requests, on every link e. The objective is to minimize the sum of the additional bandwidth for protection.

In order to find an ideal exact solution, we assume that the network management is aware of all the details of the physical topologies of the domains, and propose a centralized scheme to compute such exact solution. In reality, this assumption is not satisfied as protection in multi-domain networks is inherently a distributed problem in the sense that some relevant information to solve the problem is only available locally. Hence, we focus on distributed protection schemes. We then propose parallel strategies for each of these schemes to obtain solutions for very large multi-domain optical networks, up to 45 domains.

1.3 Articles produced during the thesis

In the following, we present the list of the articles published or submitted to publication to journals and international conferences with peer review during the thesis. Those that have been included as chapters are indicated by a star ($\star$).

1. B. Jaumard, D.T. Kien, M. Toulouse and H.A Hoang. p-Cycle based protection mechanisms in multi-domain optical networks. In *Proceedings of the International Conference on Communications and Electronics (ICCE)*, August 2012, pages 19-24.
2. $\star$ B. Jaumard, D.T. Kien and M. Toulouse. A distributed p-cycle protection scheme in multi-domain optical networks. In *Proceedings of the IEEE Global Communications Conference (GLOBECOM)*, December 2012, pages 3019-3025.

3. B. Jaumard and D.T. Kien. Distributed design and provisioning of survivable multi-domain optical networks. In *Proceedings of the International Conference on Optical Network Design and Modeling (ONDM)*, April 2013, pages 101-106.

4. ⋆ B. Jaumard and D.T Kien. A p-cycle protection scheme in multi-domain optical network, 2014 (submitted for publication in *Optical Switching and Networking*).

5. B. Jaumard and D.T. Kien. Distributed resilient design of very large multi-domain optical networks. In *Proceedings of the International Telecommunications Network Strategy and Planning Symposium (Networks)*, 2014 (to appear).

6. ⋆ B. Jaumard and D.T. Kien. Resilient design of very large multi-domain optical networks, 2014 (submitted for publication in *JOCN - Journal of Optical Communications and Networking*).

7. ⋆ B. Jaumard, H.A Hoang and D.T. Kien. Robust FIPP p-cycles against dual link failures. *Telecommunications Systems*, 2013, pages 1-12.

8. B. Jaumard and D.T. Kien. ROADM optimization in WDM networks. In *Proceedings of the International Telecommunications Network Strategy and Planning Symposium (Networks)*, 2014 (to appear).

9. ⋆ B. Jaumard and D.T. Kien. Optimal provisioning of optical networks with asymmetric nodes, 2014 (submitted for publication in *Photonic Network Communications*).

1.4 Plan of the thesis

The thesis is organized as follows.

Chapter 2 provides background information on optical networks. It contains concepts and terms relevant to optical networks, routing and wavelength assignment, network survivability and the difference between protection and restoration.

Then, we describe different categories of protection mechanisms according to dedicated or shared backup resources and protection structures. We also discuss the characteristics of ROADM-based networks and multi-domain networks. Finally, we introduce the column generation technique which is suitable to solve large scale linear programing problems.

Chapter 3 reviews the existing solutions for the RWA problem. Then, we discuss the existing solution methods found in the literature for the design of p-cycles and FIPP/FDPP p-cycles. We also present the literature on multi-domain protection with heuristic solutions and ILP models, as well as with centralized and distributed schemes. Finally, the literature on the column generation method is covered.

In Chapter 4, we propose a new CG-ILP model for the RWA_AN problem. The resulting model is a large scale optimization ILP model, which allows the exact solution of quite large RWA instances in WDM networks with given asymmetric nodes. We then propose a CG-ILP model for the RWA_OAS problem in order to find an optimized asymmetric switch matrix for ROADM-based networks and compare the resulting GoS with the one of the first model.

Chapter 5 describes our proposal for protection in optical networks against multiple failures. We propose a solution in a single domain network against multiple failures using FIPP and FDPP p-cycles.

Chapter 6 describes our proposal for protection schemes in multi-domain optical networks against single failures. First, we propose two original CG-ILP models, one for a centralized protection scheme and another for a distributed protection scheme. The model relies on an hybrid protection scheme where p-cycles are used to protect the inter-domain links, while FIPP p-cycles are used for the protection of paths or subpaths in each individual domain. The resulting algorithms obtain optimal or near optimal solutions with very reasonable computing times.

Chapter 7 is dedicated to the enhancement of the above protection schemes. We improve the value of the objective function of previous CG-ILP models with bandwidth sharing. Then, we investigate two methods to construct a virtual aggregated network and consider the impact of the number of inter-domain links on

the bandwidth requirement while still keeping a survivable multi-domain network.

In Chapter 8, we investigate an hybrid protection scheme where inter-domain links are protected by a shared link protection model, while a shared path protection model are used for the protection of paths or subpaths in each individual domain. We then propose parallelization strategies in order to obtain solutions for very large multi-domain optical networks.

Finally, Chapter 9 concludes the thesis and suggests future research directions.

CHAPTER 2

BACKGROUND

We introduce a description of optical networks and concepts related to routing and wavelength assignment, as well as protection models in optical networks. We also introduce the solution methodologies which are used to tackle large scale optimization problems arising in the modeling of protection or provisioning problems in single and multi-domain networks. But first, we list some basic terms used in the context of optical networks and survivability to which we will refer frequently in the sequel of thesis.

2.1 Basic terminology

Some important terms in optical networks and survivability are summarized as follows [64]:

- ◇ **Channel:** Wavelength on a fiber link.
- ◇ **Connection:** Capacity occupied by a request over a path.
- ◇ **Lightpath:** All-optical path between a pair of nodes which may go through multiple fiber links, i.e., a path that optically bypasses intermediate nodes. Occasionally, we will also refer to it as an optical segment.
- ◇ **Path:** Route in the physical network.
- ◇ **Protection capacity:** Capacity used by the protection paths on a link.
- ◇ **Working capacity:** Capacity used by the working paths on a link.
- ◇ **Protection path:** Alternate path to carry traffic in the '*failed*' state, also called backup path.
- ◇ **Recovery time:** Time elapsed between the time at which a failure occurs and the time at which traffic is restored.
- ◇ **Request:** Demand of traffic with a given bandwidth requirement between

two end nodes.

- ◇ **Span:** Physical entity collecting all channels between two adjacent nodes.
- ◇ **Working path (connection):** Path to carry traffic under normal operation conditions, also called primary path.
- ◇ **Optical cross-connection:** Switching action performed by a device called optical crossconnect (OXC) in order to setup a lightpath.
- ◇ **OC-*n*:** Transmission rate (OC means Optical Carrier). OC-n corresponds to a $n \times 51,84$ Mb/s signal, e.g., OC-192 $\simeq$ 10 Gb/s and OC-768 $\simeq$ 40 Gb/s.

2.2 Optical networks

Optical networks offer the promise to solve many problems, such as providing enormous capacities in communication networks, providing a common infrastructure where a variety of services can be delivered. They increasingly become capable of delivering bandwidth in a flexible manner where and when needed. There are three basic generations of optical networks.

2.2.1 First-generation optical networks

In the first generation, optics was essentially used for transmission, simply to provide capacity. Optical fiber provided lower bit error rates and higher capacities than copper cables which lead optical fibers to be widely deployed in all kinds of telecommunication networks. Examples of first-generation optical networks are SONET (synchronous optical networks) and the essentially similar SDH (synchronous digital hierarchy) networks, which form the core of the telecommunication infrastructure in North America, in Europe and Asia, as well as in a variety of enterprise networks such as Fibre Channel. However, in the first generation of optical networks, all the switching and other intelligent network functions were handled by electronics.

2.2.2 Second-generation optical networks

The second generation of optical networks have routing, switching, and intelligence performed in the optical layer as well. So, they can more easily process the enormous amount of data than electronics. Moreover, the electronics at a node only need to handle the data addressed (origin/destination) to that node while all the remaining data is routed through in the optical domain, significantly reducing the need for electronic equipments. These networks are based on WDM (Wavelength-Division Multiplexing) transmission and are called wavelength-routed networks.

WDM networks correspond to a type of high-speed transport network in which wavelength division multiplexing is applied to simultaneously transmit multiple distinct wavelengths in a single fiber. Depending on the spacing between two neighboring wavelengths, we can have dense WDM (DWDM) or coarse WDM (CWDM).

WDM systems use different wavelengths for different channels. Each channel may transport homogeneous or heterogeneous traffic, such as SONET/SDH (synchronous optical network/synchronous digital hierarchy) over one wavelength, ATM (Asynchronous Transfer Mode) over another, and yet another may be used for TDM voice, video or IP (Internet Protocol). WDM also makes it possible to transfer data at different bit rates. Thus, it offers the feature that one channel may carry traffic at 2.5 Gbps, 10 Gbps, 40 Gpbs or up to 100 Gbps rate while another channel may carry traffic at a different rate transmission; all on the same fiber. The technology applied to a WDM network node must support some functionalities, among which, wavelength routing (or switching) and multiplexing/demultiplexing are the most important ones.

The key network elements that enable optical networking are *optical line terminals* (OLTs), *optical add/drop multiplexers* (OADMs), and *optical crossconnects* (OXCs). An OLT multiplexes multiple wavelengths into a single fiber and demultiplexes a set of wavelengths on a single fiber into separate fibers. OLTs are used at the ends of a point-to-point WDM link. An OADM takes in signals at multiple wavelengths and selectively drops some of these wavelengths locally while letting

others pass through. It also selectively adds wavelengths to the composite outbound signal. An OADM has two line ports where the composite WDM signals are present, and a number of local ports where individual wavelengths are dropped and added. An OXC essentially performs a similar function but at much larger sizes. OXCs have a large number of ports (ranging from a few tens to thousands) and are able to switch wavelengths from one input port to another.

2.2.3 Third-generation optical networks (ROADM-based networks)

In WDM optical networks, the introduction of fixed OADMs provided the opportunity to save cost by eliminating unnecessary optical to electrical to optical conversion, but carried with it a number of key limitations that ultimately limited their application. Network operators were required to carefully plan the network topology at the time of deployment based on how they expected the network traffic to evolve. When these predictions were not accurate, it could have costly consequences such as the initial network having unused or even inaccessible bandwidth. Therefore, many have turn to the reconfigurable optical add/drop multiplexer (ROADM) technology to provide an optical network infrastructure over which they can flexibly deploy wavelengths.

ROADMs are the key elements in building the next-generation, dynamically reconfigurable optical networks [89]. ROADMs are software-provisionable that enable dynamic add/drop or express pass through individual wavelength division multiplexed (WDM) channels or group of channels at network nodes without the need for costly optical-electrical-optical (O-E-O) conversions. Hence, it influences cost, optical performance, and configuration flexibility. The technologies used include wavelength blocking, planar lightwave circuit (PLC), and wavelength selective switching (WSS) - though the WSS has become the dominant technology.

While the first generation ROADMs were of degree two and could be used only in ring or line architectures, new ROADMs are expected to support high-degree nodes. This is essential for the design and deployment of future optical networks. To do this, multi-degree ROADMs based on WSS have been proposed and are

very promising in order to build flexible and degree upgradeable fully functional ROADMs, see [89].

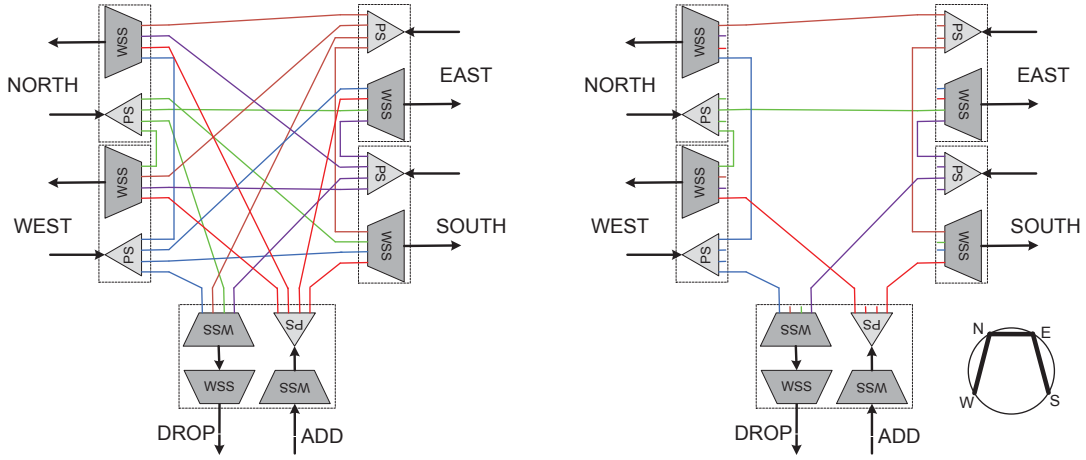

(a) Symmetric Architecture

(b) Asymmetric Architecture

Figure 2.1: A 4-degree ROADM (adapted from [14])

Figure 2.1(a) shows a diagram of a 4-degree ROAM using WSS elements located at a node in a network. Such a node can reach its neighbours from East, West, North, and South directions, and vice-versa. The optical signal coming into each direction is split by a Power Splitter (PS) and then directed to WSSs positioned on the outbound side of the other three directions and of the local DROP module. Each WSS selects and combines wavelengths from the other three directions and from local ADD module and direct to the desired direction. Figure 2.1(a) also shows that individual wavelengths can be locally added and dropped at the node. Therefore, with this architecture, any wavelength entering a node can be routed to the output of any one or more other directions. However, this is not necessary and the service providers always keep a "pay as you grow" investing approach. It means that asymmetric switching nodes are preferred in practice. Figure 2.1(b) shows a possible architecture of a 4-degree asymmetric ROADM. In Figure 2.1(a), we can still use 1×4 WSSs and 1×4 PSs, but only a subset of their ports can reach a subset of the other directions and the remaining ports are reserved for scaling in

the future [89].

The switching connectivity among the four directions of the above asymmetric ROA-DM can be simply represented by the small circle on the lower right corner in Figure 2.1(b). The three bold lines in the circle connect reachable directions and are called Internal Port Connections (IPCs).

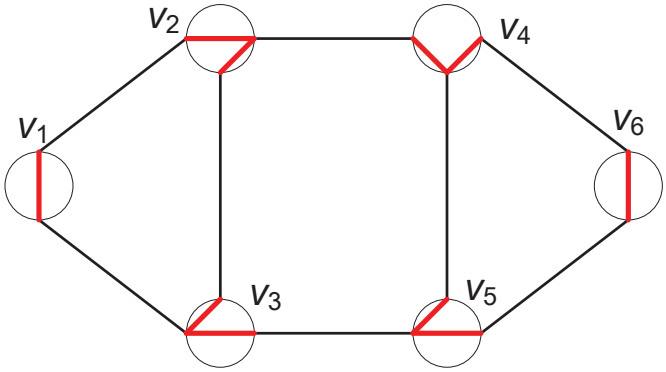

Figure 2.2: A network with asymmetric nodes

A ROADM-based network can be represented by a graph with asymmetric nodes as Figure 2.2. All the RWA computation for connection requests will be based on this simple asymmetric node model. When a lightpath traverses an asymmetric node, it must be along one of the internal lines (bold lines) and it cannot go through multiple internal lines for a given node.

2.3 Routing and wavelength assignment

The RWA problem considers either networks without any wavelength converters or networks with wavelength converters at nodes. There exist some research on networks with wavelength converters at every node [11, 27], or on networks with sparse wavelength conversion [62, 79]. However, Jaumard *et al.* [42] have shown that wavelength conversion does not help very much in order to reduce the blocking rate when the number of wavelengths are large. Hence, we restrict here to the RWA problem with wavelength continuity assumption, i.e., the same wavelength is used from the source to the destination for all connection requests.

Formally, the RWA problem can be stated as follows [63, 69]:

◇ Input: the network topology, a set of connection requests and a set of available wavelengths.

◇ Output: the lightpaths to be established, each lightpath defined by the path along which it is set up and wavelength.

◇ Constraints: there are some basic constraints:

- Wavelength continuity constraint for network without wavelenth conversion: The same wavelength must be assigned to all the links along the path traversed by a lightpath.
- Distinct wavelength constraint, or so-called *clash* constraint: If two or more lightpaths share a common link, each must be assigned a distinct wavelength.

◇ Objective: several objectives have been considered:

- Maximimizing the number of accepted connections (or equivalently minimizing the blocking rate). This objective is most relevant when there is not enough transport capacity, i.e., enough avaiable wavelengths, to accommodate all connection requests.
- Minimizing the number of used wavelengths. It is usually assumed in that case that all connections can be established given the available wavelengths and the objective is to use the smallest number of them.
- Minimizing bandwidth requirement. In this case, it is again assumed that all connections can be granted.

2.4 Protection mechanisms

We first introduce classifications for the protection mechanisms, then we focus more specifically on classical shared link/path protections as well as p-cycle based techniques in transport network survivability.

2.4.1 Classification of protection mechanisms

Protection schemes can be classified into *dedicated* or *shared* protection. In dedicated protection, each working connection has its own dedicated spare capacity for protection. For example, in 1+1 protection, the optical signals are transmitted simultaneously on two dedicated channels between end nodes. Dedicated protection is very fast in service recovery and can handle multiple failures simultaneously. In contrast, resources for protection can be saved in shared protection schemes. Shared protection requires less resources for protection. Another advantage of shared protection is that the protection bandwidth can carry low-priority traffic under normal operational conditions. When the bandwidth is needed to protect a connection in the event of a failure, this low-priority traffic is preempted for restoration of a higher priority request.

Protection schemes can also be classified according to the type of protection they provide to working connections, i.e., link-based, path-based, or segment-based schemes, which we now describe in more details.

Link-based Protection

This protection scheme assigns a pre-determined backup path to each link of a working path. The backup path and its capacity are stored in the end nodes of the protected link. Backup paths in this scheme may share reserved spare capacity which is set up only after the failure occurs.

Figure 2.3(a) illustrates how protection is provided using link-based schemes. For example, if a failure on link $v_4 - v_5$ occurs, the traffic going through this link is rerouted over a backup path and then continue its way over the subsequent working links. Each working link (solid lines) has its own protection path (dashed lines). From this example, we can also see that it corresponds to a shared protection scheme as links $v_3 - v_4$ and $v_4 - v_5$ on the working path have backup paths that share the link $v_3 - v_4$.

Link-based schemes provide very fast service restoration. However, they are less efficient in utilizing network capacity. Link-based protections include the clas-

sical Shared Link Protection (SLP), Dedicated Link Protection (DLP), and link-protecting p-cycles, which are discussed in Section 2.4.3.

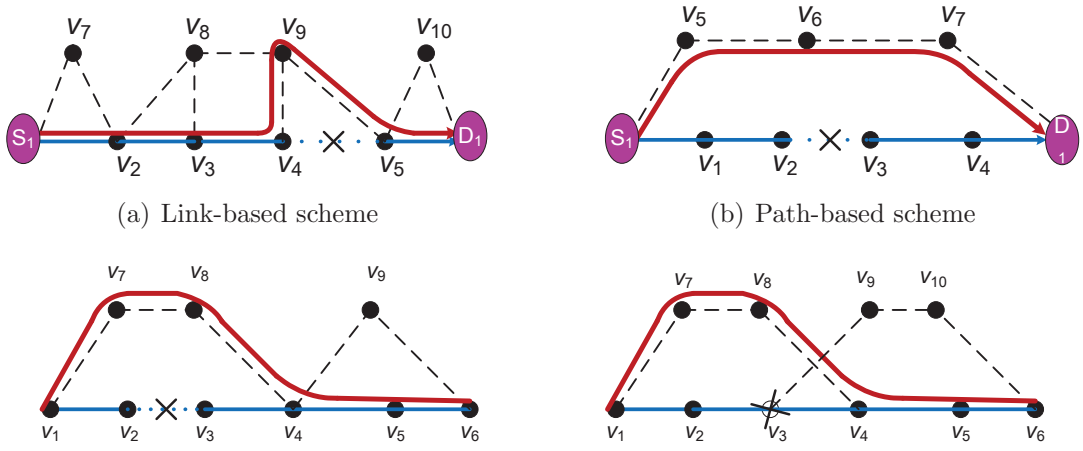

(a) Link-based scheme

(b) Path-based scheme

(c) Segment-based scheme

(d) Overlapping Segment-based scheme

Figure 2.3: Protection mechanisms

Path-based Protection

Path-based schemes provide an end-to-end backup path to protect each working path individually. In case of a link failure, a notification signal is sent to the end nodes of each connection traversing the failed link in order for them to switch the traffic from the working path to the backup path. The techniques in this category include Shared Path Protection (SPP) [84], and path-protecting p-cycles (see Section 2.4.4). Path-based schemes are more efficient than link-based schemes in terms of network capacity utilization.

In SPP, the backup path requires to be disjointly routed from its working path, as shown in Figure 2.3(b). The backup path can be link or node-disjoint from its corresponding working path depending on the type of protection to be provided.

Segment-based Protection

Segment-based schemes are based on a concept generalized from the two previous schemes. These schemes consist in dividing each working path into a sequence of path segments, which can overlap or not, and protecting them separately. When

a failure occurs, only the affected segment performs protection switching and the other unaffected segments are oblivious to the failure. In the classical segment protection, the working segments are concatenated but not overlapping, as illustrated in Figure 2.3(c). As in link-based schemes, segment-based schemes are not able to protect end nodes of the segments. However, they have the advantages of faster restoration and more spare capacity efficiency compared to path-based schemes, despite the complexity in network planning and operation.

Protection using overlapping working segments was introduced in [53] and further developed in [37]. The most important advantage of this scheme over the classical segment protection is that it provides recovery against node failure, as shown in Figure 2.3(d), although they consume more spare capacity.

2.4.2 Classical shared link/path protection

Shared protection schemes are used in order to save resources for protection [60]. In shared-link protection, at the time of call setup, for each link of the working path, a backup path and resource are reserved around that link. However, the backup resources reserved on the links of the backup path may be shared with other backup paths.

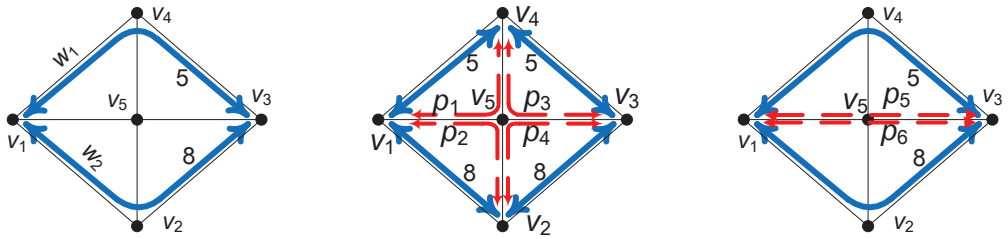

(a) Two working paths

(b) Classical shared link protection

(c) Classical shared path protection

Figure 2.4: Shared link/path protection

In shared-path protection, at the time of call setup for a primary path, a link-disjoint backup path and resource are also reserved. However, the backup resources

reserved on the links of the backup path may be shared with other backup paths. The eligible condition is subject to the constraint that "*the working paths, whose backup paths share bandwidth, never fail simultaneously*"'.

Let us consider a shared protection example in Figure 2.4. In Figure 2.4(a), two bold blue lines describe working paths w_1 and w_2 that require 5 and 8 bandwidth units respectively. Figure 2.4(b) describes a classical link shared protection where the links on working paths are protected by (dashed red lines) backup paths p_1, p_2, p_3 and p_4. These backup paths share bandwidth on common link. For example, the link connecting $\{v_1, v_5\}$ only needs 8 spare capacity units for both p_1 and p_2. Similarly, figure 2.4(c) presents a classical path shared protection where the working paths w_1 and w_2 are protected respectively by backup paths p_5, p_6. The two backup paths share bandwidth on link connectiong $\{v_1, v_5\}$ and $\{v_5, v_3\}$. Clearly, in the shared protection schemes, the total backup bandwidth is smaller than if dedicated protection is employed.

2.4.3 *p*-Cycles

p-Cycles were introduced in 1998 by Grover and Stamatelakis [32], they are linked-based protection mechanisms using fully preconnected cyclic protection structures with preplanned spare capacity. When a link fails, only the two end-nodes of the link perform protection switching, therefore no switching actions are required at any intermediate node of the cycle. Unlike rings, p-cycles protect against straddling link (chord) failures as well as failures on links over the ring itself. Besides, under p-cycles, the working paths are routed independently, i.e., they are not restricted to follow a cyclic structure. These characteristics make p-cycle based networks much more capacity efficient than ring-based networks, while providing "ring-like" speed switching [33]. Figure 2.5 illustrates the operation of basic link-protecting p-cycles. A same single p-cycle is shown by the red bold line. In Figure 2.5(a), a link on the cycle fails (dash line) and the surviving part of the cycle is used to provide a protection path (arrowed dotted line), just like rings. In Figure 2.5(b), a straddling link is protected by the same p-cycle. Each unit of spare capacity on a p-cycle

can protect two units of working capacity on a failed straddling link because two protection paths are provided in this case. In the example, both $v_5 - v_1 - v_2 - v_3$ and $v_5 - v_4 - v_3$ can be used to protect two units of working traffic on link $v_3 - v_5$.

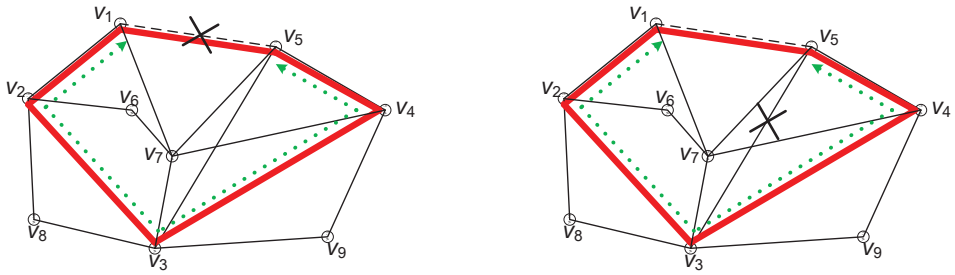

(a) On-cycle link failure (b) Straddling link failure

Figure 2.5: Basic concept of p-cycles

The p-cycle concept has been extended to more elaborated techniques (which are more bandwidth efficient), such as path-protecting p-cycles, which we introduce in the next section.

2.4.4 FIPP and FDPP p-cycles

Basic link-protecting p-cycles were further extended with the goal of providing end-to-end path protection with the Failure Independent Path-Protecting (FIPP) p-cycles [49] and Failure Dependent Path-Protecting (FDPP) p-cycles [38].

The FIPP p-cycle concept is explained using the example illustrated in Figure 2.6. FIPP p-cycles and working paths are represented by red bold and dashed lines respectively. In Figure 2.6(a), path $v_3 - v_{10} - v_5$ is a straddling working path since it is link-disjoint from the cycle. If link $v_3 - v_{10}$ or $v_{10} - v_5$ fails, protection paths $v_3 - v_4 - v_5$ and $v_5 - v_6 - v_1 - v_2 - v_3$ over the cycle can be used to restore the traffic on this path. In Figure 2.6(b), if link $v_5 - v_6$ or $v_6 - v_1$ of on-cycle working path $v_5 - v_6 - v_1$ fails, it can be recovered by using protection path $v_1 - v_2 - v_3 - v_4 - v_5$. More complicated relationships between a working path and a FIPP p-cycle can appear as shown in Figure 2.6(c). In this case, called z-relationship, the whole cycle is needed for protecting working path $v_6 - v_5 - v_{10} - v_3 - v_4$ and the protection

path used depends on which working link is affected. For example, protection path $v_6 - v_1 - v_2 - v_3 - v_4$ can be used to recover from a failure on links $v_5 - v_6, v_5 - v_{10}$ and $v_{10} - v_3$, and protection path $v_4 - v_5 - v_6$ protects against a failure on link $v_3 - v_4$. Although it is presented by A. Kodian and D. Grove [49] as a FIPP p-cycle enhancement, it is a step toward FDPP p-cycles.

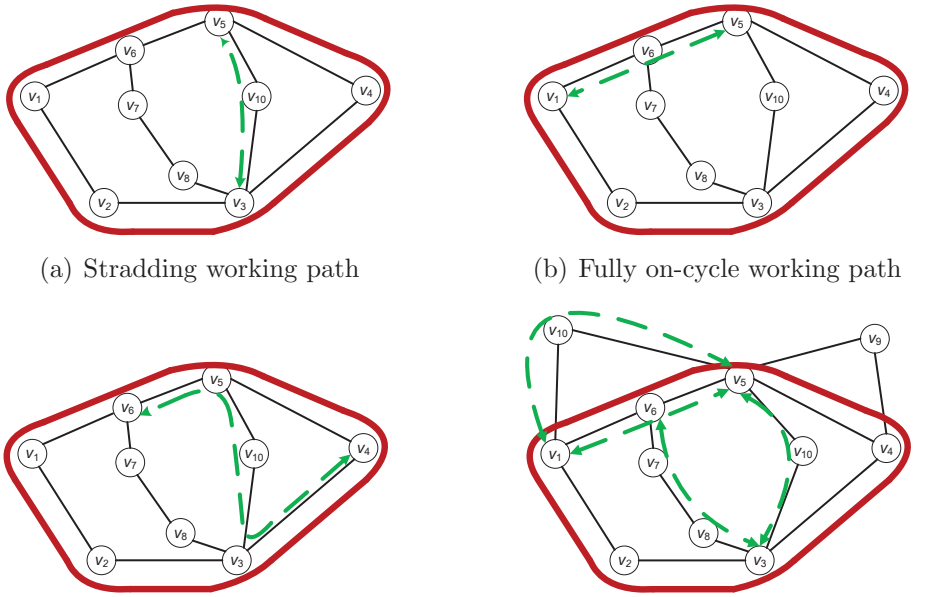

(a) Stradding working path

(b) Fully on-cycle working path

(c) Partially on-cycle working path

(d) Pairwise link-disjoint working paths

Figure 2.6: Basic concept of FIPP p-cycles

Under FIPP p-cycles, the cyclical protection structures can be shared by a set of working paths for protection as long as the working paths in this set are mutually disjoint or, if they are not, their protection paths must be mutually disjoint. If these criteria are met, there will be no contention for spare capacity after a failure. Furthermore, the end nodes of the working paths must also be crossed by the cycle assigned to protect them. Let us consider the example illustrated in Figure 2.6(d). In FIPP p-cycles, only one route will require protection under a single failure scenario because of the disjointness property of the set. Some of the routes in the example fully straddle the FIPP p-cycle, such as $v_6 - v_7 - v_8 - v_3$ and $v_5 - v_{10} - v_3$. These routes can have two working paths protected per unit of spare capacity on

the cycle. In addition, there are some routes lying fully over the cycle ($v_5 - v_{10} - v_1$ and $v_5 - v_6 - v_1$) and others partially over the cycle ($v_9 - v_4 - v_3$).

The main properties of FIPP p-cycle, presented in [49], are as follows:

- ◇ Only cross-connections at the end nodes are needed in real time to compose the protection paths which result in fast restoration.
- ◇ The protection paths are fully pre-cross-connected, providing certainty about functioning in case of a failure.
- ◇ Protection switching is end-node controlled, entirely failure-independent, and can recover either link or node failure along the path. Only a single switching action is pre-programmed at each end-node.
- ◇ Straddling routes can have two working paths protected by each unit-capacity p-cycle.
- ◇ Node-failure protection is achievable if working routes are node (and consequently link) disjoint. Node-disjointness can be relaxed to link-disjointness if only link failure is required.

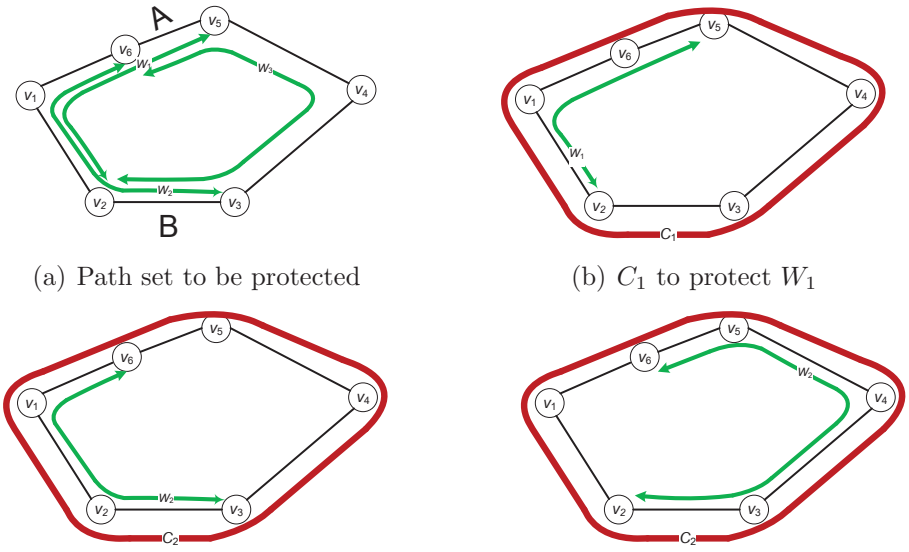

(a) Path set to be protected

(b) C_1 to protect W_1

(c) C_2 to protect W_2

(d) W_3 cannot be assigned a cycle for protection prior to failure

Figure 2.7: A FDPP p-cycles example

Under FDPP p-cycles, working paths can be protected using multiple protection

paths as part of different configurations depending on where the working paths are affected by failure. For example, consider Figure 2.7 where three unit working paths W_1, W_2 and W_3 are shown. In order to protect these paths, three unit cycles would have to be placed because the working paths are non-disjoint. However, in this category we use only two unit cycles : W_1 is protected using cycle C_1 as in Figure 2.7(b), W_2 is protected using C_2 as in Figure 2.7(c) and W_3 is left unassigned, shown in Figure 2.7(d). If link $(v_5 - v_6)$ fails, W_1 and W_3 are affected. W_1 is simply restored using C_1 and W_3 can be restored using C_2. However, if link $v_2 - v_3$ fails then W_2 and W_3 are affected. W_2 can be restored using C_2, while C_1 is chosen to restore W_3. W_3 can be restored using either cycle, and the cycle that is actually used is dependent on where the network is affected by failure.

2.5 Multi-domain optical networks

These are transport networks that contain multiple single-domain optical mesh networks. Each domain is independent of the others in routing and resource management. Each domain is connected to individual neighboring domains through inter-domain links associating the domains' border nodes. Connection requests are made between nodes that belong to different domains. A domain that does not contain any of the two end-nodes of a connection request is called a *transit* domain. Domains can reach each other via neighboring and transit domains.

Every node of one domain has the complete knowledge of the domain to which it belongs. In contrast, due to domain autonomy, security problems and scalability constraints, the complete topology, resource availability and resource allocation of one domain is hidden to the other domains. The border nodes rather than internal nodes know the connectivity between domains. Border nodes see each external domain as a set of border nodes fully interconnected by virtual links. Each virtual link represent the physical connectivity between pairs of border nodes based on intra-domain physical paths between the border nodes. The capacity of this connectivity is represented through the TE information of the virtual link,

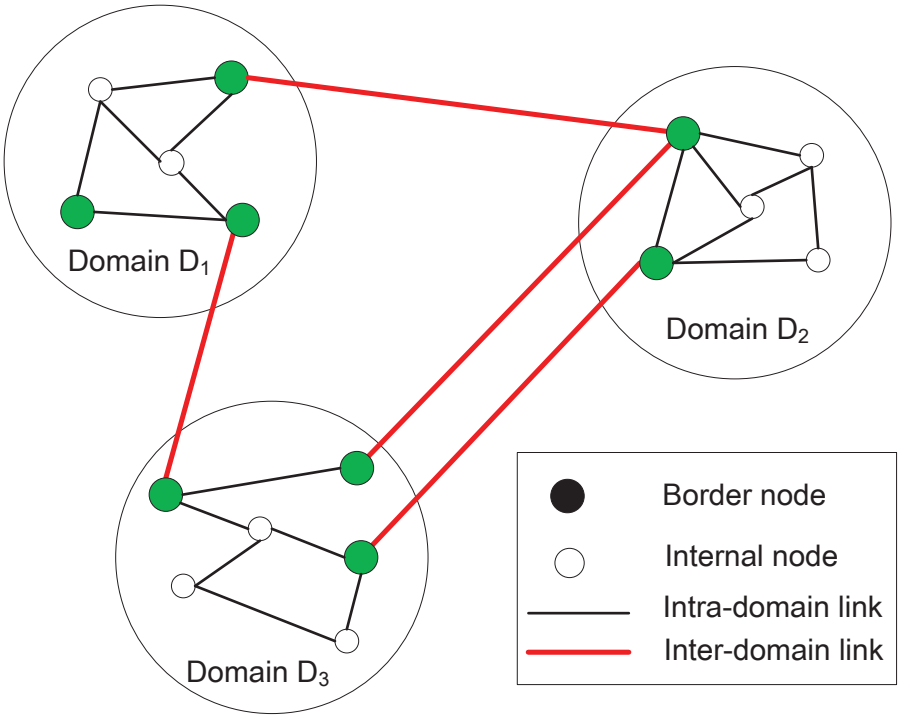

Figure 2.8: A multi-domain network

which is the aggregated information of those paths.

A border node views the multi-domain network as the combination of its domain, the border nodes, the inter-domain links and the virtual links of the other domains (Figure 2.8). We refer to the topology and resource allocation viewed by a border node as *inter-domain topology* and *inter-domain resource allocation*. N. Ghani *et al.* [28] address the survey of control plane design in multi-domain network.

Protection in multi-domain networks is characterized by difficulties that do not appear in single-domain networks:

- ◇ The working and backup paths are longer, resulting in longer failure notification and backup path activation.
- ◇ Due to security and scalability constraints, domains normally do not flood their internal link state messages throughout the large network. Thus, the domains' internal topology and their resource allocation information are hid-

den from the outside. The assumption that the entire network is visible from a computation center, as in single domain network, is no longer valid.

2.6 Large-scale optimization

In this section we review two techniques we will use to solve large scale optimization problems. The first technique is column generation, a scalable solution method requiring only a subset of the decision variables. The second technique is parallel computation, that allow spread over several processors the computation load of solving large optimization problems.

2.6.1 Column generation

Column generation is a well known technique for solving efficiently large scale optimization problems, see, e.g., [10, 17, 20]. It can be used whenever the original problem can be decomposed into a so-called master problem (MP) and one or several so-called pricing problems. The master problem is a linear program subject to a first set of explicit constraints and a second set of implicit constraints expressed throughout properties of the coefficients of the constraint matrix. The pricing problems consist in the optimization of the so-called reduced cost subject to the set of implicit constraints: It either identifies augmenting [1]configurations/columns to be added to the master problem or indicates that no such column exists. In Figure 2.9, we describe a "*base*" framework of ILP & column generation algorithm that we use for solving efficiently large scale optimization ILP problems in the next chapters.

In order to solve the master problem, we first generate a set of initial configurations (they can be dummy ones) in order to set the so-called Restricted Master Problem (RMP) built with all the constraints of the master problem but with only a subset of configurations (i.e., variables). The solution process is iterative (see Figure 2.9) and can be described as follows. At each iteration, the RMP is optimally

1. i.e., columns such that, if added to the current constraint matrix of the master problem, improve the value of the master objective function

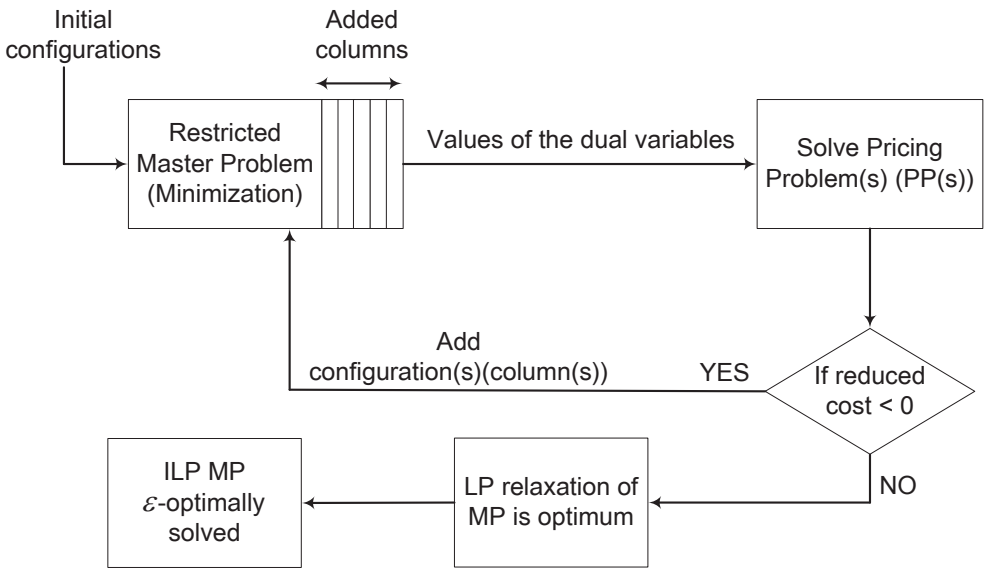

Figure 2.9: A "*base*" framework of ILP & column generation algorithm

solved and its optimal dual values are used to define the objective function of the pricing problem, which corresponds to the minimization of the so-called reduced cost of the configuration under construction (constraints of the pricing problem). If a new configuration is found with a negative reduced cost (even if not the minimum reduced cost configuration), then its addition in the RMP will allow a reduction of the value of the objective function of the RMP. However, if no such configuration can be found, the current solution of the master problem is an optimal one (for the continuous relaxation of the RMP), see, e.g., Chvatal [17] if not familiar with generalized linear programming concepts.

The solution scheme of a ILP column generation model is a two step process where we first solve the linear relaxation of the master problem using column generation techniques, and then design an algorithm (e.g., rounding off algorithm or the ILP solution of the restricted master problem) in order to derive an integer solution such that the so-called optimality gap $\left(\tilde{z}_{\mathrm{ILP}} - z^{\star}_{\mathrm{LP}}\right)/z^{\star}_{\mathrm{LP}}$, (where $z^{\star}_{\mathrm{LP}}$ is the optimal value of the linear relaxation, and $\tilde{z}_{\mathrm{ILP}}$ is the incumbent integer solution) is as small as possible. A well known integer programming technique, that complemented with column generation in solving many large scale integer programmes,

is branch-and-price [9, 85]. However, we have not used this type because we never encountered large gaps for the our problems. Indeed, several other techniques have been used, but vary depending on the problems, and therefore are described in the subsequent chapters.

2.6.2 Parallel and distributed implementations

With respect to centralized scheme for protection in multi-domain networks, we have designed a column generation solution that decomposes into several dual pricing problems. These pricing problems can be solved independently, i.e., they can be solved in parallel in order to speed up the computation of the solution, allowing to tackle larger problem instances.

With respect to distributed scheme, protection in multi-domain networks is a distributed problem for which processing has to be executed at the locations where information is available, i.e., at the level of each domain. Each domain has a full representation of its local state and the aggregated state of the whole multi-domain network. Hence, problem formulations for protection in multi-domain networks can be decomposed into independent subproblems along each domain. Formulations that satisfy this constraint are inherently parallel, and allow direct parallel solutions. A computing node can be allocated to each domain of the multi-domain network to compute the protection solution.

CHAPTER 3

LITERATURE REVIEW

This chapter presents a literature review on several protection and provisioning mechanisms. In Section 3.1, we discuss the existing solutions for the RWA problem in optical networks with asymmetric nodes. Section 3.2 reviews the protection mechanisms based on p-cycles. In Section 3.3, we review the literature on multi-domain protection and the solution approaches that have been proposed, in particular heuristics and ILP models. Finally, in Section 3.4 we cover the current literature on column generation techniques.

3.1 RWA in optical networks with asymmetric switching nodes

In WDM networks, many papers have already appeared on the RWA problem. As it is a highly combinatorial problem, various heuristic scheme solutions have been proposed under different traffic assumptions with static or dynamic patterns, with single or multi hops, and for various objectives. Several compact ILP formulations have been also proposed for this problem: see [43] and [41] for surveys in the asymmetrical and symmetrical traffic cases respectively. Several improvements as well as comparisons of all these formulations can be found in [46]. However, none of the above studies consider the internal switching structures of optical nodes.

Chen *et al.* in [14] proposed two solution schemes, link-state (LS) and distance vector (DV) schemes, for dynamic lightpath provisioning in optical WDM mesh networks with asymmetric nodes. In LS schemes, two proposed algorithms are the asymmetric switching-aware (ASA) Dijkstra's algorithm (the K-shortest path-based algorithm) and the entire path searching (EPS) algorithm. Results show that the ASA Dijkstra's algorithm has a high blocking probability while the computational complexity of the EPS algorithm is factorial, therefore non-polynomial. Hence, those algorithms cannot scale well when the network size increases. For the

DV scheme, the authors proposed a routing solution based on information diffusion. Results show that the resulting algorithm can achieve a low blocking probability with a low computational complexity.

In [36], the authors study how to provide resilience against node failures in WDM networks with asymmetric nodes. It implies the search for pairs of node disjoint paths, one for a working path and another for a backup path. While the Bhandari's method [13] (indeed, Suurballe and Tarjan's algorithm [81]) can quickly compute optimal disjoint paths in WDM networks with symmetrical nodes, the same algorithm may fail in networks that have asymmetric nodes. The authors proposed an approach for adapting the Bhandari's method such to avoid the trap issues due to asymmetric nodes. However, the time complexity of the resulting algorithm is exponential and the proof of the optimality is not provided.

3.2 Protection mechanisms

This section divides the protection mechanisms based on p-cycles into three subsections according to the type of protection provided by the p-cycles and their variants. Firstly, a review of survivable networks based on link-protection p-cycles is presented. Secondly, we summarize the literature on FIPP p-cycles. Finally, we discuss current literature on FDPP p-cycles.

3.2.1 *p*-Cycles

As described in Section 2.4.3, p-cycles are pre-cross-connected cyclic protection structures that use preplanned spare capacity, an idea that was first introduced by Grover and Stamatelakis in 1998 [32]. In our work, we consider a scenario where the objective is to minimize the amount of spare capacity needed to provide full protection. This objective is achieved through an optimal selection of p-cycles using usually an ILP formulation of the selection problem. But as the number of cycles grows exponentially with the network size, most authors propose to enumerate or pre-select candidate cycles before applying integer linear programming or any

other solution approach. Few authors propose an ILP-model to minimize the overall protection cost while using column generation to solve it.

There exists already several surveys on the p-cycles concept and associated solution methods to protect against single failures in single-domain networks, we refer the reader more specifically to the following surveys [8, 22, 40, 48]. While there exists substantial research on p-cycles against single failures, there is few research on multiple failures in single-domain networks (and virtually none on multiple failures in multi-domain networks). We review briefly the literature on p-cycles for protection against multiple failures in single-domain.

In reference [18], the authors investigate the design of p-cycles with complete or enhanced dual failure recoverability. Therein, three ILP models are proposed. The first one, which minimizes the spare bandwidth usage, is used to select p-cycles such that 100% survivability is guaranteed against any dual link failures. The second one aims to select p-cycles such to maximize the dual failure restorability under a given spare capacity budget. The third one is formulated to deploy p-cycles with minimum spare bandwidth usage such that only the specifically intended services or customers obtain full dual failure restorability.

The studies in [6, 21, 51] focus on the design of p-cycles networks with a specified minimum dual-failure restorability. The problem is formulated as an ILP model in each of these studies. The difference between the work in [51] and [21] lies in the way they calculate the dual failure recovery ratio, i.e, the restorability of working channels on span ℓ and ℓ' when those two spans simultaneously fail (or when their failures have overlapped in time). The work in [6] extends the one in [21] through a proposed enhanced dual failure recovery strategy. With this enhanced strategy, the numerical results show that the spare bandwidth cost is reduced considerably compared with [21]. To solve these ILP models, therein, a subset of p-cycle candidates is off-line pre-enumerated, thus optimality of the solution cannot be guaranteed.

Sebbah and Jaumard in [74] propose a scalable optimization solution method for the p-cycle design such that a specific protection level against dual link failures

can be guaranteed. Therein, the p-cycle design problem is formulated as an ILP. In contrast with all previous related studies, a solution method based on column generation is proposed. Using column generation, a limited number of promising p-cycles are calculated on the fly in the course of the optimization process. Thereby, this solution approach is more scalable than the previous studies on dual link failures.

The work in [55, 73, 80] also investigates, based on reconfigurable p-cycles, the design of survivable networks against dual failures. The assumption is that the second failure occurs after the first one has been recovered by p-cycles. The objective is to minimize spare capacity usage such that 100% guaranteed survivability can be ensured against dual link failures. In these studies, different strategies have been proposed for p-cycle reconfiguration, and different ILP models have been developed accordingly. The efficiency of the solutions from these designs is ranked as the order shown, i.e., [55] is less efficient than [73], which is less efficient than [80]. To solve these ILP models, a subset of p-cycle candidates are off-line enumerated with/without length limitation. Clearly, in these studies, the authors compromise on the quality of the solution in order to obtain scalability.

In reference [34], the authors propose an ILP-model for protection against shared risk link group (SRLG). A SRLG refers to a set of links which share the same risk of failure. However, the model is complex and difficult to solve for large networks. To overcome this drawback, Liu and Ruan in [52] investigate the p-cycle design problem in the presence of the failure of any SRLG. For this, an ILP model is formulated. The objective of the model is to minimize the spare capacity usage such that 100% survivability can be guaranteed against any single SRLG failure. The p-cycle candidates are off-line enumerated and supplied to the ILP for p-cycle selection. To avoid enumeration of all possible cycles in a network, a heuristic is proposed to generate a basic p-cycle candidate set. Here also, the authors compromise on the optimality of the spare capacity usage, i.e., the ILP solution in order to reduce the computational time.

Wang and Mouftah in [86] study the p-cycle design problem to survive against

multiple failures that may occur in large networks. They propose a pure two-stage heuristic for recovery from multiple failures, i.e., an off-line centralized p-cycle calculation and on-line distributed p-cycle selection. With this method, it is reported that a high probability of multiple failure recovery can be obtained without adding extra spare bandwidth.

3.2.2 FIPP p-cycles

Recall that FIPP p-cycles are an extension of p-cycles to provide end-to-end path protection. FIPP p-cycles have been introduced by Kodian and Grover in [49]. The authors suggest two principles on which solution approaches for the design of FIPP p-cycle networks could be based. The first one consists in identifying sets of mutually disjoint working routes, and then to define suitable FIPP p-cycles with adequate capacity to protect each set so that every demand is protected by at least one cycle. The second principle, in turn, consists in identifying a subset of working routes which can be protected by a given FIPP p-cycle which is selected from a set of candidate cycles. Following the second principle, the authors propose an ILP model, which receives as input the set of candidate cycles as well as the working routes. For a survey on the FIPP p-cycles concept and existing solution methods for related problems against single failure, we refer the reader to [8, 40, 48].

Jaumard *et al.* in [45] propose a first column generation model for solving the FIPP p-cycles design problem against a single link failure. Following the approach of column generation techniques, the FIPP p-cycle design problem is decomposed into a master problem and a pricing problem. The master problem is used to select FIPP p-cycles from candidate cycles that are generated when needed by solving the pricing problem dynamically in the course of the optimization process. Further improvement of this column generation solution is reported in [67], where two pricing problems are exploited for generating FIPP p-cycles. Thereby, the solution process is much faster than the previous two CG models.

Eiger *et al.* in [26] investigate the FIPP p-cycle design problem such that demands in the network can survive from single or dual failures depending on

each demand requirement. The problem is formulated as an ILP model with the objective of minimizing spare capacity usage. To solve the ILP model, a subset of FIPP p-cycle candidates are pre-enumerated with the proposed algorithm. As only a subset of FIPP p-cycle candidates is pre-enumerated, the solution accuracy remains unpredictable.

3.2.3 FDPP p-cycles

In [38], the authors study the FDPP p-cycle design against multiple link failures. To do this, they determine the set of all possible single link failure sets, indexed by $\mathcal{F}$. For each given failure set F, they calculate how many bandwidth units need to be rerouted, and which links cannot be used for establishing a protection structure. Then, FDPP p-cycles are constructed to protect the amount of working capacity that needs to be re-routed in protection fibers between node pair v_s, v_d whenever F occurs. For small to medium size networks, the proposed model remains fairly scalable for increasing percentages of dual failures, and requires much less bandwidth than p-cycles protection schemes. For larger networks, heuristics are required in order to keep computing times reasonable [47].

3.3 Multi-domain protection

This section reviews the literature on protection against failures in multi-domain optical networks. Several studies show solutions that are link-based, path-based or segment-based, few consider p-cycles. The allocation of spare capacities for protection is usually based on heuristics, very few studies propose integer linear programming solutions.

3.3.1 Heuristic based solutions

In [84], Truong and Thiongane proposed a shared-path protection algorithm for multi-domain optical networks. A virtual topology including gateway nodes, intra-virtual links, and inter-physical links is extracted from a multi-domain optical

network. Coarse inter-routes are then computed for working paths and link-disjoint backup paths. Intra virtual links in every domain are then mapped to physical intra-routes, and inter-routes are obtained by combining coarse inter-routes with physical intra-routes.

Segment protection has been studied by several authors. Xie *et al.* [87] consider segment protection where each working path is partitioned into several working segments based on the different domains the working path go through. Each working segment is then protected by a link-disjoint backup segment in each corresponding domain. While this approach is more scalable than the previous one as each domain is independently protected, it offers no protection for the inter-domain links. Segment protection was further investigated in [83], where end-to-end working paths are divided into overlapping segments in order to ensure inter-link and node protection, including the protection of border nodes. Heuristics are developed and tested against an exact algorithm on small instances.

More recently, p-cycles (pre-configured cycles) were studied by Szigeti *et al.* [82] who combined the inter-domain p-cycle protection with different intra-domain protection schemes (p-cycle protection or dedicated protection). They used a heuristic to enumerate potential p-cycles. Experiments were conducted on three different networks. The largest one, TNET, has eight domains. In [24], Drid *et al.* also proposed p-cycles for the protection of multi-domain optical networks. However, they mostly focused on a topology aggregation model adapted to p-cycle computations.

In general, the work in [24, 82] uses the entire multi-domain virtual topology to compute the p-cycles. As result, the backup paths (i.e., p-cycles) are overly lengthy routes with unacceptably high impairments. Moreover, computational complexities can also grow to prohibitive levels here. To overcome this drawback, the authors in [23] apply domain partitioning strategies (based upon spectral clustering) to segment domains into smaller "sub-multi-domain" networks. Localized p-cycle protection is then applied within these reduced entities and further provisions are also introduced to protect inter-domain links connecting the partitions. Extensive experiments were successfully conducted on a large multi-domain network with 17

domains. Results show much-improved computational scalability, by almost two orders of magnitude, with a very small increase in redundancy overheads, i.e., 2–4% range.

3.3.2 ILP based solutions

There are a very few solutions applying integer linear programming in multi-domain optical networks. In reference [59], the authors proposed subpath protection, which is a generalization of shared-path protection. The main ideas of subpath protection are: 1) to partition a large optical network into smaller domains and 2) to apply shared-path protection to the optical network such that an intradomain lightpath does not use resources of other domains. In this case, the primary/backup paths of an interdomain lightpath exit a domain (and enter another domain) through a common domain-border node. The authors proposed a ILP-model for the routing and wavelength-assignment (RWA) problem under subpath protection for a given set of lightpath requests. However, the model was proposed for large networks but not for multi-domain networks, i.e, inter-domain links do not exist. The solution cannot be used for generic multi-domain networks due to the absence of inter-domain links.

3.4 Column generation techniques

Column generation is a linear programming method that is designed for solving problems that have a huge number of variables, but also with a structure such that coefficients of the columns can be implicitly defined. Column generation has been proposed and discussed for integer programming with the pioneering work of Gilmore and Gomory [29, 30] on the cutting stock problem, however, with the derivation of heuristic ILP solutions Minoux [54] shows how several important combinatorial optimization problems can be reformulated and tackled by column generation. In reference [20], the authors offer an insightful overview of the state-of-the-art in integer programming column generation and its many applications,

such as shortest path problems with resource constraints, vehicle routing problem with time windows, airline crew and flight scheduling problems. Many reasearches show that column generation complemented with a suitable integer programming technique is a success story in large scale integer linear program. A well known strategy of this type is branch-and-price, where column generation and branch-and-bound scheme can be combined to obtain guranteed optimal solutions, see Barnhart *et al.* [9]. Vanderbeck [85] surveys some of the recent work in this area where the branching is made on the variables of the master problem (using cuts) rather than on the variables of the pricing problems.

There has been, even recently, several enhancements and extensions to the column generation technique. In [31], the authors consider new developments in the primal-dual column generation technique. In the standard column generation technique, an unstable behavior is caused by the use of optimal dual solutions that are extreme points of the restricted master problems. To overcome this drawback, an interior point method is used to obtain non-optimal solutions that are well-centered in the dual feasible set of the corresponding restricted master problem. The authors have presented theoretical analysis that guarantees the convergence of the primal–dual approach. Promising computational results on applications, such as the cutting stock problem, the vehicle routing problem with time windows, and the capacitated lot sizing problem with setup times, have been reported. In [68], the authors proposed column generation approaches for set partitioning problems. The set partitioning polytope has the quasi-integrality property, which enables the use of simplex pivots for finding improved integer solutions, each of which is associated with a linear programming basis. By combining such pivots with column generation, one obtains a method where each found solution to a restricted master problem is feasible, integer, and associated with a dual solution that can be used in a column generation step. The authors presented a framework for such an all-integer column generation approach to set partitioning problems. Although the overall approach is primarily introduced as being of a metaheuristic nature, criteria for determining whether a solution is optimal or near-optimal are also available.

CHAPTER 4

OPTIMAL PROVISIONING OF OPTICAL NETWORKS WITH ASYMMETRIC NODES

4.1 Chapter presentation

The chapter consists of the article (entitled as this chapter) which was submitted for publication in *Photonic Network Communications*. A shorter version of this paper with preliminary results was accepted in the *Proceedings of the International Telecommunications Network Strategy and Planning Symposium (Networks 2014)* under the title of "ROADM optimization in WDM networks".

This chapter is organized as follows. Section 4.2 describes the motivation towards our problems, the RWA_AN and RWA_OAS problems (see Section 1.2.1). In Section 4.3, we present the formal statements of two problems. In Sections 4.4 and 4.5, we propose two new optimization models and their solution processes for solving the RWA_AN and RWA_OAS problems respectively. Numerical results are presented in Section 4.6, where comparisons are made between the grades of service (GoS) of the two models, as well as the GoS sensitivity to the number of ports and to the number of switching connections. Conclusions are drawn in the last section.

4.2 Introduction

Recent developments in the Wavelength Selective Switch (WSS) technology enable multi-degree Reconfigurable Optical Add/Drop Multiplexers (ROADM) architectures with colorless, directionless and even contentionless switching. WSS is regarded as a very promising enabler for future reconfigurable wavelength division multiplexing (WDM) mesh networks, see, e.g., [89] [12]. WSS selects individual wavelengths from multiple ingress ports and switches them to a common egress port, a key property of the WSS based ROADM referred as Asymmetric Switching: in an optical switching element, the optical signal from one port can only

reach a subset of other ports. Such restrictions have been hardly considered in the studies on the RWA (Routing and Wavelength Assignment) problem.

Currently, most of the proposed RWA algorithms either assume a network with ideal physical layer ([44, 88]) or a network with physical layer impairments ([71]), with node architectures that are fully flexible. Very few studies (see Section 3.1) consider RWA algorithms assuming nodes with architectural constraints such as the ones associated with asymmetric switching.

In this study, we propose a new ILP (Integer Linear Programming) model, called RWA_AN (RWA with asymmetric nodes), derived from the one of Jaumard, Meyer and Thiongane [46] for the classical RWA problem. The resulting model is a large scale optimization ILP model, which allows the exact solution of quite large RWA instances, i.e., up to 670 wavelengths, assuming all nodes are asymmetric and that the switching connectivity matrix is given. We next modify the RWA_AN Model and design the RWA_OAS Model (RWA with an optimized asymmetric switch matrix) in order to find the best switching connectivity matrix for a given number of ports and a given number of switching connections, with respect to the grade of service (GoS), and compare the resulting GoS with the one of the first model.

4.3 Statement of the RWA_AN and RWA_OAS problems

We consider a WDM optical network represented by a directed multigraph $G = (V, L)$ with node set $V = \{v_1, v_2, ..., v_n\}$ where each node is associated with a node of the physical network, and with arc set $L = \{\ell_1, \ell_2, ..., \ell_m\}$ where each arc is associated with a fiber link of the physical network: the number of arcs from v to v' is equal to the number of fibers supporting traffic from v to v'. See Figure 4.1(a) for an example of a multigraph representing a multifiber optical network.

We will also use a so-called expanded directed graph $G^{\mathrm{E}} = (V^{\mathrm{E}}, L^{\mathrm{E}})$ where $V^{\mathrm{E}} = \bigcup_{v \in V} \mathrm{PORT}^v$ where PORT^v is the set of ports of node v, and $L^{\mathrm{E}} = \left(\bigcup_{v \in V} L^v \right) \cup L$ where L^v is the set of links connecting the ports of node v. An example of an expanded directed graph is shown in Figure 4.1(b).

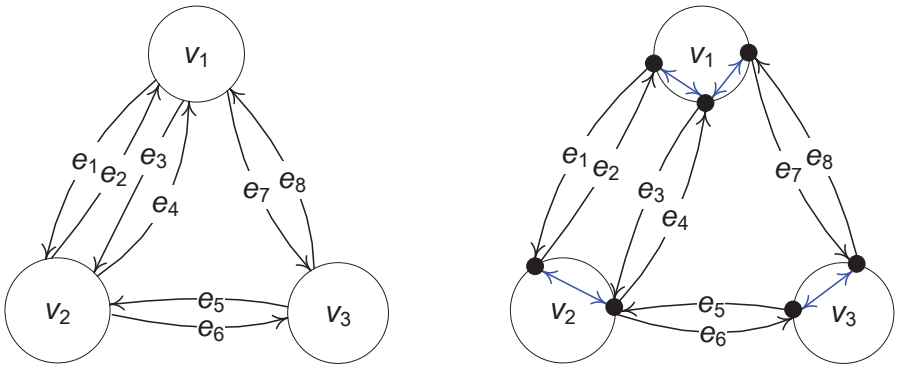

(a) Multigraph (b) Expanded Multigraph

Figure 4.1: Directed multigraphs and expanded multigraphs

The set of available wavelengths is denoted by $\Lambda = \{\lambda_1, \lambda_2, ..., \lambda_W\}$ with $W = |\Lambda|$. Traffic is described by set T where T_{sd} defines the number of connection requests from v_s to v_d. Let $\mathcal{SD} = \{(v_s, v_d) \in V \times V : T_{sd} > 0\}$. We only consider single-hop routing, i.e., the same wavelength is used from source to destination for each requested connection.

We give the detailed definition of the two following RWA problems with asymmetric nodes:

Problem RWA_AN, i.e., RWA with asymmetric nodes. Given an expanded multigraph G^{E} corresponding to a WDM optical network with asymmetric nodes (for a given set of asymmetric switch connections), and a set of requested connections, find a suitable lightpath (p, λ) for each granted connection, where a lightpath is defined by the combination of a routing path p and a wavelength λ, so that no two paths sharing an arc of G^{E} are assigned the same wavelength. We study the objective of maximizing the Grade of Service (GoS).

Problem RWA_OAS, i.e., RWA with an optimized asymmetric switch matrix. Given an expanded multigraph G^{E} corresponding to a WDM optical network with limited switching capabilities (i.e., number of switch connections between the ports of a node v, denoted by S_v), find the (asymmetric) switching node configuration and the provisioning (lightpaths) of the demand that maximizes the GoS.

4.4 RWA with asymmetric nodes

4.4.1 RWA_AN model

The proposed optimization model relies on the concept of configurations. Let C define the set of all wavelength configurations where a wavelength configuration is associated with a maximal set of link disjoint paths, all routed on the same wavelength, that can be used for satisfying a given fraction of the connections. A wavelength configuration c is represented by a vector a^c such that: a^c_{sd} = number of connection requests from v_s to v_d that are supported by configuration c. A wavelength configuration c is maximal if there does not exist another wavelength configuration c' such that $a^{c'} \geq a^c$.

There are two sets of variables in the model. Let z_c represent the number of selected occurrences of configuration c, each with a different wavelength. Variables y_{sd} define the number of accepted connections from v_s to v_d for all (v_s, v_d) in $\mathcal{SD}$.

The objective function can be formulated as follows:

$$\max \sum_{(v_s,v_d)\in\mathcal{SD}} y_{sd} \tag{4.1}$$

subject to:

$$\sum_{c\in C} z_c \leq W \tag{4.2}$$

$$\sum_{c\in C} a^c_{sd} z_c \geq y_{sd} \quad (v_s, v_d) \in \mathcal{SD} \tag{4.3}$$

$$y_{sd} \leq T_{sd} \quad (v_s, v_d) \in \mathcal{SD} \tag{4.4}$$

$$z_c \in \mathbb{N} \quad c \in C. \tag{4.5}$$

Constraints (4.2) ensure that we assign no more than the number of available wavelengths. Constraints (4.3) guarantee a full support for each requested connection. Constraints (4.4) ensure that the number of accepted connections for a given pair source-destinaton does not exceed the demand.

4.4.2 Solution of the RWA_AN model

In order to generate the wavelength configurations, we need to solve the so-called pricing problem, assuming the model of the previous section is solved using a column generation (CG), see Section 2.6.1 for the "*base*" framework of ILP & column generation algorithm.

We introduce one set of decision variables $\alpha = (\alpha_\ell^{sd})$ such that $\alpha_\ell^{sd} = 1$ if there exists a lightpath from v_s to v_d, which goes through link ℓ, 0 otherwise.

The objective of the pricing problem, $\textsc{redcost}(\alpha)$, is weighted with the dual variables. Let $u^{(4.2)} \geq 0$ be the value of the dual variable associated with constraint (4.2) and $u_{sd}^{(4.3)} \geq 0$ the values of the dual variables associated with constraint (4.3) in the optimal linear relaxation solution of the restricted master problem, i.e., the problem (4.1)-(4.5).

The pricing problem can be written as follows:

$$\textsc{redcost}(\alpha) \;=\; -u^{(4.2)} + \sum_{(v_s,v_d)\in\mathcal{SD}} \sum_{\ell\in\omega^+(v_s)} u_{sd}^{(4.3)} \alpha_\ell^{sd} \tag{4.6}$$

subject to:

$$\sum_{(v_s,v_d)\in\mathcal{SD}} \alpha_\ell^{sd} \leq 1 \qquad \ell \in L^{\mathrm{E}} \tag{4.7}$$

$$\sum_{\ell\in\omega^+(v)} \alpha_\ell^{sd} = \sum_{\ell\in\omega^-(v)} \alpha_\ell^{sd} \quad (v_s,v_d) \in \mathcal{SD}, \quad v \in V^{\mathrm{E}}\backslash(v_s,v_d) \tag{4.8}$$

$$\sum_{\ell\in\omega^+(v_s)} \alpha_\ell^{sd} \leq T_{sd} \qquad (v_s,v_d) \in \mathcal{SD} \tag{4.9}$$

$$\sum_{\ell\in\omega^-(v_s)} \alpha_\ell^{sd} = 0 \qquad (v_s,v_d) \in \mathcal{SD} \tag{4.10}$$

$$\sum_{\ell\in L^v} \alpha_\ell^{sd} = \sum_{\ell\in\omega^-(v)} \alpha_\ell^{sd} \quad (v_s,v_d) \in \mathcal{SD}, \quad v \in V^{\mathrm{E}}\backslash(v_s,v_d) \tag{4.11}$$

$$\alpha_\ell^{sd} \in \{0,1\} \qquad (v_s,v_d) \in \mathcal{SD}, \ell \in L^{\mathrm{E}}. \tag{4.12}$$

Constraints (4.7) and (4.8) define a set of link disjoint paths, i.e., a configuration. Constraints (4.9) and (4.10) ensure that we grant no more than the number of requested connections. Constraints (4.11) ensure that each path only goes through at most one internal connection of a asymmetric node.

The restricted master problem, i.e., the master problem with a very limited number of configurations, and the pricing problem are solved alternately until the optimality condition is met, i.e., the pricing problem cannot generate any new configuration with a positive reduced, see again Section 2.6.1 for more details on a CG-ILP solution scheme. Consequently, if $\textsc{redcost}(\alpha) \leq 0$, then problem (4.1)-(4.5) has been solved to optimality. Otherwise, the routing configuration c defined by the vector (a_{sd}^c) with $a_{sd}^c = \sum_{\ell\in\omega^+(v_s)} \alpha_\ell^{sd}$ for $(v_s,v_d) \in \mathcal{SD}$ is added to the current restricted master problem, which is solved again. Once the linear relaxation of the restricted master is optimally solved, we solve the ILP model resulting from the set of columns of the last solved restricted master problem in order to output an ILP solution for RWA_AN Problem (4.1)-(4.5).

4.5 RWA with optimal asymmetric switch node configurations

4.5.1 RWA_OAS model

We modify the definition of the wavelength configurations we used in the previous section as follows. Each configuration c is now represented by two binary vectors a^c (same definition as before) and b^c where $b^c_\ell = 1$ if configuration c uses link $\ell \in L^v$ (i.e., internal port connection) and 0 otherwise.

We also need to introduce one more set of variables: $x_\ell = 1$ if link ℓ is chosen for an internal port connection of an asymmetric node, and 0 otherwise.

RWA_OAS model has the same objective as RWA_AN, and includes the same set of constraints, as well as the following set of additional constraints:

$$\sum_{c \in C} b^c_\ell z_c \leq W x_\ell \qquad v \in V, \ell \in L^v \tag{4.13}$$

$$\sum_{\ell \in L^v} x_\ell \leq S_v \qquad v \in V \tag{4.14}$$

$$\sum_{\ell \in \omega^+(v)} x_\ell \geq 1; \sum_{\ell \in \omega^-(v)} x_\ell \geq 1 \qquad v \in V^{\mathrm{E}}. \tag{4.15}$$

Constraints (4.13) ensure that link ℓ is used in a configuration only if it is selected for an internal port connection in a switching matrix (i.e., $x_\ell = 1$). Constraints (4.14) ensure that the number of internal port connections of an asymmetric node does not exceed the limit on the number of internal port connections for that node. Constraints (4.15) ensure that there is at least one internal port connection per node in the expanded graph (G^{E}).

4.5.2 Solution of the RWA_OAS model

The solution scheme of RWA_OAS model follows the one for the RWA_AN model, i.e., a CG-ILP solution scheme, which requires the definition and the solution of a pricing problem in order to generate the configurations. Let $u^{(4.13)}$ be the dual value associated with constraint (4.13). The objective function of the pricing

problem can be written as follows:

$$\text{REDCOST}(\alpha) = u^{(4.2)} + \sum_{(v_s,v_d)\in\mathcal{SD}} \sum_{\ell\in\omega^+(v_s)} \alpha_\ell^{sd} u_{sd}^{(4.3)} - \sum_{v\in V} \sum_{\ell\in L^v} x_\ell u^{(4.13)}. \tag{4.16}$$

We use the same set of constraints as for the pricing problem of RWA_AN, together with some modified constraints that are next described. Replace the set of constraints (4.7) by the following constraint set:

$$\sum_{(v_s,v_d)\in\mathcal{SD}} \alpha_\ell^{sd} \leq x_\ell \quad \ell \in L^{\text{E}}. \tag{4.17}$$

Constraints (4.17) ensure that link ℓ is only chosen for the configuration under construction if $x_\ell = 1$, i.e., it is chosen for connection of a switching matrix.

Add the following new set of constraints:

$$\sum_{\ell\in L^v} x_\ell \leq S_v \quad v \in V, \tag{4.18}$$

In order to ensure that the number of internal port connections (IPC) (see Section 2.2.3) of an asymmetric node does not exceed the IPC number for that node.

The initial step of the solution process, i.e., the solution of the linear relaxation of the RWA_OAS model is the same as for the RWA_AN model, using a column generation algorithm. Next, we aim at finding an integer solution of the RWA_OAS problem. We found that this integer solution consists in the integer solution of the RWA_AN model and its respective set of asymmetric switch connections which is defined by combination of values x_ℓ for $\ell \in L^v, v \in V$. Hence, we propose a two step process. In the first step, we identify the binary values of the x variables using a sequential rounding-off mechanism (see Algorithm 1 below). Once all the x variables have been set to either 0 or 1 (i.e., internal port connections have been selected), we solve the remaining problem with an ILP solver.

Algorithm 1 Rounding-based algorithm for setting the integer values of the x variables

$x^{\text{IP}} \leftarrow x^{\text{LP}}$
while $\exists x_\ell^{\text{IP}} \notin \mathbb{Z}^+$ **do**
Select the variable x_ℓ^{IP} with the largest fractional value
$x_\ell^{\text{IP}} \leftarrow \text{ROUND}(x_\ell^{\text{LP}})$
Solve the CG-ILP model where the restricted master problem is (4.1)-(4.5), (4.13)-(4.15) and the pricing problem (4.6), (4.8)-(4.12), (4.17)-(4.18) with the additional constraint $x_\ell = x_\ell^{\text{IP}}$
$x^{\text{IP}} \leftarrow x^{\text{LP}}$
end while

Algorithm 1 is started with the optimal LP (Linear Programming) relaxation solution, x^{IP}, as output by the column generation algorithm. If all x_ℓ^{IP} for $\ell \in L^v, v \in V$ have integer values, an optimum asymmetric switch matrix has been found for all asymmetric nodes and there is no need to proceed with Algorithm 1, we use the same solution approach as for finding an integer solution for Model RWA_AN. On the other hand, if at least one variable x_ℓ has a fractional value in x^{IP}, one of them with maximum fractional value is selected and rounded to its closest integer value. Then, the resulting restricted master problem with one more integer x_ℓ variable is re-optimized, meaning the pricing problem is solved until the LP optimality condition is met again. This process continues until there is no remaining variable x_ℓ with a fractional value.

4.6 Numerical results

The two RWA_AN and RWA_OAS models were solved using the solution process described in Section 4.4 and 4.5. Algorithms were implemented using the OPL programming language and solved using CPLEX 12.5. Programs were run on a 2.2 GHz AMD Opteron 64-bit processor with 4GB of RAM.

We next describe the network and data instances, and then discuss the quality of the solutions provided by both models. We then look at grade of service vs. switching connectivity for a given number of ports.

4.6.1 Network and data instances

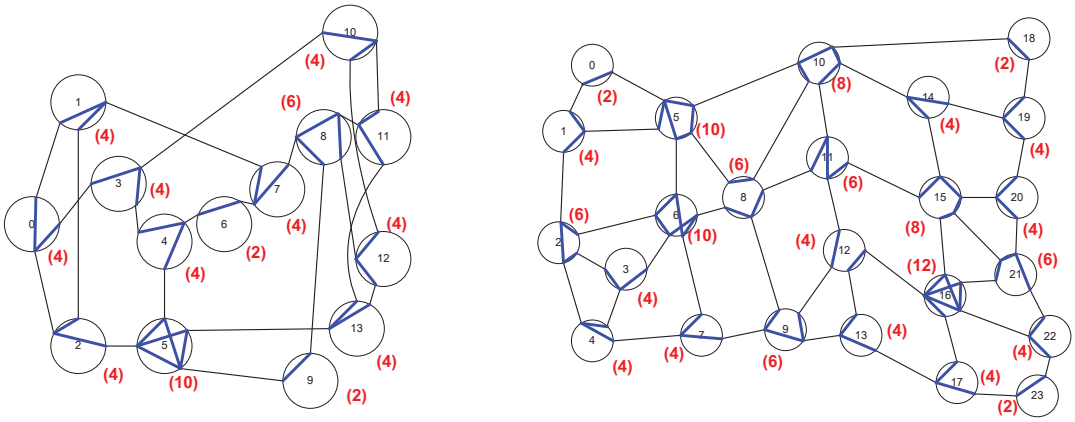

(a) NSFNET backbone network

(b) USANET backbone network

Figure 4.2: Network topology

We run experiments on two different topologies: the 14-node, 42-(directed) link NSFNET and the 24-node, 86-(directed) link USANET [77]. The topologies of the networks are depicted in Figure 4.2. The bold blue lines describe the internal port connections for each node. They are randomly generated for the RWA_AN model such that any ingress port is connected to at least one egress port in a node. The red numbers beside nodes define the limit on the number of node internal switching capabilities for RWA_OAS model: (x) indicates that they can be $x/2$ bidirectional switching capabilities between the ports, i.e., whenever one can transfer from port π to port π', we assume it is also possible from π' to port π.

For each network topology, we consider 20 traffic instances. For the first traffic instance (i.e., SD_0), the asymmetric traffic demand matrix $T = [T_{sd}]$ is generated by drawing the (integer) traffic demands (in units of lightpaths) uniformly at random in $\{0, 1, 2, 3, 4, 5\}$. The following traffic instances correspond to incremental traffic: SD_i $\subseteq$ SD_$(i + 1)$ where SD_$(i + 1)$ is built upon SD_i by deciding at random whether or not to add from 1 up to 5 more requests for each pair of nodes. Table 4.I gives the detailed characteristics of the request sets. For each traffic instance, we provide the number of node pairs with requests ($|\mathcal{SD}|$) and the overall

Traffic instances	NSFNET				USANET			
	$\lvert\mathcal{SD}\rvert$	$\sum_{\{v_s,v_d\}\in\mathcal{SD}} d_{sd}$	Sc1 (#W)	Sc2 (#W)	$\lvert\mathcal{SD}\rvert$	$\sum_{\{v_s,v_d\}\in\mathcal{SD}} d_{sd}$	Sc1 (#W)	Sc2 (#W)
SD_0	142	346		30	444	1,049		100
SD_1	171	696		60	539	2,168		130
SD_2	179	1,043		90	548	3,246		160
SD_3	180	1,413		120	552	4,373		190
SD_4	182	1,797		150	552	5,477		220
SD_5	182	2,191		180	552	6,560		250
SD_6	182	2,541		210	552	7,670		280
SD_7	182	2,880		240	552	8,802		310
SD_8	182	3,229		270	552	9,897		340
SD_9	182	3,611		300	552	11,041		370
SD_10	182	3,973	30	330	552	12,147	100	400
SD_11	182	4,364		360	552	13,266		430
SD_12	182	4,739		390	552	14,321		460
SD_13	182	5,103		420	552	15,483		490
SD_14	182	5,488		450	552	16,539		520
SD_15	182	5,828		480	552	17,662		550
SD_16	182	6,198		510	552	18,762		580
SD_17	182	6,538		540	552	19,872		610
SD_18	182	6,900		570	552	20,932		640
SD_19	182	7,300		600	552	22,044		670

Table 4.I: Characteristics of the request sets

number of traffic requests ($\sum_{\{v_s,v_d\}\in\mathcal{SD}} d_{sd}$).

We investigate two scenarios of the number of wavelengths. In the first study, the number of wavelengths is set to 30 for NSFNET and 100 for USANET. In the second study, these values are increased uniformly by 30 going from one instance to the next one (i.e., from SD_i to SD_$(i+1)$).

4.6.2 Quality of the RWA_AN and RWA_OAS solutions

In Tables 4.II and 4.III, we provide the solutions that are output by the solution process: z^{LP} is the optimal solution of the LP relaxation, hence a lower bound on the optimal ILP solution, z^{ILP} is the integer solution, it is an ε-optimal solution, with the

ε accuracy as indicated in the columns entitled ε. Indeed, ε varies from 0.00 to 9.15, meaning that the output solutions are always within a 10% accuracy. Computing times are within few seconds to few hours for traffic instances of NSFNET, while the computing times of USANET would benefit from the help of a heuristic in order to speed up the solution. However, note that the results corresponds to the largest traffic instances solved ε-optimally so far with 30 wavelengths on the NSFNET network and 100 wavelengths on the USANET network.

Herein, we also compare the grades of service resulting from the solutions of models RWA_AN and RWA_OAS. The last columns of Table 4.II and 4.III describe these comparisons on the NSFNET and USANET networks respectively. We can observe an average 17.3% and 28.9% increase of the grades of service, GoS^1_{AN} and $\text{GoS}^1_{\text{OAS}}$ for all traffic instances of the NSFNET and USANET networks, respectively. Therefore optimizing the switching configurations for a given number of ports makes a significant difference.

4.6.3 Performance of solutions vs. the number of wavelengths

In order to make the investigations more realistic, we increase the number of wavelengths for each instance. Indeed, the number of wavelengths increase uniformly by 30 going from one instance to the next one (i.e., from SD_i to SD_$(i+1)$) in order to ensure that GoS are always around 95%. The results are documented in Tables 4.IV and 4.V. We can observe that the solutions obtained with proposed models are still optimal or close to optimality. Indeed, ε accuracy varies from 0.00 to 7.52 for the traffic instances of the NSFNET and the USANET networks. Moreover, we can observe that the larger network is, the more significant the difference of optimizing the switching configurations is. Indeed, the difference between the solutions of models RWA_AN and RWA_OAS is 38.06% on average in USANET while it is 4.06% in NSFNET. This means that re-optimizing the switching configurations is very meaningful in large networks.

Traffic instances	RWA_AN model						RWA_OAS model						Comparison
	z_{AN}^{LP}	z_{AN}^{ILP}	ε (%)	# Bandwidth requirements	CPU times (sec.)	GoS (%)	z_{OAS}^{ILP}	z_{OAS}^{ILP}	ε (%)	# Bandwidth requirements	CPU times (sec.)	GoS (%)	$\frac{z_{OAS}^{ILP} - z_{AN}^{ILP}}{z_{AN}^{ILP}}(\%)$
SD_0	345.0	332	3.77	988	3,857	95.95	346.0	336	2.80	997	110	97.11	1.20
SD_1	486.5	442	9.15	1,060	1,179	63.51	548.0	506	7.66	1,138	395	72.70	14.48
SD_2	595.0	552	7.23	1,135	940	52.92	682.7	658	3.61	1,219	614	63.09	19.20
SD_3	676.0	636	5.92	1,140	592	45.01	767.3	699	8.91	1,217	392	49.47	9.91
SD_4	742.0	720	2.96	1,172	375	40.07	834.5	781	6.41	1,243	365	43.46	8.47
SD_5	794.5	743	6.48	1,190	332	33.91	884.5	850	3.90	1,250	277	38.80	14.40
SD_6	843.0	839	0.47	1,201	203	33.02	925.0	903	2.38	1,251	310	35.54	7.63
SD_7	891.0	891	0.00	1,231	102	30.94	967.0	951	1.65	1,243	248	33.02	6.73
SD_8	905.0	903	0.22	1,223	79	27.97	1,008.0	992	1.59	1,239	210	30.72	9.86
SD_9	921.0	915	0.65	1,219	63	25.34	1,049.0	1,024	2.38	1,234	230	28.36	11.91
SD_10	933.0	929	0.43	1,210	48	23.38	1,086.0	1,070	1.47	1,232	285	26.93	15.18
SD_11	942.0	942	0.00	1,189	36	21.59	1,128.0	1,044	7.45	1,257	213	23.92	10.83
SD_12	947.0	947	0.00	1,184	13	19.98	1,157.0	1,110	4.06	1,260	109	23.42	17.21
SD_13	951.0	951	0.00	1,217	24	18.64	1,185.0	1,159	2.19	1,260	73	22.71	21.87
SD_14	953.0	953	0.00	1,170	10	17.37	1,206.0	1,206	0.00	1,248	65	21.98	26.55
SD_15	955.0	955	0.00	1,154	9	16.39	1,228.0	1,228	0.00	1,254	45	21.07	28.59
SD_16	955.0	955	0.00	1,150	7	15.41	1,241.0	1,241	0.00	1,260	32	20.02	29.95
SD_17	958.0	958	0.00	1,138	7	14.65	1,253.0	1,253	0.00	1,260	42	19.16	30.79
SD_18	960.0	960	0.00	1,140	5	13.91	1,257.0	1,257	0.00	1,260	41	18.22	30.94
SD_19	960.0	960	0.00	1,140	5	13.15	1,259.0	1,259	0.00	1,260	28	17.25	31.15

Table 4.II: Performance of the RWA_AN/RWA_OAS model solutions - NSFNET network - with 30 wavelengths

Traffic instances	RWA_AN model						RWA_OAS model						Comparison
	z_{AN}^{LP}	z_{AN}^{ILP}	ε (%)	# Bandwidth requirements	CPU times (sec.)	GoS (%)	z_{OAS}^{ILP}	z_{OAS}^{ILP}	ε (%)	# Bandwidth requirements	CPU times (sec.)	GoS (%)	$\frac{z_{OAS}^{ILP} - z_{AN}^{ILP}}{z_{AN}^{ILP}}(\%)$
SD_0	918.0	849	7.52	4,165	12,751	80.93	1,049.0	1,049	0.00	5,692	72,155	100.00	23.56
SD_1	1,476.0	1,359	7.93	5,319	35,541	62.68	2,089.0	1,945	6.89	6,823	118,508	89.71	43.12
SD_2	1,908.0	1,802	5.56	6,028	61,951	55.51	2,640.2	2,438	7.66	7,268	89,783	75.11	35.29
SD_3	2,225.0	2,083	6.38	6,362	46,101	47.63	3,103.0	2,931	5.54	7,745	65,296	67.02	40.71
SD_4	2,473.3	2,378	3.85	6,419	34,852	43.42	3,480.6	3,170	8.92	8,008	85,404	57.88	33.31
SD_5	2,699.0	2,574	4.63	6,628	22,930	39.24	3,742.1	3,430	8.34	7,986	74,883	52.29	33.26
SD_6	2,892.0	2,768	4.29	6,604	20,643	36.09	3,968.0	3,647	8.09	8,075	63,822	47.55	31.76
SD_7	3,088.0	3,014	2.40	6,904	25,379	34.24	4,149.8	3,955	4.69	7,983	69,937	44.93	31.22
SD_8	3,248.0	3,203	1.39	6,985	24,391	32.36	4,322.4	3,985	7.81	8,046	84,192	40.26	24.41
SD_9	3,423.0	3,359	1.87	7,137	14,024	30.42	4,516.3	4,269	5.47	8,095	84,899	38.66	27.09
SD_10	3,570.0	3,463	3.00	7,223	19,885	28.51	4,661.5	4,267	8.46	8,179	73,952	35.13	23.22
SD_11	3,723.0	3,529	5.21	7,274	30,197	26.60	4,822.0	4,629	4.00	8,163	89,096	34.89	31.17
SD_12	3,835.0	3,777	1.51	7,343	20,321	26.37	4,956.2	4,708	5.01	8,213	112,008	32.87	24.65
SD_13	3,985.0	3,922	1.58	7,446	19,370	25.33	5,109.7	4,805	5.96	8,214	108,303	31.03	22.51
SD_14	4,117.0	4,014	2.50	7,482	23,261	24.27	5,243.9	4,995	4.75	8,288	102,793	30.20	24.44
SD_15	4,236.0	4,159	1.82	7,570	18,096	23.55	5,405.1	5,287	2.18	8,356	83,583	29.93	27.12
SD_16	4,346.0	4,294	1.20	7,540	15,449	22.89	5,522.9	5,312	3.82	8,353	54,462	28.31	23.71
SD_17	4,455.0	4,360	2.13	7,512	14,538	21.94	5,639.4	5,533	1.89	8,372	66,947	27.84	26.90
SD_18	4,541.0	4,441	2.20	7,517	8,465	21.22	5,725.6	5,591	2.35	8,377	61,655	26.71	25.90
SD_19	4,647.0	4,591	1.21	7,523	9,057	20.83	5,820.7	5,689	2.26	8,389	37,970	25.81	23.92

Table 4.III: Performance of the RWA_AN/RWA_OAS model solutions - USANET network - with 100 wavelengths

Traffic instances	RWA_AN model						RWA_OAS model						Comparison
	z_{AN}^{LP}	z_{AN}^{ILP}	ε (%)	# Bandwidth requirements	CPU times (sec.)	GoS (%)	z_{OAS}^{ILP}	z_{OAS}^{ILP}	ε (%)	# Bandwidth requirements	CPU times (sec.)	GoS (%)	$\frac{z_{OAS}^{ILP} - z_{AN}^{ILP}}{z_{AN}^{ILP}}(\%)$
SD_0	345	332	3.77	988	3,857	95.95	346.0	336	2.80	997	110	97.11	1.20
SD_1	691	642	7.09	1,957	5,072	92.24	696.0	693	0.43	1,939	208	99.57	7.94
SD_2	1,040	975	6.25	2,867	4,755	93.48	1,043.0	1,034	0.86	2,927	176	99.14	6.05
SD_3	1,406	1,346	4.27	3,888	5,418	95.26	1,413.0	1,413	0.00	4,982	166	100.00	4.98
SD_4	1,780	1,686	5.28	4,812	5,915	93.82	1,797.0	1,797	0.00	4,985	240	100.00	6.58
SD_5	2,139	2,043	4.49	5,758	4,035	93.25	2,191.0	2,186	0.23	5,727	201	99.77	7.00
SD_6	2,486	2,419	2.70	6,717	3,948	95.20	2,541.0	2,532	0.35	6,819	230	99.65	4.67
SD_7	2,846	2,783	2.21	7,812	5,258	96.63	2,880.0	2,866	0.49	8,001	210	99.51	2.98
SD_8	3,188	3,126	1.94	8,761	4,736	96.81	3,229.0	3,224	0.15	8,997	220	99.85	3.13
SD_9	3,559	3,514	1.26	9,618	4,549	97.31	3,611.0	3,606	0.14	9,713	238	99.86	2.62
SD_10	3,895	3,832	1.62	10,484	3,926	96.45	3,973.0	3,973	0.00	10,951	258	100.00	3.68
SD_11	4,271	4,197	1.73	11,397	4,053	96.17	4,364.0	4,360	0.09	11,579	232	99.91	3.88
SD_12	4,641	4,506	2.91	12,531	4,465	95.08	4,739.0	4,733	0.13	12,715	250	99.87	5.04
SD_13	5,001	4,949	1.04	13,459	4,673	96.98	5,103.0	5,103	0.00	13,687	221	100.00	3.11
SD_14	5,361	5,307	1.01	14,475	4,448	96.70	5,488.0	5,488	0.00	14,667	254	100.00	3.41
SD_15	5,724	5,647	1.35	15,529	4,680	96.89	5,828.0	5,828	0.00	15,694	197	100.00	3.21
SD_16	6,076	5,991	1.40	16,423	4,525	96.66	6,198.0	6,187	0.18	16,558	197	99.82	3.27
SD_17	6,423	6,338	1.32	17,446	4,726	96.94	6,538.0	6,533	0.08	17,970	214	99.92	3.08
SD_18	6,790	6,699	1.34	18,403	4,692	97.09	6,900.0	6,899	0.01	18,659	217	99.99	2.99
SD_19	7,167	7,123	0.61	19,188	4,490	97.58	7,300.0	7,300	0.00	19,890	223	100.00	2.48

Table 4.IV: Performance of the RWA_AN/RWA_OAS model solutions - NSFNET network - when the number of wavelengths increase from 30 to 600

Traffic instances	RWA_AN model						RWA_OAS model						Comparison
	z_{AN}^{LP}	z_{AN}^{ILP}	ε (%)	# Bandwidth requirements	CPU times (sec.)	GoS (%)	z_{OAS}^{ILP}	z_{OAS}^{ILP}	ε (%)	# Bandwidth requirements	CPU times (sec.)	GoS (%)	$\frac{z_{OAS}^{ILP} - z_{AN}^{ILP}}{z_{AN}^{ILP}}$(%
SD_0	918.0	849	7.52	4,165	12,751	80.93	1,049.0	1,049	0.00	5,692	72,155	100.00	23.56
SD_1	1,626.0	1,516	6.77	6,494	45,880	69.93	1,049.0	1,049	0.00	5,692	72,155	100.00	23.56
SD_2	2,269.0	2,193	3.35	8,404	44,401	67.56	2,168.0	2,116	2.40	8,201	126,574	97.60	39.58
SD_3	2,901.0	2,833	2.34	10,470	68,706	64.78	3,129.0	3,060	2.21	10,658	122,637	94.27	39.53
SD_4	3,551.0	3,444	3.01	12,708	86,435	62.88	4,069.0	3,865	5.01	13,132	148,329	88.38	36.43
SD_5	4,176.0	4,082	2.25	14,529	77,293	62.23	4,947.0	4,757	3.84	15,299	129,711	86.85	38.12
SD_6	4,784.0	4,695	1.86	16,350	73,014	61.21	5,810.0	5,669	2.43	17,528	135,416	86.42	38.88
SD_7	5,383.0	5,313	1.30	18,260	68,276	60.36	6,668.0	6,459	3.13	19,683	124,987	84.21	37.57
SD_8	5,967.0	5,894	1.22	19,906	81,584	59.55	7,516.0	7,173	4.56	21,930	117,446	81.49	35.01
SD_9	6,608.0	6,421	2.83	21,820	93,498	58.16	8,365.3	8,206	1.90	24,161	105,137	82.91	39.23
SD_10	7,204.3	7,106	1.36	24,073	94,758	58.50	9,247.1	9,021	2.45	26,440	92,564	81.70	40.49
SD_11	7,821.7	7,680	1.81	25,929	85,979	57.89	10,079.2	9,840	2.37	28,828	64,069	81.01	38.47
SD_12	8,419.5	8,347	0.86	27,635	73,453	58.29	10,952.8	10,710	2.22	31,012	52,212	80.73	39.45
SD_13	9,067.0	8,956	1.22	29,553	73,982	57.84	11,788.0	11,597	1.62	33,343	70,520	80.98	38.94
SD_14	9,668.3	9,532	1.41	31,439	86,294	57.63	13,492.0	13,210	2.09	37,871	63,716	79.87	38.59
SD_15	10,289.0	10,203	0.84	33,369	75,487	57.77	14,401.0	14,191	1.46	40,273	74,186	80.35	39.09
SD_16	10,884.0	10,692	1.76	34,980	79,671	56.99	15,249.0	15,138	0.73	42,433	72,452	80.68	41.58
SD_17	11,481.5	11,411	0.61	37,295	83,241	57.42	16,103.9	15,905	1.24	44,937	58,230	80.04	39.38
SD_18	12,064.0	11,977	0.72	38,677	81,199	57.22	16,956.9	16,692	1.56	47,034	69,912	79.74	39.37
SD_19	12,674.0	12,576	0.77	41,058	76,367	57.05	17,816.0	17,626	1.07	48,971	79,692	79.96	40.16

Table 4.V: Performance of the RWA_AN/RWA_OAS model solutions - USANET network - when the number of wavelengths increase from 100 to 670

4.6.4 Characteristics of the RWA_AN solutions

In Tables 4.VI and 4.VII, we provide the percentage of *lightpaths* based on the number of hops (i.e., the number of links) in the optimal integer solutions. Indeed, columns entitled "1-hop", "2-hops", "3-hops" and "$\geq$ 4-hops" describe the proportion of *lightpaths* with 1, 2, 3 or more than 4 link of the length respectively. When the number of traffic demands increase, going from SD_0 to SD_19, we can see that the number of "1-hop" *lightpaths* grows up while the number of "$\geq$ 4-hops" *lightpaths* reduce down, even to zero for almost traffic instances of NSFNET. The results show that: with respect to the objective of maximizing the number of requests in a network with a fixed number of wavelengths, when traffic demands are increased, the solution try to assign to 1-hop lightpaths which are completely disjoint with other 1-hop lightpaths and the 1-hop lightpaths have low conflicting probability with other longer lightpaths.

Tables 4.VI and 4.VII also show the number of generated configurations. We observe that only a very small number of configurations are generated while there are millions of possible configurations, thanks to the column generation technique which allows reaching an optimal solution of the linear relaxation without the requirement of an explicit enumeration of all the configurations. The number of selected configurations, which are part of the near optimal ILP solutions, is even smaller as can be observed in these tables. We can see that these values reduce down, resulting from the increase in "1-hop" *lightpaths* and the reduction of "$\geq$ 4-hops" *lightpaths*, when the number of traffic demands increase. Consquently, the computing times go down from SD_0 to SD_19 on the NSFNET network with 30 wavelengths (see Table 4.II)

4.7 Conclusion

We have proposed a scalable and efficient optimization model for determining the best switching matrices for each ROADM, for a given number of ports, and have shown how critical is such a choice in order to maximize the grade of service.

Traffic instances	1-hop (%)	2-hops (%)	3-hops (%)	≥ 4-hops (%)	# Generated config	# Selected config	GoS (%)
SD_0	26.88	24.46	22.85	25.81	835	29	95.95
SD_1	31.91	33.74	21.95	12.40	329	25	63.51
SD_2	38.74	38.58	18.87	3.81	294	25	52.92
SD_3	47.24	37.41	13.56	1.79	216	26	45.01
SD_4	54.91	32.57	12.38	0.13	160	25	40.07
SD_5	60.48	29.86	9.54	0.13	154	21	33.91
SD_6	65.64	26.92	7.44	0.00	99	19	33.02
SD_7	68.27	25.92	5.81	0.00	53	14	30.94
SD_8	69.46	26.35	4.08	0.11	42	15	27.97
SD_9	70.98	25.54	3.48	0.00	32	11	25.34
SD_10	74.17	21.97	3.86	0.00	26	11	23.38
SD_11	76.19	21.80	2.01	0.00	20	8	21.59
SD_12	76.79	21.52	1.69	0.00	6	5	19.98
SD_13	75.50	21.03	3.47	0.00	13	6	18.64
SD_14	77.91	21.68	0.42	0.00	5	4	17.37
SD_15	79.37	20.42	0.21	0.00	4	4	16.39
SD_16	79.58	20.42	0.00	0.00	3	2	15.41
SD_17	81.21	18.79	0.00	0.00	3	3	14.65
SD_18	81.25	18.75	0.00	0.00	2	2	13.91
SD_19	81.25	18.75	0.00	0.00	2	2	13.15

Table 4.VI: Characteristics of the RWA_AN model Solutions - NSFNET network - with 30 wavelengths

Future work will include the adaptation of the proposed models to dynamic traffic, in order to take advantage of the flexibility of ROADMs.

Traffic instances	1-hop (%)	2-hops (%)	3-hops (%)	$\geq$ 4-hops (%)	# Generated config	# Selected config	GoS (%)
SD_0	13.44	18.65	16.88	51.03	609	79	80.93
SD_1	18.17	21.44	18.10	42.29	985	79	62.68
SD_2	20.49	21.97	21.30	36.24	1,654	74	55.51
SD_3	22.07	24.49	22.39	31.05	1,368	74	47.63
SD_4	25.16	27.52	24.04	23.28	1,078	69	43.42
SD_5	28.77	28.88	22.63	19.72	750	63	39.24
SD_6	30.61	28.29	25.19	15.90	692	53	36.09
SD_7	31.90	31.48	22.84	13.78	829	54	34.24
SD_8	34.04	32.78	20.98	12.20	810	59	32.36
SD_9	35.77	32.92	21.55	9.77	503	52	30.42
SD_10	37.16	33.25	21.44	8.15	701	54	28.51
SD_11	39.53	33.26	20.37	6.84	1,046	59	26.60
SD_12	39.76	34.96	20.01	5.27	734	53	26.37
SD_13	42.14	34.29	18.85	4.72	710	48	25.33
SD_14	43.81	34.92	17.84	3.43	851	51	24.27
SD_15	45.03	35.43	16.29	3.25	682	43	23.55
SD_16	47.66	34.27	15.33	2.74	568	43	22.89
SD_17	49.32	34.57	14.16	1.94	538	41	21.94
SD_18	50.49	34.82	12.79	1.90	319	41	21.22
SD_19	53.21	33.85	11.02	1.92	348	43	20.83

Table 4.VII: Characteristics of the RWA_AN model Solutions - USANET network - with 100 wavelengths

CHAPTER 5

ROBUST FIPP *P*-CYCLES AGAINST DUAL LINK FAILURES

5.1 Chapter presentation

This chapter presents the article entitled "Robust FIPP p-cycles against dual link failures", published in *Telecommunications Systems*. The article aims at developing protection schemes of a single domain network against multiple link failures, using FIPP and FDPP p-cycles.

We propose a new generic flow formulation for FIPP p-cycles subject to multiple failures. While our new model resembles the decomposition model formulation proposed by Orlowski and Pioro (2011) in the case of classical shared path protection, its originality lies in its adaptation to FIPP p-cycles. When adapted to that last pre-configured pre-cross connected protection scheme, the bandwidth sharing constraints must be handled in a different way in order to take care of the sharing along the FIPP p-cycles. It follows that, instead of a polynomial-time solvable pricing problem as in the model of Orlowski and Pioro (2011), we end up with a much more complex pricing problem, which has an exponential number of constraints due to some subtour elimination constraints. Consequently, in order to efficiently solve the pricing problem, we consider: *(i)* a hierarchical decomposition of the original pricing problem; *(ii)* heuristics in order to go around the large number of constraints in the pricing problem.

Performance evaluation is made in the case of FIPP p-cycles subject to dual failures. For small to medium size networks, the proposed model remains fairly scalable for increasing percentages of dual failures, and requires much less bandwidth than p-cycle protection schemes (ratio varies from 2 to 4). For larger networks, heuristics are required in order to keep computing times reasonable. In the particular case of single link failures, it compares very favorably (5 to 10% of bandwidth saving) to the previously proposed column generation ILP model of Rocha, Jaumard and

Stidsen (2012).

The chapter is organized as follows. Section 5.2 describes the motivation to study the problem. Section 5.3 reviews related works. Section 5.4 presents definitions, notations, and the new proposed mathematical model. Section 5.5 discusses the solution process, and the heuristics for solving the pricing problems. Section 5.6 describes the data instances and present the numerical results. Finally, conclusions are drawn in the last section.

5.2 Introduction

Internet traffic has been growing rapidly and is expected to increase more than fourfold in the next few years. Such a traffic growth led to the generation of Wavelength Division Multiplexing Networks (WDM) networks for taking advantage of the very high capacity of optical fibers ($\sim$50 Tbps).

The design of survivable WDM networks has already received considerable attention as therein, service downtime and data losses due to a single link failure, such as a fiber cut, are highly critical issues. Two survivability approaches have been proposed in the literature, namely restoration and protection. The protection approach has been a common choice for designing survivable WDM networks as, thanks to shared backup path bandwidth reservation, some survivability quality can be guaranteed, e.g., 100% protection against any single link failure. Fast recovery is another advantage.

Protection solutions can be classified as either (end-to-end) path, segment or link protection. Path protection consumes less protection capacity but has longer restoration times than link protection. Thus, when it comes to spare capacity, in particular for WDM mesh networks where bandwidth is quite costly, path protection schemes are preferred.

Line-switched self-healing rings have been, and are still in some cases, the standard in survivable SONET/SDH ring networks due to their very fast recovery speed ($\sim$50ms). This led to the particular class of pre-configured pre-crossed connected

protection schemes. In the case of link protection, it corresponds to the now well-known p-cycles [32], and in the case of path protection, to the so-called FIPP (Failure Independent Path Protecting) p-cycles [49].

FIPP p-cycles offer a path protection within backup ring structures, and provide a rapid restoration service while requiring an economic amount of reserved capacity [45, 49, 50]. Other path protection configurations than paths and cycles have been studied, e.g., p-trees, p-trails, or p-structures [76]. So far, p-structures appear to be the most general and efficient path protection scheme, in terms of bandwidth requirements, as no condition is a priori set on the shape on the protection structures at the outset.

Moreover, most previous publications have focused on using a path protection scheme to guarantee the traffic connections in the event of single link failures. However, path protection design against single link failures turns out not be to always sufficient to keep the WDM networks away from many downtime cases as other kinds of failures, such as node failures, dual link failures, triple link failures, etc., become common nowadays due, e.g., to shared risk link groups [78]. Recently, several works partially dealt with this issue [16, 19, 39, 73, 75]. However, those works cannot be generalized for multiple failures or are far from being scalable in terms of performance.

In our work, we aim to develop a generic model which can be customized to represent whatever path protection structures. It is equivalent to the model of Orlowski and Pioro [57] in the case of the classical shared path protection, but new in the case of FIPP p-cycles. Both models can be efficiently solved using column generation techniques, combined with either heuristics or a branch-and-price method in order to derive an integer solution. In order to adapt the generic model to the case of FIPP p-cycles, bandwidth sharing constraints need to be moved to the pricing problems, and then, the master problem looses its decomposability structure and the pricing problem is no more polynomially solvable. We therefore need to propose another algorithm to solve efficiently the pricing problems in practice. This is done using a hierarchical decomposition of the pricing problems similar to

the one of Rocha *et al.* [67]. In order to keep computing times reasonable even for large instances, we also designed two heuristics which contribute to speeding up the solution of the pricing problems. Experiments show that high quality solutions are then obtained in acceptable computing times.

As a side but quite interesting result, it should be noted that the proposed model is the first one which encompasses all the different cases in which the previous ones differed (see, e.g., [45, 49, 67]) with respect to either the assumption of link disjointness for a subset of requests to be protected by a given FIPP pcycle or the so-called Z-case with refers to requests such that their protection path depends on which link fails along the working path (see [49] for more details).

5.3 Related works

Protection and restoration are important in designing reliable optical networks and have been widely studied in the literature. Most studies assume only a single-link or single-node failure model. As networks grow in size and complexity, the likelihood of multiple failures increases, and the impact of such failures can be measured in millions of losses. We review below the studies on link or path protection in the context of multiple failures, which may or may not occur in the context of a Shared Risk Link Group (SRLG) failure, i.e., a failure of multiple links due to a failure of a common resource.

Most studies dealing with multiple failures limit themselves to dual failures, and usually do not address node failures.

Choi *et al.* [16] proposed three loopback link protection heuristics for recovering from double link failures. The first two heuristics consist primarily in computing two link disjoint backup paths for each link, while the third one consists in computing a backup path p_ℓ^{B} for each link ℓ, such that the backup path of the links of p_ℓ^{B} does not contain ℓ. Such heuristics are difficult to extend to higher order of failures, especially in terms of the signalling that they entail. The authors also observe that it is possible to achieve almost 100 % recovery from double link failures

with a modest increase of the backup capacity, a conclusion that is quite surprising taking into account the results reported by other studies.

Schupke *et al* [73], Ramasubramanian and Chandak [61], Clouqueur and Grover [19] proposed each an ILP (Integer Linear Program) model to deal with dual link failures, assuming a p-cycle protection scheme, i.e., a link based protection. Those models cannot be easily generalized for handling multiple link failures. Moreover, the scalability of those models is questionable for realistic sized networks.

Sebbah and Jaumard [75] also considered dual link failures within the p-cycle framework. Their CG model is more efficient and more scalable than the previously proposed ones, but not easy to adapt to higher order failures.

An extension of p-cycle survivable network design to support multiple link failure is proposed in [52]. Only a subset of p-cycle candidates is enumerated during the design process, thus there is no available estimation of the solution quality. Huang *et al.* [39] introduced a path protection scheme for multiple link failures in WDM networks. However, the restoration is implemented under a dynamic routing scheme, which is not the focus of our study.

Eiger *et al.* [25] developed a heuristic method to fully protect WDM networks against single and dual link failures using FIPP p-cycles. Candidate FIPP p-cycles are pre-enumerated by an ad hoc procedure, again not easy to extend to higher order failures. Moreover, no tool is available for assessing the accuracy of the solutions.

Several decomposition models of path protection are proposed in [57] in order to protect WDM networks against multiple link failures. The study primarily focuses on the complexity analysis without providing any numerical experiments. In those models, a column is an optical path while our concept of column is a traffic flow associated with one or more paths. This way, we expect to generate less columns than when using path-based columns and then have a faster solution process. There is no comparative performance between the proposed models of [57] and the other path-based protection models.

We next discuss a generic exact ILP model which can fully protect the WDM

mesh networks against multiple link failures under a pre-configured path protection scheme while minimizing the bandwidth requirements. We believe such a model can serve as a unification tool for several protection schemes such as FIPP p-cycles, p-trees, p-trails, or p-structures.

5.4 Decomposition model

We first introduce the concepts and notations in Section 5.4.1, and then we set the newly proposed column generation model for multiple link failure protection, called FIPP_MULFAIL in Section 5.4.2.

5.4.1 Definitions and notations

We assume the WDM network to be represented by an undirected graph $G = (V, L)$ where V denotes the set of nodes (indexed by v) and L denotes the set of links (indexed by ℓ), each with a fiber capacity of W wavelengths. We denote by $\omega(v)$ the set of adjacent links of node v, $v \in V$.

Under a multiple link failure scenario, let $\mathcal{F}$ be the set of all possible link failure sets, indexed by F. We denote by $\mathcal{F}^k \subseteq \mathcal{F}$ the set of failure sets containing each k spans. We assume that all dominated failure sets have been eliminated, i.e., for any F, F' belonging to $\mathcal{F}$, we assume that $F \not\subseteq F'$ and $F' \not\subseteq F$.

We assume that the primary routing of the requests has been done, e.g., along the shortest paths between source and destination nodes.

In order to deal with a given failure set, say F, we need to know how many bandwidth units need to be rerouted, and which links cannot be used for establishing a protection structure. Let d_{sd}^F be the amount of working capacity which needs to be re-routed in protection fibers between node pair $\{v_s, v_d\}$ whenever F occurs. For instance, in Figure 5.1, lightpaths p_1, p_2, and p_4 transfer 5, 4, and 9 working units, respectively. If the failure set associated with set $F = \{\ell_6, \ell_7, \ell_3\}$ occurs, then we need to recover 9 $(= 4 + 5)$ units between s_1 and d_1 and 9 other units between s_2 and d_2, meaning that $d_{s_1 d_1}^{\{\ell_6,\ell_7,\ell_3\}} = 9$ and $d_{s_2 d_2}^{\{\ell_6,\ell_7,\ell_3\}} = 9$.

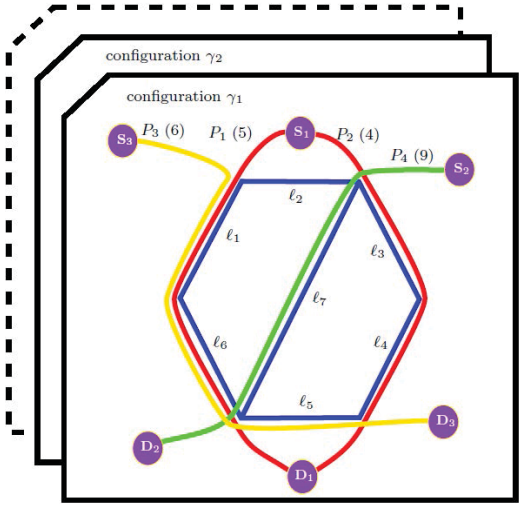

Figure 5.1: A WDM Network

In our model, the protection solution is provided by a set of configurations, where each configuration γ is defined as follows:

Definition 1 *A configuration $\gamma = (\varphi, p)$ is represented by a pair of vectors φ and p such that $\varphi = (\varphi_{sd}^{F,\ell})$ and $p = (p_{sd}^{F})$, for $F \in \mathcal{F}$, $\{v_s, v_d\} \in \mathcal{SD}$ and $\ell \in L$, where:*

$\varphi_{sd}^{F,\ell}$ *is the number of protection units on link ℓ which are used for protecting part of all the traffic going between v_s and v_d against failure set F.*

p_{sd}^{F} *is the number of protected units provided by configuration γ for the traffic between v_s and v_d against failure set F.*

Let Γ denote the set of all possible configurations.

Note that, with such a configuration definition, each configuration can be selected more than once. Moreover, in general, a given configuration only protects a fraction of the working capacity. By aggregating several configurations, the overall network is then protected. Indeed, for a given set of configurations $\{\gamma_1, \gamma_2, \ldots, \gamma_n\}$, we can build a new configuration γ as an aggregate configuration defined by a linear combination (with coefficients $\alpha_1, \alpha_2, \ldots, \alpha_n$) of the protection elements $\varphi_{sd}^{F,\ell}$ and p_{sd}^{F} of each of the "elementary" configurations as follows:

For all $F \in \mathcal{F}, \{v_s, v_d\} \in \mathcal{SD}$,

$$\varphi_{sd}^{F,\ell,\gamma} = \sum_{i=1..n} \alpha_i \, \varphi_{sd}^{F,\ell,\gamma_i} \qquad \ell \in L \tag{5.1}$$

$$p_{sd}^{F,\gamma} = \sum_{i=1..n} \alpha_i \, p_{sd}^{F,\gamma_i}. \tag{5.2}$$

In order to reduce the number of potential configurations, one may consider only maximal configurations, i.e., configurations γ such that there exists no configuration γ' satisfying: For all $F \in \mathcal{F}, \{v_s, v_d\} \in \mathcal{SD}$,

$$\varphi_{sd}^{F,\ell,\gamma} \leq \varphi_{sd}^{F,\ell,\gamma} \qquad \ell \in L \tag{5.3}$$

$$p_{sd}^{F,\gamma'} \leq p_{sd}^{F,\gamma} \tag{5.4}$$

i.e., no configuration that can offer less protection with more protection bandwidth requirement. But then, on the one hand, there would still be many potential configurations, and on the second hand, there is no guarantee that an optimal solution could be made of only maximal configurations, while maximizing protection bandwidth sharing and consequently minimizing the protection bandwidth requirements (see constraint (5.7) in the mathematical model). Pushing the idea of maximal configurations to its extreme, one could think about the definition of a configuration which supports the overall needed protected capacity. But then, the resulting optimization problem may be quite difficult to solve. Following those two observations, we decided to turn our attention to unit configurations:

Definition 2 *A unit configuration $\gamma = (\varphi, p)$ is a configuration such that: $\varphi_{sd}^{F,\ell} \in \{0, 1\}$.*

Using unit configuration, we propose to set an optimization model where the protection structure will be defined by a combination of several unit configurations, with some unit configuration occurring more than one.

In order to compute the traffic flow values $\varphi_{sd}^{F,\ell}$ and the protected amounts p_{sd}^{F}, we use a network flow formulation that is presented in Section 5.5.2. Those values

constitute the building blocks of the configurations.

We next have a closer look at the configurations. In order to be protected against failure F, on each link ℓ, we need a protection capacity that is equal to the sum of the protection capacities which are reserved for the traffic of each node pair $\{v_s, v_d\}$ with respect to F:

$$\varphi^{F,\ell} = \sum_{\{v_s,v_d\}\in\mathcal{SD}} \varphi_{sd}^{F,\ell} \qquad F \in \mathcal{F}, \ell \in L. \tag{5.5}$$

For a given set of values of variables $\varphi_{sd}^{F,\ell}$, the amount of protected capacity that configuration γ provides for the traffic of node pair $\{v_s, v_d\}$ against failure F is as follows:

$$p_{sd}^{F} = \sum_{\ell\in\omega(v_s)} \varphi_{sd}^{F,\ell} \qquad F \in \mathcal{F}, \{v_s, v_d\} \in \mathcal{SD}. \tag{5.6}$$

To apply the decomposition approach in a column generation method, we need to break the protection solution into several configurations. Note that the solution process consists of repeatedly solving the pricing problem and the restricted master problem (see Section 5.5 for the detailed definition of these problems), thus, in order to achieve a scalable decomposition model, a good performance trade-off between the pricing problem and the restricted master problem must be found. As configurations are generated by the pricing problem, we need to define a so-called basic configuration that can be easily generated by the pricing problem, and such that any configuration can be easily decomposed into an integer linear combination of basic configurations.

5.4.2 Optimization model: fipp_mulfail

The proposed optimization model, FIPP_MULFAIL, establishes relationships among the configurations in order to satisfy the protection bandwidth requirements, as the configurations take care (throughout the pricing problems) of generating the protection paths against the various independent failure sets. It requires one set of variables defined as follows:

$z_\gamma \in \mathbb{Z}^+$ number of selected copies of configuration γ.

The objective, which aims at minimizing the protection bandwidth requirements, can be written as follows:

$$\min \quad z^{\text{OBJ}} = \sum_{\gamma \in \Gamma} \text{COST}_\gamma \, z_\gamma$$

where $\text{COST}_\gamma = \sum_{\ell \in L} x_\ell^\gamma$.

Constraints are expressed as follows:

$$\sum_{\gamma \in \Gamma} p_{sd}^{F,\gamma} \, z_\gamma \geq d_{sd}^F \qquad \{v_s, v_d\} \in \mathcal{SD}^F, F \in \mathcal{F} \tag{5.7}$$

$$z_\gamma \in \mathbb{Z}^+ \qquad \gamma \in \Gamma \tag{5.8}$$

where d_{sd}^F is the amount of demand between v_s and v_d which needs to be rerouted following a failure $F \in \mathcal{F}$, and $\mathcal{SD}^F = \{\{v_s, v_d\}$: there exists at least one routing path between v_s and v_d which uses at least one link of $F\}$.

Note that $d_{sd}^F > 0$ for $\{v_s, v_d\} \in \mathcal{SD}^F$ as, if the demand between v_s and v_d is routed on one or several paths which do not use any link of F, then $d_{sd}^F = 0$. If $\{v_s, v_d\} \notin \mathcal{SD}^F$, then $d_{sd} \geq d_{sd}^F > 0$, with $d_{sd} = d_{sd}^F$ if all routing paths are going through at least one link of F.

5.5 Solution of the FIPP_MULFAIL model

In this section, we discuss how to solve the optimization column generation model, which was presented in the previous section. We start with generalities on column generation techniques, and then describe the pricing problem.

5.5.1 Generalities

Column Generation method is nowadays a well known technique for solving efficiently large scale optimization problems. A column generation mathematical model consists of a so-called master problem (here the linear relaxation of the model

that was presented in Section 5.4.2) and a so-called pricing problem that will be described in Section 5.5.2. The role of the pricing problem is to generate the so-called augmenting configurations, i.e., the configurations which, if added to the master problem, will improve its value, i.e., minimize further the protection bandwidth requirements as estimated by the linear relaxation of the model of Section 5.4.

In order to solve the master problem, we first generate a set of initial configurations (they can be dummy ones) in order to set the so-called Restricted Master Problem (RMP) built with all the constraints of the master problem but with only a subset of configurations (i.e., variables). The solution process is iterative and can be described as follows, see Figure 5.2 for an overview. At each iteration, the RMP is optimally solved and its optimal dual values are used to define the objective function of the pricing problem, which corresponds to the minimization of the reduced cost of the configuration under construction (constraints of the pricing problem). If a new configuration is found with a negative reduced cost (even if not the minimum reduced cost configuration), then its addition in the RMP will allow a reduction of the value of the objective function of the RMP. However, if no such configuration can be found, the current solution of the master problem is an optimal one (for the continuous relaxation of the RMP), see, e.g., Chvatal [17] if not familiar with generalized linear programming concepts.

In the next section, we provide the description of the pricing problem in the case of a path protection scheme, and show that it is easy to define additional constraints and a variable vector x (see the concise definition below in Section 5.5.2 which allows its adaptation to the case of a pre-configured protection scheme, such as the FIPP p-cycle one. Moreover, in that last particular case, it is possible to speed-up the solution process, we next explain how.

For FIPP p-cycles, a configuration $\gamma = (\varphi, p, x)$ includes: (i) the definition of one of several cycles throughout the flow variables of vectors φ and x where x is a flow vector defining the cycle(s) (there might be more than one) associated with the configuration, (ii) the number of protected units for each traffic flow between v_s and v_d against each failure set F, as identified by the variables of vector p.

Moreover, different configurations can be associated with the same cycle or set of cycles.

In order to speed up the solution of the pricing problems, which are iteratively solved, we introduced a decomposition solution scheme, as in Rocha *et al.* [67]. Let us denote by PRICING(INPUT : u; OUTPUT : φ, p, x) the current pricing problem to be solved, where u is the vector of the dual variables of the current RMP. Let C_γ be the set of cycles associated with configuration γ. We introduce the restricted pricing problem PRICING$_c(u; \varphi, p)$, for each cycle $c \in C_\gamma$, where constraints are identical to the constraints of PRICING(INPUT : u; OUTPUT : φ, p, x), except that a cycle is given (see Section 5.5.2 for more details). Before solving a new pricing problem PRICING$(u; \varphi, p, x)$, we first iterate solving restricted pricing problems PRICING$_c(u; \varphi, p)$, for all cycles $c \in C_\gamma$, until no more augmenting configuration can be generated with the set C of cycles generated so far, see Figure 5.2 for a flowchart of the algorithm.

We next provide the pricing problem formulation, and we will next discuss, in Section 5.5.4, how to derive an integer solution, once the linear relaxation of the master problem is optimally solved.

5.5.2 Pricing problem

We first write the pricing problem for the classical shared path protection and extend it later to the p-cycle protection scheme.

In the undirected case, the pricing problem PRICING(INPUT : u; OUTPUT : φ, p) has two sets of variables:

$\varphi_{sd}^{F,\ell} \in \{0, 1\}$. Those unit flow variables define potential protection path(s) for a given pair $(v_s, v_d) \in \mathcal{SD}$, against failure set F.

$p_{sd}^{F} \in \mathbb{Z}^+$. Those variables help to indicate the number of protected units with respect to protection against failure set F, for a given pair $(v_s, v_d) \in \mathcal{SD}$.

We define $\delta(S)$ for $S \subset V$, as the cut induced by S, i.e., the set of edges incident to a node in S and another node in $V \setminus S$.

For all $\{v_s, v_d\} \in \mathcal{SD}$ and for a given $F \in \mathcal{F}$, we have:

$$\varphi_{sd}^{F,\ell} = 0 \qquad \ell \in F \tag{5.9}$$

$$\sum_{\ell \in \omega(v_s)} \varphi_{sd}^{F,\ell} = \sum_{\ell \in \omega(v_d)} \varphi_{sd}^{F,\ell} = p_{sd}^{F} \tag{5.10}$$

$$\sum_{\ell \in \omega(v)} \varphi_{sd}^{F,\ell} \leq 2 \qquad v \in V \setminus \{v_s, v_d\} \tag{5.11}$$

$$\sum_{\ell \in \omega(v) \setminus \{\ell'\}} \varphi_{sd}^{F,\ell} \geq \varphi_{sd}^{F,\ell'} \qquad \ell' \in \omega(v), v \in V \setminus \{v_s, v_d\} \tag{5.12}$$

$$p_{sd}^{F} \in \{0, 1, 2\} \qquad F \in \mathcal{F}, \{v_s, v_d\} \in \mathcal{SD} \tag{5.13}$$

$$\varphi_{sd}^{F,\ell} \in \{0, 1\} \qquad \{v_s, v_d\} \in \mathcal{SD}, F \in \mathcal{F}, \ell \in L \tag{5.14}$$

The above constraints establish paths throughout a flow formulation, from a given source to a given destination, while forbidding the use of failing links. Note that constraints (5.12), together with constraints (5.11), force the "flow" degree of each node (except for the source and the destination) to be equal to 2 or 0: no flow or a unique flow going through the node.

In order to get a FIPP p-cycle protection scheme, we introduce the unit flow variables $x_\ell \in \{0, 1\}$, which enforce cycle shapes for supporting the protection paths, i.e., to guarantee that the two endpoints of each protection path lie on a

cycle. We also need the following constraints:

$$x_\ell \geq \sum_{\{v_s,v_d\}\in\mathcal{SD}} \varphi_{sd}^{F,\ell} \quad \ell \in L, F \in \mathcal{F} \tag{5.15}$$

$$\sum_{\ell\in\omega(v)} x_\ell \leq 2 \quad v \in V \setminus \{v_s, v_d\} \tag{5.16}$$

$$\sum_{\ell\in\omega(v)\setminus\{\ell'\}} x_\ell \geq x_{\ell'} \quad \ell' \in \omega(v), v \in V \setminus \{v_s, v_d\} \tag{5.17}$$

$$\sum_{\ell\in\delta(S)} \varphi_{sd}^{F,\ell} \geq p_{sd}^F \quad S \subset V, 3 \leq |S| \leq |V| - 3,$$

$$F \in \mathcal{F}, v_s \in S, v_d \in V \setminus S, \{v_s, v_d\} \in \mathcal{SD} \tag{5.18}$$

$$x_\ell \in \{0, 1\} \quad \ell \in L \tag{5.19}$$

Constraints (5.18) are subtour elimination constraints (see, e.g., [7]) which eliminates cycles isolating the source node from the destination node of a given flow. Such cases may arise when $p_{sd}^F = 2$. Note that those constraints do not eliminate all subtours, but only those disconnecting a source node to its corresponding destination node.

5.5.3 Speeding up the solution of the LP relaxation

The solution of the pricing problem, and consequently the solution of the LP relaxation, may become long when the number of failure sets increases. In order to speed it, we propose two heuristics which are next described.

Heuristic 1

Consider the heuristic solution scheme outlined in Figure 5.3. Therein, instead of solving the pricing problem with all constraints, we consider only the subset of constraints associated with a given subset $\mathcal{F}' \subseteq \mathcal{F}$, i.e., we randomly select a given number of failure sets. As guaranteeing the protection of all single link failures allow the protection of a large fraction of multiple failures, we assume that $\mathcal{F}^1 \subseteq \mathcal{F}'$, where $\mathcal{F}^1$ is the failure subset with all single link failure spans, i.e., $\mathcal{F}^1 = \{F : F = \{\ell\}, \ell \in L\}$. Consequently, the pricing problem denoted

by PP($\mathcal{F}'$), contains constraints (5.16) and (5.17), and only those associated with $F \in \mathcal{F}'$ among the remaining ones (i.e., (5.9)-(5.12), (5.15), (5.18)).

Let γ the configuration output by PP($\mathcal{F}'$). Apply a random permutation σ on the set SDF($\mathcal{F} \setminus \mathcal{F}'$) = $\{(\{v_s, v_d\}, F) : F \in \mathcal{F} \setminus \mathcal{F}'\}$ as to define a random order in which to go through the set. Let SDF$^\sigma$($\mathcal{F} \setminus \mathcal{F}'$) the resulting ordered set. We then use the following algorithm to enlarge the generated configuration so that it becomes maximal:

Configuration enlargement algorithm:

For $k = 1$ to $|$ SDF$^\sigma$($\mathcal{F} \setminus \mathcal{F}'$)$|$ **do**

let $(\{v_s, v_d\}, F)$ be the k^{th} pair of SDF$^\sigma$($\mathcal{F} \setminus \mathcal{F}'$)

if $\{v_s, v_d\}$ can be protected against F

in configuration γ **then**

update the values of $\varphi_{sd}^{F,\ell}$ and p_{sd}^F accordingly

endif

EndFor

Heuristic FIPP_MULFAIL_H1	
Selection of initial and iterative $\mathcal{F}'$ set	$\lvert L \rvert$ randomly selected failure sets in addition to the single link failure sets
ε	0.01
iter_max	3
Stopping condition: t ε'	 20 0.01 % of incumbent LP value
Enlargement of $\mathcal{F}'$	add 10% of randomly selected failure sets

Table 5.I: Parameter settings for heuristic FIPP_MULFAIL_H1

As it takes too long in practice to go through the whole (randomly) ordered list, we stop going through the list in practice if after going through, e.g., 10 pairs $(\{v_s, v_d\}, F)$, we cannot enlarge the incumbent configuration anymore.

As shown in Figure 5.2, there are two pricing problems, one where we determine a set of cycles, one where we reuse a given set of cycles. We only use the above solution for the first pricing problem (PRICING$(u; \varphi, p, x)$), as it is the one which takes the longest computing times.

In order to avoid iterating with a configuration which only improves lightly the incumbent value of the LP relaxation, we strengthen the sign condition of the reduced cost: instead of requiring it to be negative, we only care for configurations such that their reduced cost is smaller than $-\varepsilon$ with $\varepsilon > 0$.

If we are not successful with the first random selection of $\mathcal{F}'$ in order to reach a negative (or sufficiently negative) reduced cost, we make additional attempts for a maximum of iter_max attempts. If we are still unsuccessful, and if the stopping condition is not satisfied, we try to enlarge the set $\mathcal{F}'$ with randomly selected failure sets.

For the stopping condition, we look at the progress of the decrease of the objective function (z^{OBJ}). Let ∇^{ITER} be the improvement (decrease) of the value of z^{OBJ} at iteration ITER. If $\nabla^{\text{ITER}} < \varepsilon'$ during the last t iterations, then we stop iterating. Parameters used in the experiments are described in Table 5.I.

Heuristic FIPP_MULFAIL_H2

In Heuristic FIPP_MULFAIL_H2, rather than using a random selection of the constraints to be explicitly inserted, we make an attempt to take advantage of the information carried by the dual variables in order to select the sets of constraints to be fulfilled by the next generated configuration. A second difference is, instead of selecting a failure set F and then adding all the constraints associated with F (i.e., for all pairs of source and destination), we select an index subset FSD^k of $\mathcal{F} \times \mathcal{SD}$, i.e., FSD $= \{(F, (v_s, v_d)) : F \in \mathcal{F}, (v_s, v_d) \in \mathcal{SD}\}$, where k denotes the number of selected elements. Heuristic FIPP_MULFAIL_H2 is outlined in Figure 5.4 and its parameter settings in Table 5.II.

For the initial pricing problem, we order the elements of FSD in the decreasing order of the dual variables associated with constraints $(5.7)_{(F,(v_s,v_d))}$, so that FSD^k contains the indices of the constraints $(5.7)_{(F,(v_s,v_d))}$ with the dual variables (u^F_{sd})

Heuristic FIPP_MULFAIL_H2	
FSD is assumed ordered in the decreasing order of u_{sd}^F values	
Initial selection of FSD^k	add the constraints associated with the first $\|\mathcal{F}^1\| + \|L\|$ largest dual variables
ε	0.01
Stopping condition: t ε	 10 or 20 0.01 % of incumbent LP value
Enlargement of FSD^k	add the constraints associated with the next $.1 \times \|$ FSD $\|$ largest dual variables

Table 5.II: Parameter settings for heuristic FIPP_MULFAIL_H2

with the largest values. Note that those last variables are likely to minimize the most the reduced cost objective of the next pricing problem to be solved. Again, we have the configuration enlargement step with the elements of FSD ordered in the decreasing order of the dual variables u_{sd}^F (instead of the random permutation), as in Heuristic FIPP_MULFAIL_H1, and the enhanced reduced cost test.

For the stopping condition, we look at the progress of the decrease of the objective function (z^{OBJ}). Let ∇^{ITER} be the improvement (decrease) of the value of z^{OBJ} at iteration ITER. If $\nabla^{\text{ITER}} < \varepsilon'$ during the last t iterations, then we stop iterating. Otherwise, we enlarge the set FSD^k, adding in the next pricing problem a subset of constraints (those with index F, v_s, v_d) with the largest associated dual values u_{sd}^F. The size of the subset is a fraction p_2 of the size of FSD.

5.5.4 Finding an integer solution

Once the master problem has been optimally or heuristically solved, one has to derive an integer solution, ideally an optimal one, or otherwise, the best possible one. In order to get an optimal ILP solution, one should use a branch-and-price algorithm, which is usually much too costly from a computing point of view. Instead,

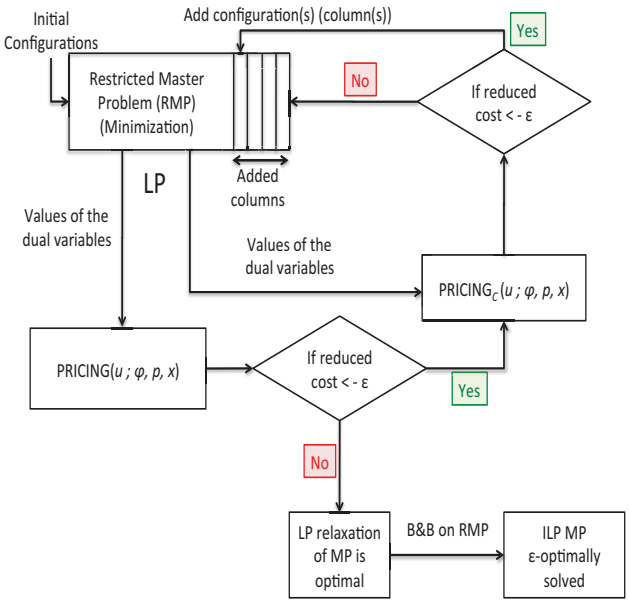

Figure 5.2: ILP & column generation algorithm

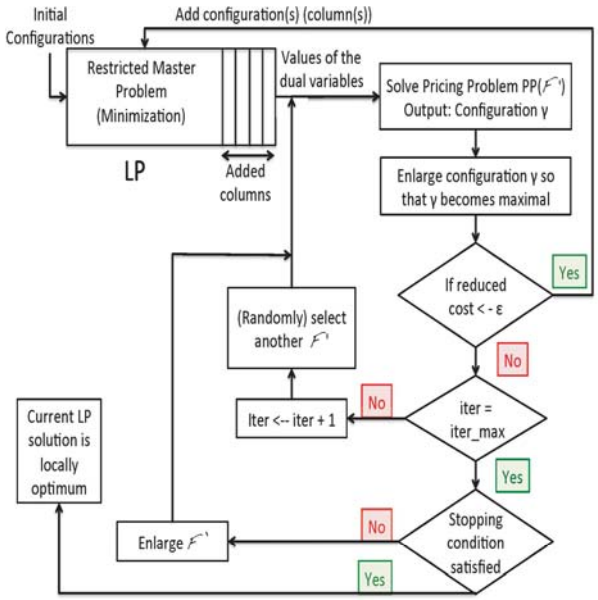

Figure 5.3: Heuristic 1

we propose to use a branch-and-bound (B&B) algorithm on the RMP made of the columns (i.e., variables) generated in order to get the optimal/heuristic solution of the linear relaxation of the master problem, see, e.g., [10] for more references.

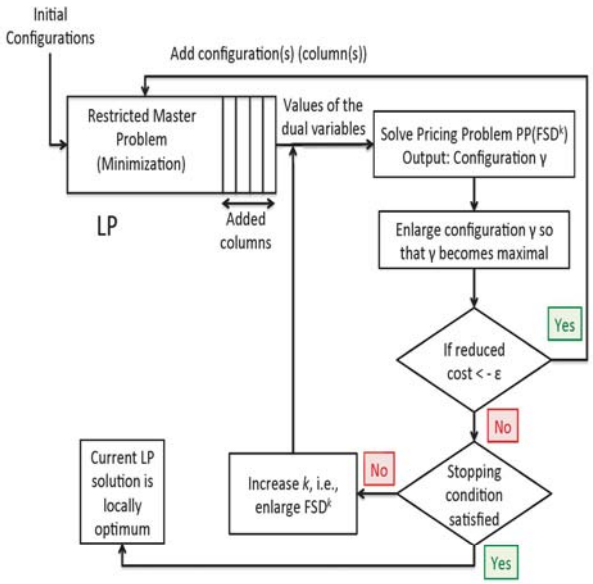

Figure 5.4: Heuristic 2

The integrality gap between the optimal ILP solution of the RMP and the optimal solution of the LP relaxation of the MP measures the accuracy of the ILP solution, and is defined as follows:

$$\text{GAP}(\%) = 100 \times \frac{\tilde{z}_{\text{ILP}^\star} - z^\star_{\text{LP}}}{\tilde{z}_{\text{ILP}^\star}}, \tag{5.20}$$

where $\tilde{z}_{\text{ILP}^\star}$ denotes the value of the obtained ILP solution, and $z^\star_{\text{LP}}$ denotes the optimal value of the linear relaxation of the master problem. Note that when the LP relaxation is solved heuristically, z^h_{LP} is not a valid lower bound. In order to get valid lower bound and then to get an optimality gap in order to estimate the accuracy of the ILP solution, one has to solve the LP relaxation with an additional constraint of the type

$$z^{\text{OBJ}} \leq z^h_{\text{LP}} - \varepsilon',$$

and identify the smallest possible value of ε' for which this latter LP (enriched with one constraint) has no feasible solution, in which case $z^h_{\text{LP}} - \varepsilon'$ is a valid lower bound on $z^\star_{\text{LP}}$.

5.6 Numerical results

This section presents the results of the article entitled "Robust FIPP p-cycles against dual link failures", accepted to *Telecommunications Systems* in 2012.

We describe the network and data instances in Section 5.6.1, and then discuss performances of the FIPP PP-FLOW model in the cases of single link failures (Section 5.6.2) and of dual link failures (Section 5.6.3). We also look at the increase of the bandwidth requirements when the number of protected pairs of links increases.

5.6.1 Network and data instances

We consider the benchmark network and data instances listed in Table 5.III for our numerical experiments. They are all from [58], except for the instances denoted by ATLANTA-2, COST239-2, US14N21S, which are taken from [67], and for the instance denoted by ELS, taken from [25]. For each network, we provide the number of nodes ($|V|$), the number of undirected links ($|L|$), the average node degree (d), the number of node pairs with requests ($|\mathcal{SD}|$), and the overall flow value ($\sum_{\{v_s,v_d\}\in\mathcal{SD}} d_{sd}$). Notice that the ATLANTA-1 and ATLANTA-2 data instances correspond to the same topology with different traffic flows, similarly for COST239-1 and COST239-2.

Network & traffic instances	$\|V\|$	$\|L\|$	d	$\|\mathcal{SD}\|$	$\sum_{\{v_s,v_d\}\in\mathcal{SD}} d_{sd}$
DFN-BWIN	10	45	9.00	45	548,388
COST239-1	11	25	4.55	55	432.5
COST239-2		26	4.73	55	176
PDH	11	34	6.18	24	4,621
POLSKA	12	18	3.00	66	9,943
NOBEL-US	14	21	3.00	91	5,420
US14N21S	14	21	3.00	91	2,710
ATLANTA-1	15	22	2.93	105	136,726
ATLANTA-2				105	74,470
ELS	20	40	2.67	57	96

Table 5.III: Description of network instances

5.6.2 Performance of the fipp pp-flow model - single link failure

As already mentioned in Section 5.4, the multiple failure model for FIPP p-cycle proposed in Section 5.5 differs from the previously proposed models for FIPP p-cycles ([45, 49, 67]). It is indeed more general in the sense that it is less constrained. For instance, the so-called Z-case is allowed (see [45] for its definition), and no restriction is made on disjointness of the working paths protected by a given FIPP p-cycle, see Table 5.IV for a summary of the assumptions in the key previous papers on FIPP p-cycles. The consequences, as illustrated by the results in Table 5.V, is some reduced bandwidth requirements.

	Model handles	
	Z-case	only link-disjoint requests for a given FIPP p-cycle
Kodian *et al.* [49]	✓	
Rocha *et al.* [45]		✓
Rocha *et al.* [65, 67]	✓	
Our Model	✓	✓

Table 5.IV: Comparison of FIPP p-cycle models

Experiments reported in Table 5.V have been made on the same network and traffic instances than in Rocha *et al.* [67] with exactly the same set of working paths (shortest paths). We observed that the reduction in the bandwidth requirements for protection against single link failure range from 5.6% for the ATLANTA-2 instance up to 12.9 % for the US14N21S instance, which is quite meaningful. In the particular context of the comparison, it corresponds to the bandwidth saving we can get when removing the assumptions of link disjoint requests for a given FIPP p-cycle. In addition, the optimality gaps are comparable between the two models, see the two columns entitled "Gaps". As observed in other experiments in the literature, the gap is relatively high for the COST239 instance (i.e., around 10%), but much smaller for the other instances (between 1% and 2%), and indeed optimal from a practical point of view.

Instances	FIPP p-cycles Model of [67]		FIPP PP-FLOW Model		Band-width
	z^{ILP}	Gaps	z^{ILP}	Gaps	Saving
ATLANTA-2	135,951	0.0	128,318	0.0	5.6 %
COST239-2	70,065	16.3	65,045	10.7	7.2 %
US14N21S	5,939,776	1.1	5,174,280	2.6	12.9 %

Table 5.V: Comparison of FIPP p-cycle models (single link failures)

5.6.3 Performance of the fipp pp-flow model - dual link failure

We first discuss the performance, i.e., solution accuracy and scalability, of the FIPP PP-FLOW model. We solved the FIPP PP-FLOW model for different values of dual failure rates (R_2), on different traffic and network instances of Table 5.III. Accuracy of the solutions are given in Table 5.VI, where we report the values of the optimality gaps, see formula (5.20). Those values are average values on the number of R_2 rate values (with a step size of 10) for which each particular instance was solved, within the time limit of 24 hours. Except for the COST239-1 and COST239-2 instances, solutions have been obtained with a very small optimality gap.

Instances	Range of R_2	Gaps
ATLANTA-1	[0, 60]	0.1
ATLANTA-2	[0, 40]	0.05
COST239-1	[0, 20]	12.2
DFN-BWIN	[0, 20]	0.01
NOBEL-US	[0, 30]	2.12
PDH	[0, 30]	1.41
POLSKA	[0, 70]	0.87
US14N21S	[0, 30]	2.57

Table 5.VI: Accuracy of the solutions

In Figure 5.5, we look at the ratio of the number of generated configurations over the number of selected configurations. Firstly, while there are a priori millions of possible configurations (i.e., overall number of cycles $\times$ number of combinations of cycles, while taking into account the number of ways to protect the failure

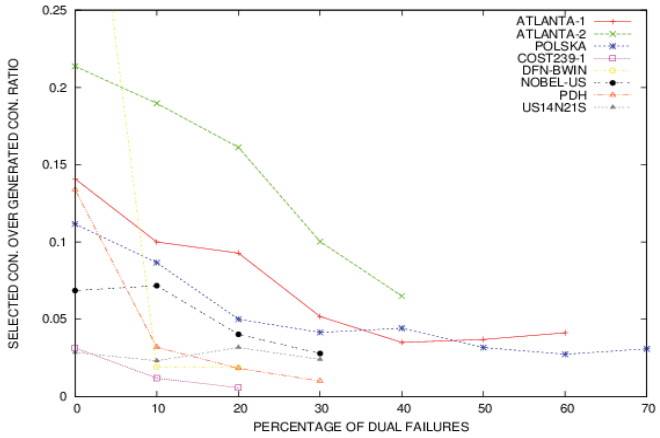

Figure 5.5: Number of generated/selected configurations

sets for each combination of cycles), only a very small number of them need to be generated, typically less than 0.1 %, e.g., 11,660 in the case of the POLSKA instance for $R_2 = 60\%$ while 319 were indeed selected for the protection scheme. Secondly, what we see in Figure 5.5, is that the number of selected configurations over the number of generated ones decreases while R_2 increases, typically from around 10% for $R_2 = 0$ to around 5% for $R_2 = 70\%$. It means that: *(i)* the number of generated configurations which are not selected remains reasonable with respect to the number of selected configurations, taking into account that the most time consuming part of the solution process is the solution of the pricing problems, especially the PRICING$(u; \varphi, p, x)$ ones, *(ii)* the decrease of the ratio translates that the configuration selection becomes more complex when R_2 increases, the search of sharable protection structures is more difficult.
Any improvement of the solution process should go with an attempt for reducing the number of generated configurations which do not belong to the final solution.

Figure 5.6 shows us the relationship between the percentage R_2 of protected dual failures and the protection bandwidth over the working bandwidth ratio. Note that when R_2 is equal to zero, it corresponds to the classical FIPP p-cycle protection scheme with 100% protection against single failures. Depending on the network connectivity, the capacity redundancy ratio can vary from a range of .6 (PDH topol-

ogy with a nodal degree of 6.18) to 1.3 (ATLANTA-1 topology with a nodal degree of 2.93) for $R_2 = 30\%$. When $R_2 = 60\%$, we observe an increase of the redundancy ratio leading to a range of values between 1.1 for POLSKA and 1.4 for ATLANTA-2. Such values for the redundancy ratio are much smaller than what has been observed with a p-cycle link protection scheme, see [75], i.e., bandwidth redundancy ratio values ranging from 2 to 4 for $R_2 = 60$ % depending on the traffic instances.

Instances	% dual failures	Exact solution			Heuristic solution			
					Random		Deterministic	
		z^{ILP}	Gap (%)	CPU (sec.)	z^{ILP}	CPU (sec.)	z^{ILP}	CPU (sec.)
POLSKA	0	11,175	.6	468	11,207	1,127	11,419	375
	20	20,081	.5	4,111	24,282	2,331	20,464	2,112
	50	21,518	.9	23,483	23,654	8,169	22.642	5,141
	100	24,111	1.4	86,829	31,452	12,834	34,770	5,291
ATLANTA-2	0	107,390	.6	4,165	107,776	2,985	107,391	1,770
	20	133,406	.9	10,486	133,601	17,810	135,291	5,551
	50	181,240	1.7	62,646	191,980	40,109	224,963	9,674
	100	220,592	1.6	128,157	228,508	81,127	263,605	32,721
ELS	10	177,802	-	24,119	203,584	12,316	175,895	8,778
	20	213,945	-	66,461	257,291	18,047	284,415	4,458
	50	343,165	-	438,460	465,462	26,683	484,346	25,528
	100	OUT OF MEMORY					570,425	34,981

Table 5.VII: Comparison of exact/heuristic solution of the PP-FLOW model

5.6.4 Comparative performance of the fipp_mulfail_h heuristics

Performance comparison of the heuristics and of the exact model is summarized in Table 5.VII. For both heuristics, we conducted many experiments in order to identify the best parameters values. The values for which we report the results are described in Tables 5.I and 5.II. Although the best parameters are not the same for each data instance, we selected the values for which we get the best performances at a whole, taking into account a reasonable compromise between the quality (i.e., accuracy) of the solutions and the computing times.

For single link failures, both heuristics are very efficient, as they reach an ε-optimal value with an accuracy of 1% in smaller computing times, or with larger

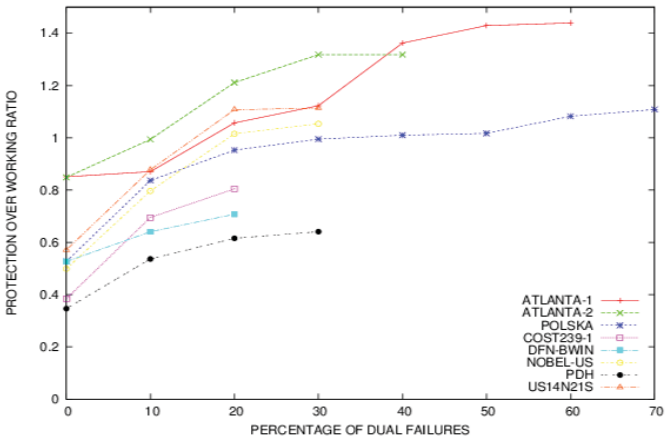

Figure 5.6: R_2 ratio vs. capacity redundancy

computing times (POLSKA instance with the FIPP_MULFAIL_H1 heuristic) than the ILP algorithm for the FIPP_MULFAIL model, but with a better accuracy (.5% instead of .6 %).

For dual link failures, there is a compromise to be made between the accuracy of the heuristic solution and the computing times. Moreover, there is no clear dominance of one heuristic over the other, although only the FIPP_MULFAIL_H2 heuristic is able to solve the ELS-4 instance (the largest one) in reasonable time: both alternate solutions fail due to lack of sufficient memory.

5.7 Conclusions

We proposed a new flow formulation for FIPP p-cycles subject to multiple failures, derived from a generic flow formulation for shared path protection, which resembles the model of Orlowsky and Pioro [57]. Although it corresponds to a column generation formulation, the pricing problem may have many constraints, and it is difficult to design an efficient exact algorithm to solve it. We therefore develop two heuristics in order to efficiently solve the pricing problems. Future work will include further investigations of the heuristic strategies in order to reach a better accuracy without increasing the computing times, and ultimately with multiple failure sets not limited to dual failure sets.

CHAPTER 6

CENTRALIZED AND DISTRIBUTED *P*-CYCLE PROTECTION SCHEME IN MULTI-DOMAIN OPTICAL NETWORKS

6.1 Chapter presentation

This chapter contains and merges the contribution of two articles. The first article entitled "*p*-Cycle based protection mechanisms in multi-domain optical networks" was published in the *Proceeding of the International Conference on Communications and Electronics (ICCE)* in August 2012, and the second article was published under the title of "A distributed *p*-cycle protection scheme in multi-domain optical networks" in *Proceeding of the IEEE Global Communications Conference (GLOBECOM 2012)*, December 2012.

Due to scalability issues, almost all previous studies focused on heuristics for solving the protection of multi-domain networks. In the first article, we propose a large scale optimization ILP centralized model, which allows the exact solution of quite large instances for the fist category of protection optimization problem: "*Best possible protected dimensioning*" (see Section 1.2). In a centralized model, it is assumed that the network management is aware of all the details of the physical topologies of the domains. The model relies on an hybrid protection scheme where *p*-cycles are used to protect the inter-domain links, while FIPP *p*-cycles are used for the protection of paths or subpaths in each individual domain. Extensive experiments were successfully conducted on a multi-domain network with 5 domains. Results show that the obtained optimality gaps are very small for all benchmark instances, meaning our solutions are all nearly optimal. Moreover, computing times are all very reasonable for a network planning tool.

Because protection in multi-domain networks is inherently a distributed problem in the sense that some relevant information to solve the problem is only available locally. In the second article, we propose and analyze a solution that satisfies

the assumptions under which optical multi-domain networks operate (see Section 2.5). It is based on a distributed representation of the protection problem into sub-problems which are then solved independently. We propose a model for the second category of protection optimization problem: *"Full protected dimensioning"* (see Section 1.2). In order to compare distributed solutions with an ideal exact solution, we adapted the previous optimization ILP centralized model to this problem. Experiments were successfully conducted on a multi-domain network with 5 domains. They include a comparison of bandwidth requirements between the proposed distributed scheme and a centralized scheme.

The chapter is organized as follows. Section 6.2 introduces notations and definitions. Optimization models for designing a protection scheme, for both a centralized and a distributed scheme, are proposed and detailed in Section 6.3 and 6.4 respectively. Solutions of the proposed models with large scale optimization tools are also discussed in these sections. Computational results are discussed in Section 6.5, where the centralized and distributed schemes are compared with respect to their bandwidth requirements. Section 6.6 concludes the chapter.

6.2 Notations and definitions

A multi-domain network is represented by a graph $G = (V, E)$ where V represents the set of nodes in the network and E represents the set of bi-directional physical links between pairs of nodes. Let D denotes the set of domains, with generic index d. The set V is partitioned into subsets V_d, $d \in D$, along the domains to which the corresponding nodes belong. We denote by $E^{\text{INTER}} \subset E$ the set of edges that represent bi-directional physical links between a pair of nodes that belong to two different domains. Consequently, $E \setminus E^{\text{INTER}}$ represents the set of links between pairs of nodes that belong to a same domain. Furthermore, as for the set V, $E \setminus E^{\text{INTER}}$ is partitioned into subsets E_d, $d \in D$, along the domains to which the physical links belong. It follows that:

$$V = \bigcup_{d \in D} V_d \quad \text{and } E = \left(\bigcup_{d \in D} E_d \right) \cup E^{\text{INTER}}. \tag{6.1}$$

The routing traffic over the multi-domain network is defined by a set K of aggregated requests (generic index k), where 1 unit corresponds to, e.g., an OC-192 (10 Gbps) or an OC-768 (40 Gbps) wavelength capacity. For each request $k \in K$, b_k denotes the required bandwidth (number of optical channels) while WP_k denotes the working route (i.e., shortest path) between the origin and destination nodes, which we denote respectively by s_k and d_k. We distinguish two types of requests: the *intra-domain requests* where the source and destination nodes are in the same domain and the *inter-domain requests* where the source and destination nodes are in different domains. Inter-domain requests are subdivided into a set of *intra-domain sub-requests* and a set of *inter-domain sub-requests* (see Figure 6.1), which are independently protected.

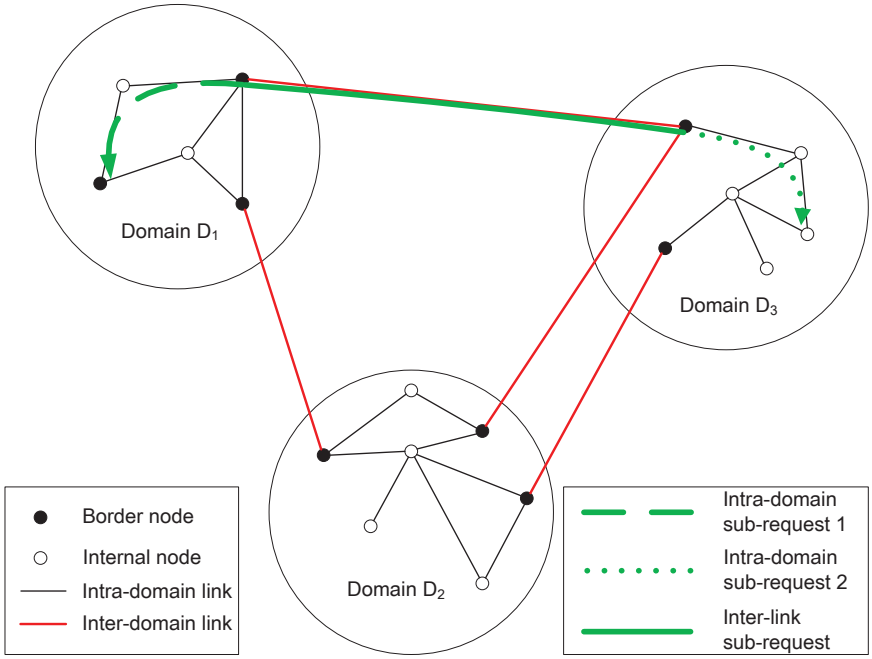

Figure 6.1: A multi-domain network

Once the routing of the working paths has been completed, let CAP_e^W be the

bandwidth requirement for working traffic on edge e, CAP_e^P the available spare capacity for protection on edge e, and b_κ the working demand traffic for the intra-domain sub-request κ.

In order to solve the protection problem in multi-domain networks, we propose a decomposition of this problem into a two-level protection scheme, where p-cycles are generated to protect the inter-domain links, and FIPP p-cycles are generated on each original domain to protect the intra-domain paths or segments. This is illustrated in Figure 6.2. The (dash followed by dot) red cycle connecting border nodes $v_1, v_2, \ldots, v_{10}$ in Figure 6.2 pictures a p-cycle which protects inter-domain physical links $\{v_3, v_4\}$ and $\{v_1, v_6\}$. Note that each inter-domain edge in a p-cycle is in an one-to-one mapping relation with an inter-domain physical link. FIPP p-cycles are represented by dash blue cycles.

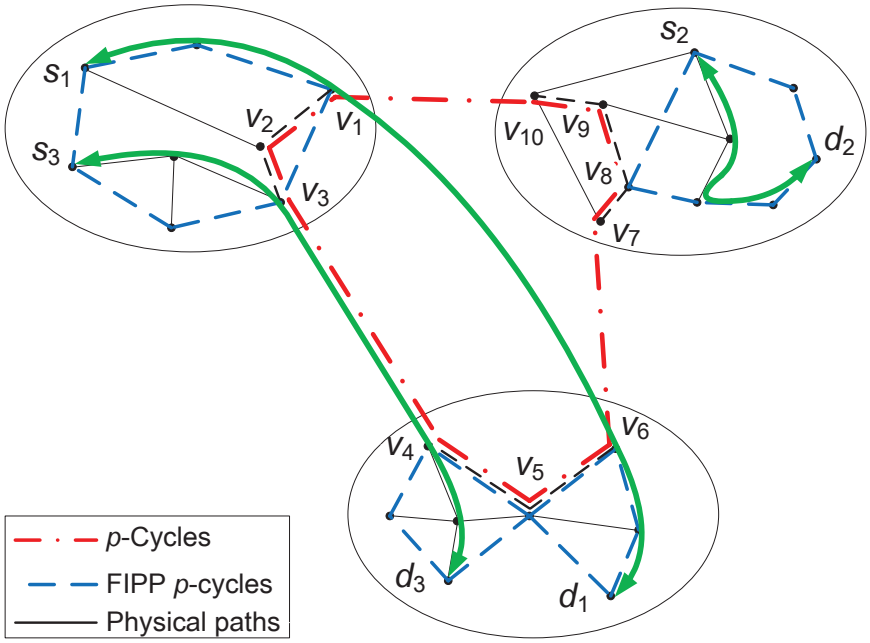

Figure 6.2: An illustration of the 2-level protection scheme

The models that we propose to compute the p-cycles that protect inter-domain links rely on an aggregated representation of multi-domain networks called *virtual network*. A virtual network derives in fact from an aggregation of the single do-

main networks that are part of a multi-domain network. Figure 6.3 illustrates the aggregation of a single domain network. A physical network is depicted in Figure 6.3(a). It comprises 5 nodes, of which three (1, 3, 5) are border nodes, and 6 physical links, each associated with an integer indicating its residual capacity. The corresponding single domain aggregated topology is represented by the solid lines in Figure 6.3(b). A virtual network $G^{\text{VIRTUAL}} = (V^{\text{BORDER}}, E^{\text{INTER}} \cup E^{\text{VIRTUAL}})$ is therefore defined by the set V^{BORDER} of border nodes in the multi-domain network, E^{INTER} the set of inter-domain links and E^{VIRTUAL} the set of so-called virtual edges, i.e., the solid lines that connect border nodes in single domain networks.

Note there is a virtual edge between each pair of border nodes belonging to a same domain and that each virtual edge is mapped to a physical path, the dashed lines in Figure 6.3(b). Each virtual edge has a capacity and cost which are calculated based on its associated path. For example, from the path $\{\{v_3, v_4\}, \{v_4, v_5\}\}$ associated with virtual edge $\{v_3, v_5\}$ we deduce the residual capacity $b_{\{v_3,v_5\}} = \min_{e \in p_{\{v_3,v_5\}}} c_e^{\text{res}} = 4$ and $\text{COST}_{\{v_3,v_5\}} = 2$. More generally, each virtual edge e' [1] must be mapped onto a physical path $p_{e'}$. The residual transport capacity of virtual link e', which is available for protection, denoted by $b_{e'}$, is given by $b_{e'} = \min_{e \in p_{e'}} c_e^{\text{res}}$, where e is a physical link and c_e^{res} is the residual spare capacity on physical link e, e.g., the bandwidth that remains available for the routing of the p-cycles once the FIPP p-cycles have been set, while taking bandwidth sharing into account. The value $\text{COST}_{e'}$ indicates the cost of the virtual edge e', e.g., the length of physical path $p_{e'}$ if we assume a cost proportional to the edge length.

The mapping of physical paths to virtual links is obtained through a k-shortest path algorithm. Weights or lengths of the edges, to be used in the k-shortest path algorithm, correspond to the (residual) spare transport capacities available for protection. We use this algorithm in both the centralized and the distributed models below. The difference between the two models lies in the order in which the mappings are computed. In the centralized scheme, the mapping of virtual/physical

1. We will use e' refer to virtual edge and e to physical link when defining the notations in multi-domain networks

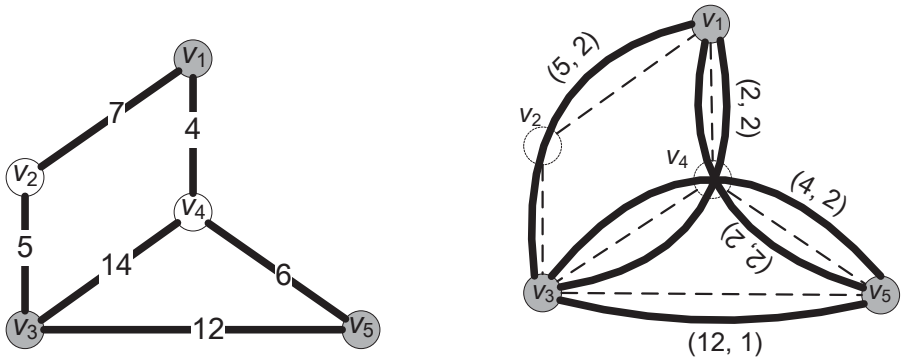

(a) Original Domain Network

(b) Virtual Aggregated Domain Network

Figure 6.3: An illustration of virtual aggregated topology

paths is computed prior to the computation of p-cycles as this model is based on the assumption that the detailed network information is available to all domains. On the other hand, in the distributed scheme, the mappings are independently computed after the computation of the p-cycles, which rises infeasibility issues in case the spare capacities are smaller than the bandwidth requirements. As will be seen in Section 6.4.2, we allow an increase of the transport capacities, with a penalty, in order to go around those infeasibility issues.

6.3 Centralized model

Protection in multi-domain networks is inherently a distributed problem in the sense that some relevant information to solve the problem is only available locally. As many inherently distributed problems, the exact solution may not be computable. However, the problem has distributed approximate solutions. In order to compare distributed solutions with an ideal exact solution, this section makes abstraction of the conditions that prevent the computation of exact solutions, and propose an ILP centralized model to compute such exact solution. This centralized model makes abstraction of the main condition that prevent exact solutions, i.e., it is assumed that the network management is aware of all the details of the physical topologies of the domains. We propose a model for the first category of protection

optimization problem: *"Best possible protected dimensioning"*

In the description of this model, we first introduce the concept of *configurations* which is central to the model, and which represent mappings between p-cycles, FIPP-p-cycles and the inter-domain links or intra-path segments they protect in a given solution. There is also a similar notion of configuration for virtual links. Next we describe the variables of the model, its objective function and constraints. Finally, we propose a column-generation approach that solves exactly this model.

6.3.1 Configurations

p-Cycle Configurations.

Each such configuration is associated with a p-cycle and the subset of inter-domain links protected by that p-cycle. Let C be the overall set of potential p-cycle configurations in the virtual (aggregated) network G^{VIRTUAL}. Any $c \in C$ is characterized by vector $\alpha^c = (\alpha_e^c)_{e \in G^{\text{VIRTUAL}}}$ where $\alpha_e^c \in \{0, 1, 2\}$ represents the protection provided by p-cycle c for link e: $\alpha_e^c = 1$ if e lies on cycle c, $\alpha_e^c = 2$ if e straddles cycle c, and $\alpha_e^c = 0$ otherwise. Similarly, parameter $\overline{\alpha}_e^c \in \{0, 1\}$ is such that $\overline{\alpha}_e^c = 1$ if e lies on cycle c, and 0 otherwise.

FIPP p-Cycle configurations.

Each such configuration consists in one FIPP p-cycle and the traffic (intra-domain requests and sub-requests) it protects in a given single domain. Let F_d be the overall set of potential FIPP p-cycle configurations in domain d. Any $f \in F_d$ is characterized by vector $\beta^f = (\beta_\kappa^f)_{\kappa \in K_d}$ where $\beta_\kappa^f \in \{0, 1, 2\}$ defines the level of protection (the number of protection paths) provided by the FIPP p-cycle associated with f for intra-domain segment κ. Similarly parameter $\overline{\beta}_e^f \in \{0, 1\}$ is such that $\overline{\beta}_e^f = 1$ if e lies on the cycle associated with configuration f, and 0 otherwise.

Path Configurations.

They are only defined in the centralized scheme. Therein, for each virtual intra-domain edge $e' \in E^{\text{VIRTUAL}}$, the set of path configurations for the mapping of e' onto

an intra physical path is characterized by: $\gamma_e^p \in \{0,1\}$ such that $\gamma_e^p = 1$ if physical link e lies on path p, 0 otherwise.

6.3.2 Variables

For both generalized and distributed schemes, there are three sets of variables which keep track of the number of copies of selected configurations: z^c for the number of unit-capacity copies of p-cycle configuration c, z^f for the number of unit copies of FIPP p-cycle configuration f, and z^p for the amount of bandwidth associated with the mapping of virtual link e onto the physical path $p \in P$.

6.3.3 Objective function

The objective function consists in minimizing the overall spare capacity cost for protection, i.e., the sum of the p-cycle spare capacity for the protection of the inter-links, of the FIPP p-cycle spare capacity for the protection of the intra-requests (or sub-requests). Indeed, such capacity corresponds to the sum of the required bandwidth by p-cycles on inter-domain links, by FIPP p-cycles on intra-domain links, and by the mappings of the virtual links to physical paths belonging to p-cycles. It can be written as follows:

$$\min \quad \sum_{c \in C} \sum_{e \in E^{\text{INTER}}} \overline{\alpha}_e^c c_e z^c + \sum_{d \in D} \sum_{f \in F_d} \text{COST}_f \, z^f + \sum_{e' \in E^{\text{VIRTUAL}}} \sum_{p \in P_{e'}} \text{COST}_p z^p, \qquad (6.2)$$

where c_e designates the unit spare capacity cost of link e, $\text{COST}_f = \sum_{e \in E_d} \overline{\beta}_e^d$ and $\text{COST}_p = \sum_{e \in E_d} c_e \gamma_e^p$.

6.3.4 Constraints

Constraints can be written as follows:

$$\sum_{c \in C} \alpha_e^c z^c \geq b_{e'^i}^{\text{REQ}} \qquad e \in E^{\text{INTER}} \tag{6.3}$$

$$\sum_{c \in C} \overline{\alpha}_e^c z^c \leq b_{e'}^{\text{RES}} \qquad e \in E^{\text{INTER}} \tag{6.4}$$

$$\sum_{f \in F_d} \beta_\kappa^f z^f \geq b_\kappa \qquad \kappa \in K_d, d \in D \tag{6.5}$$

$$\sum_{e \in E_d^{\text{VIRTUAL}}} \sum_{p \in P} \gamma_e^p z^p + \sum_{f \in F_d} \overline{\beta}_e^f z^f \leq b_e^{\text{RES}} \qquad e \in E_d, d \in D \tag{6.6}$$

$$\sum_{p \in P} z^p - \sum_{c \in C} \overline{\alpha}_e^c z^c \geq 0 \qquad e \in E_d^{\text{VIRTUAL}}, d \in D \tag{6.7}$$

$$z^c \in \mathbb{Z}^+ \qquad c \in C \tag{6.8}$$

$$z^f \in \mathbb{Z}^+ \qquad f \in F = \bigcup_{d \in D} F_d \tag{6.9}$$

$$z^p \in \mathbb{Z}^+ \qquad p \in P, e \in E_d^{\text{VIRTUAL}} \tag{6.10}$$

Constraints (6.3) ensure that the working traffic on each inter-domain link is fully protected by p-cycles. Constraints (6.4) ensure that the required bandwidth by p-cycles on an inter-domain link is smaller than its residual capacity. Constraint (6.5) guarantee a FIPP p-cycle protection for each intra-domain segment. Constraints (6.6) ensure that the amount of bandwidth requested from an intra-domain link $e \in G$ by the mapping of virtual links to physical paths and for the protection provided by FIPP p-cycles does not exceed the residual capacity of link e. Constraints (6.7) check that enough spare capacity is available for the mapping of virtual link e' to one or more physical paths in order to carry the traffic of the p-cycles using link e'.

6.3.5 Solution of the ILP model

A straightforward way to solve the ILP model of the previous would be to enumerate all potential configurations, for the p-cycles, the FIPP p-cycles and the intra paths. Although easy, it will not be scalable. Indeed, the ILP model of Section 6.3 has a natural decomposition scheme which allows its linear relaxation to be solved by column generation techniques, see Section 2.6.1 for the "*base*" framework of ILP & column generation algorithm.

The previous optimization model corresponds to a master problem with three different pricing problems, one for p-cycle generation, one for FIPP p-cycle generation and one for the mapping of virtual links to physical paths. Formulations of the pricing problems are defined as follows:

p-Cycle generation pricing problem

The pricing problem, denoted by PP(c) for $c \in C$, corresponds to the optimization problem of minimizing the reduced cost (with respect to linear programming definition) subject to the constraints that must be satisfied by a given configuration, which are: definition of a cycle, identification of the inter-domain sub-requests that can be protected by the cycle, prohibition for a span to be used as a working and a protection span at the same time for the same demand.

The reduced cost objective, REDCOST_c, depends on dual variables $u_e^{(6.3)}$, $u_e^{(6.4)}$, and $u_{e'}^{(6.7)}$ associated with constraints (6.3), (6.4), and (6.7) respectively:

$$\text{REDCOST}_c = \sum_{e \in E^{\text{INTER}}} x_e^c c_e - \sum_{e \in E^{\text{INTER}}} (2s_e^c - x_e^c) u_e^{(6.3)} + \sum_{e \in E^{\text{INTER}}} x_e^c u_e^{(6.4)} + \sum_{e' \in E^{\text{VIRTUAL}}} x_{e'}^c u_{e'}^{(6.7)}. \quad (6.11)$$

where $x_e^c = 1$ if link e supports the sought cycle in configuration c, 0 otherwise; $s_e^c = 1$ if link e is protected by configuration c, and 0 otherwise. Column coefficients associated with c are then deduced as follows: $\alpha_e^c = 2s_e^c - x_e^c, \overline{\alpha}_e^c = x_e^c$. For the set

of constraints, refer to [66].

FIPP *p*-cycle generation pricing problem

The pricing problem, denoted by PP(f, d) for $f \in F_d$, $d \in D$, is set and and solved for a given domain d. Indeed, it consists in definding a cycle and dentification of the intra-domain sub-requests that can be protected by the cycle while optimizing a reduced cost objective.

The reduced cost objective, REDCOST_{fd}, can be expressed using $u_{\kappa d}^{(6.5)}$ and $u_{ed}^{(6.6)}$, the dual variables associated with constraints (6.5) and (6.6):

$$\text{REDCOST}_{fd} = \sum_{e \in E_d} c_e x_e^f - \sum_{\kappa \in K_d} (s_\kappa^f + w_\kappa^f) u_{\kappa d}^{(6.5)} + \sum_{e \in E_d} x_e^f u_{ed}^{(6.6)} \,. \tag{6.12}$$

where $x_e^f = 1$ if and only if link e belongs to the FIPP p-cycle associated with configuration f, $s_\kappa^f = 1$ if and only if working sub-path κ is protected, and $w_\kappa^f = 1$ if and only if working sub-path κ is protected and straddles cycle associated with f. Column coefficients associated with f, d are then deduced as follows: $\beta_\kappa^f = s_\kappa^f + w_\kappa^f, \overline{\beta}_e^f = x_e^f$. For the set of constraints, refer to [67].

Path generation pricing problem

The pricing problem, denoted by PP(p, e', d) for $p \in P_{e'}$, $e' \in E_d^{\text{VIRTUAL}}$, $d \in D$, is set and solved for a given virtual link e'. It consists in finding a physical path $p \in P_{e'}$ to map virtual link e' with minimum reduce cost.

The reduced cost objective, $\text{REDCOST}_{e'pd}$, can be expressed using dual variables $u_{e'd}^{(6.6)}$ and $u_e^{(6.7)}$ from constraints (6.6) and (6.7):

$$\text{REDCOST}_{epd} = -u_{e'd}^{(6.6)} + \sum_{e \in E_d} \gamma_e^p c_e + \sum_{e \in E_d} \gamma_e^p u_e^{(6.7)} \tag{6.13}$$

subject to:

$$\sum_{e \in \omega(v)} \gamma_e^p = 2d_v \qquad v \in V_d \setminus \{o_e, d_e\} \tag{6.14}$$

$$\sum_{e \in \omega(o_e)} \gamma_e^p = \sum_{e \in \omega(d_e)} \gamma_e^p = 1 \tag{6.15}$$

$$\gamma_e^p \in \{0, 1\} \qquad e \in E_d \tag{6.16}$$

$$d_v^p \in \{0, 1\} \qquad v \in V_d. \tag{6.17}$$

where $\gamma_e^p = 1$ if physical link e lies on path p, $d_v^p = 1$ if path p goes through node v.

All nodes which are on the physical path p are required to have two incident links, which is ensured by constraints (6.14). Constraints (6.15) arrange for the generation of at most one physical path in order to map virtual link e'.

6.3.6 Column generation algorithm

As part of the input data, we assume working paths have been computed for all inter/intra-domain requests, and that the working paths for inter-domain requests are decomposed into *inter-domain sub-requests* and *intra-domain sub-request*.

The general framework of the proposed column generation algorithm is depicted in Figure 6.4. Initially, the algorithm starts with a set of artificial (dummy) columns, one for each *inter-domain sub-request* or *intra-domain sub-request*, leading to the definition of the so-called Restricted Master Problem (i.e., (6.2)-(6.10) with a restricted set of configurations made of the set of initial columns). Then, the Restricted Master Problem (RMP) is solved and its optimal dual values are used to guide the pricing problems searching for new configurations with negative reduced cost. These new configurations are added to the current RMP and the current RMP is optimally solved again until the reduced costs of all pricing problems are positive, meaning that the optimal solution of the continuous relaxation of the master problem has been obtained. Note that the pricing problems do not need to be solved exactly as long as we are able to find a new configuration with a

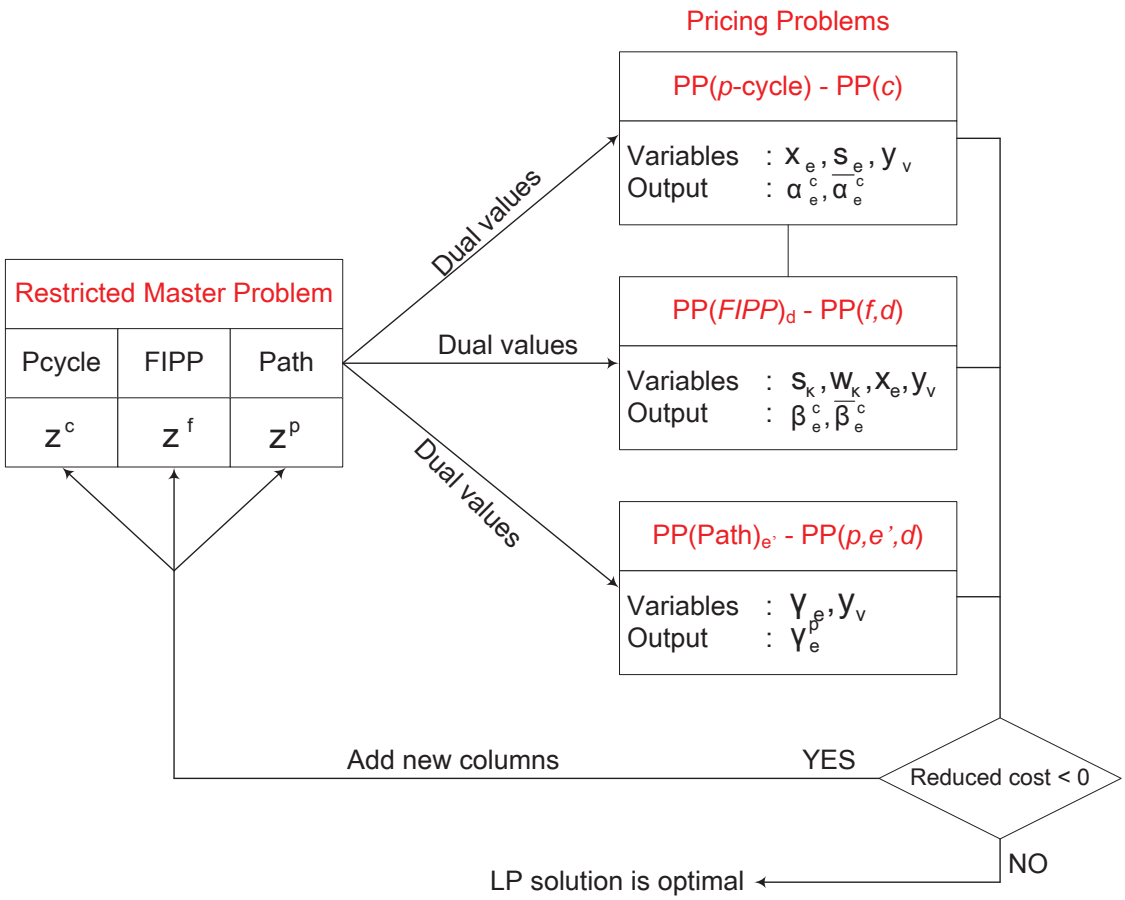

Figure 6.4: Flowchart of the column generation algorithm

negative reduced cost for improving the solution of RMP. This approach does not hamper the optimality of the master problem solution, instead, it often speeds up the solution process.

Once the optimal solution of the linear relaxation of the master problem has been reached, we solve the ILP formed of the columns generated for reaching the optimal solution of the master problem. It can be done using, e.g., the CPLEX package.

6.4 Distributed model

In this section, we propose and analyze a solution that satisfies the assumptions under which optical multi-domain networks operate, see, e.g., [28]. It is based on a distributed representation of the protection problem into sub-problems which are then solved independently. As for the centralized model, inter-domain working traffic is protected with p-cycles and intra-domain working traffic is protected with FIPP p-cycles. We propose a model for the second category of protection optimization problem: *"Full protected dimensioning"*.

6.4.1 Outline

The distributed model relies on the usual assumption that each domain is not aware of the details of the physical topologies of the other domains. Consequently, the upper management of the overall multi-domain optical network relies on the virtual network, assuming each domain provides a virtual link satisfying the bandwidth requirements (and the quality of service parameters) provided by upper management entity.

The distributed model is depicted in Figure 6.5. Initially, FIPP p-cycles solutions are independently generated in each domain, in order to protect intra-domain (sub-)requests. Then, virtual links are mapped onto intra-domain physical paths to obtain some initial values for their cost and residual/spare capacity. Next, there is an iterative process such that, each iteration ends with the computation of a p-cycle solution that protect the inter-domain working traffic given the current FIPP p-cycles solutions and intra-domain residual capacities allocated to the virtual links. If a feasible solution (with respect to the available transport capacities) can be found, a new iteration is initiated, with the release of the spare bandwidth amounts of the intra-domain links after the mapping of the virtual links onto the physical domain topologies capacities, resulting from the current p-cycle solution. FIPP p-cycles are then possibly updated in order to optimize the bandwidth usage, while taking into account the current available spare transport capacities. Last,

the mapping of the virtual links onto the physical domain topologies are revised. It leads to new residual capacity and cost for each virtual link. The value of the objective function (overall bandwidth requirements for the p-cycle and FIPP p-cycle protection structures), z^t_{OBJ} where t is the iteration index, is re-evaluated.

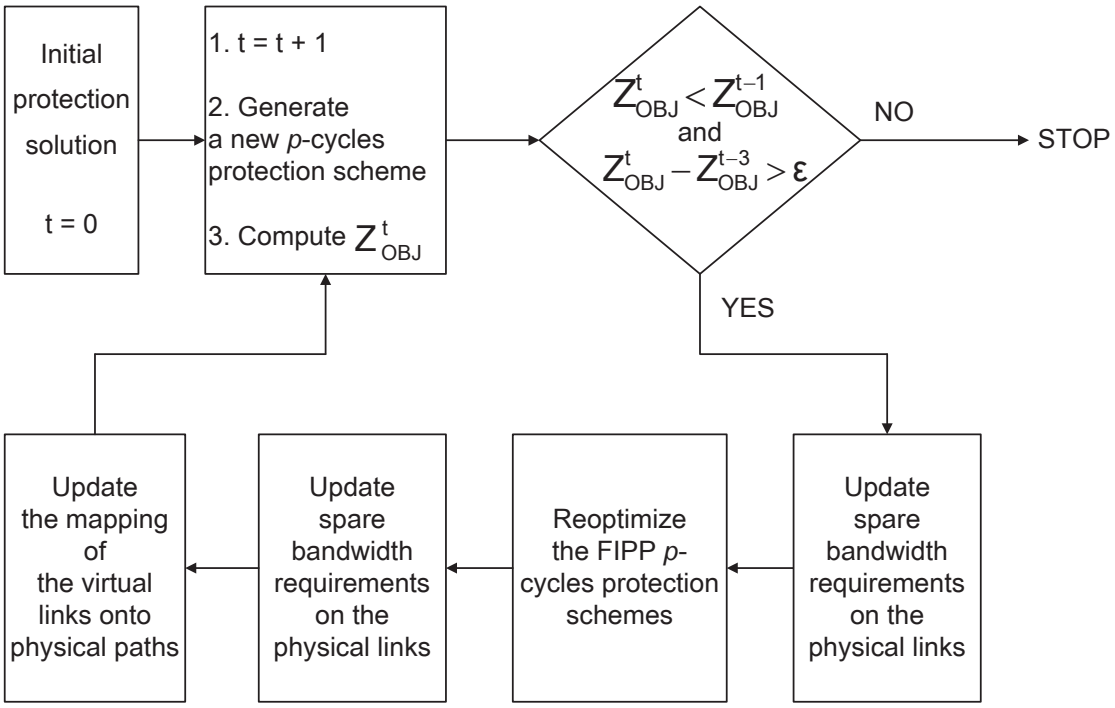

Figure 6.5: Flowchart of the distributed solution process

The computation of p-cycles requires the knowledge of the cost and capacity of the virtual links. These latter values are computed by a k-shortest path [2] algorithm that maps the virtual links onto physical paths. The computation of the FIPP p-cycles requires the knowledge of how much bandwidth is used by the p-cycles in a given domain. These values are obtained directly from the computation of the p-cycles. Therefore, the proposed distributed scheme satisfies the multi-domain network assumptions regarding the limitations on inter-domain sharing of operational information, i.e., do not assume any inter-domain information in detail sharing.

2. $k = 2$ in our numerical experiments

6.4.2 Optimization model

This section proposes the mathematical models for the placement of p-cycle structures protecting *inter-domain sub-requests* as well as FIPP p-cycle structures protecting *intra-domain sub-requests*.

The mathematical models rely on the concept of configurations and the set of variables which we define in Section 6.3. There is one more set of variables $(\text{ADD}_e)_{e \in E}$, which estimate the amount of required additional bandwidth, if any, in order to protect all demand requests, on every link e.

6.4.2.1 *p*-Cycle model

p-Cycles are computed on the virtual network in order to offer a protection to the *inter-domain links*. The p-cycle objective function aim at minimizing the spare capacity cost and added capacity for p-cycle protection. It can be written as follows :

$$\min \sum_{e \in E^{\text{INTER}} \cup E^{\text{VIRTUAL}}} \left(\sum_{c \in C} \overline{\alpha}_e^c \, \text{COST}_e \, z^c + \text{PENAL} \times \text{ADD}_e \right). \tag{6.18}$$

where COST_e designates the unit spare capacity cost of link e and PENAL is a penalty coefficient in order to discourage the addition of bandwidth in order to ensure the protection of all requests, i.e., favour the use of the available transport capacity even if it means longer cycles.

The set of constraints is made of constraints (6.3) and (6.4).

6.4.2.2 FIPP *p*-cycle model

FIPP p-cycles are constructed in each domain to protect *intra-domain requests* and *intra-domain sub-requests*. Their objective function aims at minimizing the spare capacity cost and added capacity induced by FIPP p-cycle protection. It is

written as follows:

$$\min \quad \sum_{f \in F_d} \text{COST}_f z^f + \text{PENAL} \sum_{e \in E_d} \text{ADD}_e \tag{6.19}$$

Constraints can be written as follows:

$$\sum_{f \in F_d} \beta_\kappa^f z^f \geq b_\kappa \qquad \kappa \in K_d, d \in D \tag{6.20}$$

$$\sum_{f \in F_d} \overline{\beta}_e^f z^f \leq \text{CAP}'^P_e + \text{ADD}_e \quad e \in E_d \tag{6.21}$$

$$z^f \in \mathbb{Z}^+ \qquad f \in F_d. \tag{6.22}$$

where $\text{COST}_f = \sum_{e \in E_d} \text{COST}_e \, \overline{\beta}_e^f$ and $\text{CAP}'^P_e = \text{CAP}^P_e$ - bandwidth requirement for the p-cycles. Constraints (6.20) guarantee a FIPP p-cycle protection for each intra-domain segment. Constraints (6.21) ensure that the required bandwidth by FIPP p-cycles on an intra-domain link is smaller than its residual capacity (i.e., the available spare capacity for protection minus the bandwidth required by the p-cycles) and added capacity.

6.4.3 Solution of the ILP model

We use the column generation method to solve the ILP models (see Section 2.6.1 for the "*base*" framework of ILP & column generation algorithm). There are two CG-ILP models in the distributed scheme: one for p-cycle and another for FIPP p-cycle. The optimization models of Section 6.4.2.1 and Section 6.4.2.2 are respectively the master problems for the p-cycle CG-ILP and for the FIPP p-cycle CG-ILP. Formulations of the all pricing problems can easily be derived from some previous column generation models designed for single domain optical networks, see [66] for p-cycles and [67] for FIPP p-cycles.

6.5 Computational results

6.5.1 Results of the centralized scheme

This section presents the results of the centralized scheme. Network and data instances are described in Section 6.5.1.1, followed by the performances of the proposed model in Section 6.5.1.2 (quality of the solutions) and Section 6.5.1.3 (protection characteristics).

6.5.1.1 Network and data instances

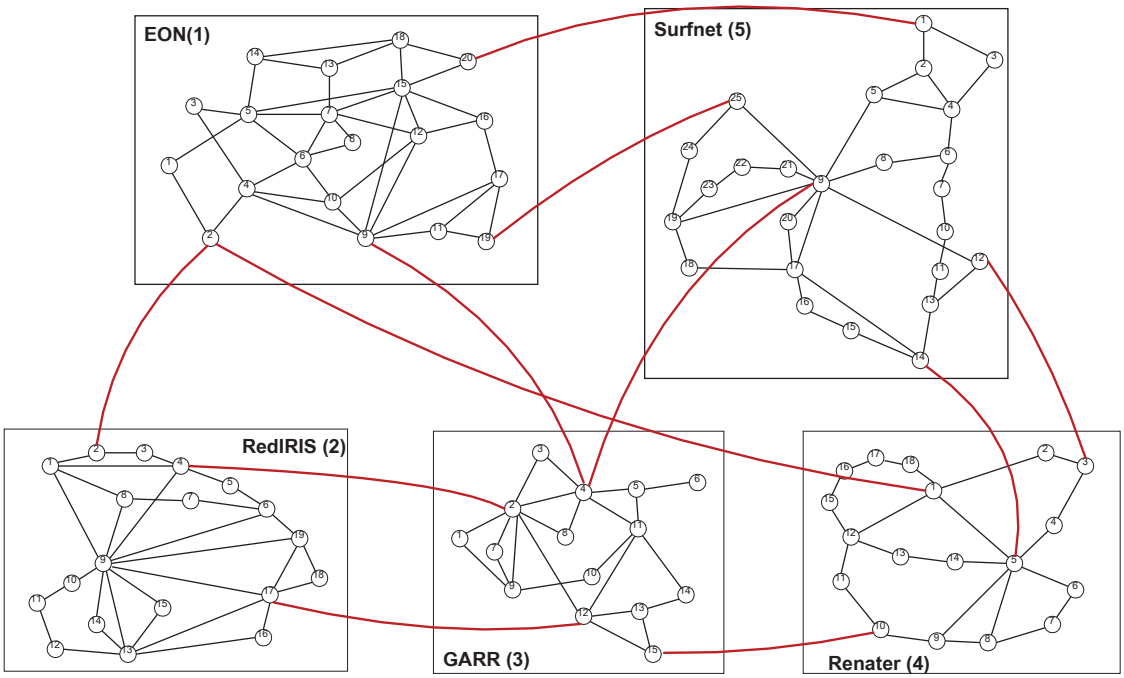

Figure 6.6: Multi-domain network used in the experiments

The multi-domain network is built from 5 real optical networks EON [56], Garr [2], Renater [4], Surfnet [5], RedIrid [3]. The numbers of nodes and links of each network are: EON (20, 39), Garr (15, 24), Renater (18, 23), Surfnet (25, 34), RedIrid (19, 31). For each optical network, we set up to 4 border nodes as well as inter-links in order to connect the border nodes from different domains such

that the degree of each border node is 1, 2 or 3. The topology of the resulting multi-domain network is depicted in Figure 6.6.

Instances	$\|K\|$	Number of requests													
		Initial							After working path routing						
			Intra							Intra					
		Inter	EON	IRIS	GARR	RENATER	SURFNET	Σ	Inter	EON	IRIS	GARR	RENATER	SURFNET	Σ
1	100	86	2	2	4	3	3	14	11	19	35	33	41	31	159
2	100	79	4	6	2	5	4	21	11	15	39	24	42	22	142
3	100	83	3	5	2	3	4	17	10	23	39	19	33	29	143
4	100	90	1	5	0	1	3	10	11	143	24	37	22	37	143
5	200	171	5	5	7	7	5	29	11	42	72	53	76	60	303
6	200	163	7	11	4	8	7	37	11	37	77	43	73	48	278
7	200	177	5	11	2	2	3	23	11	45	76	40	67	53	281
8	200	173	4	7	8	3	5	27	11	55	79	54	73	55	316
9	200	174	6	8	5	3	4	26	10	48	74	41	71	59	293
10	500	431	10	20	10	15	14	69	11	96	178	112	174	124	684
11	500	441	12	19	12	7	9	59	11	113	176	102	161	140	692
12	1,000	885	20	34	19	21	21	115	11	196	297	191	321	232	1,237

Table 6.I: Characteristics of the request sets

Experiments are conducted on sets of 100, 200, 500, and 1,000 requests. Requests have been randomly generated with a demand bandwidth in {OC-1, 3, 6, 9, 12}. Working paths are established using a shortest path algorithm. Once working routing is completed, we can define the set of inter-link requests that will be protected by p-cycles and the sets of intra-domain (sub-)requests which will be protected by FIPP p-cycles in each domain. The distribution of the various links is described in Table 6.I.

6.5.1.2 Performance evaluation : quality of the solution

Quality of solutions can be measured by the optimality gap, as defined in Section 2.6.1. As shown in Table 6.II, the obtained optimality gaps are very small for all benchmark instances, meaning our solutions are all nearly optimal. Moreover, the overall computation times, see column entitled CPU in Table 6.II are all very reasonable for a network planning tool.

Instances	z^{LP}	z^{ILP}	Gap (%)	CPU times (sec.)	Number of generated/selected configurations						
					Inter	Intra					Σ
						EON	IRIS	GARR	RENATER	SURFNET	
1	5,844.3	5,888	0.74	507	40	23/16	49/30	52/15	54/14	41/23	357
2	4,512.3	4,745	0.69	566	35	20/16	74/30	35/15	33/14	33/23	328
3	5,263.8	5,334	1.33	531	30	27/16	67/30	26/15	27/14	42/23	317
4	4,995.5	5,052	1.13	490	36	32/16	65/30	33/15	44/14	43/23	351
5	11,079.0	11,160	0.73	5,492	63	91/16	113/30	118/15	128/14	93/23	704
6	9,140.0	9,235	1.03	3,199	42	45/16	136/30	76/15	62/14	60/23	519
7	10,433.0	10,530	0.92	1,232	36	71/16	124/30	73/14	86/14	100/23	587
8	12,008.0	12,283	2.29	3,049	47	75/16	171/30	103/15	89/14	95/24	679
9	10,920.0	11,163	2.22	2,765	35	62/16	160/30	60/14	89/14	71/24	575
10	24,779.8	25,048	1.08	13,420	39	138/16	286/30	197/15	292/14	167/23	1,217
11	25,516.5	26,082	2.21	11,838	27	118/16	444/30	157/15	202/14	200/23	1,246
12	43,471.0	43,890	0.96	76,987	57	258/16	606/30	351/15	626/14	440/24	2,437

Table 6.II: Quality of the solutions

Table 6.II also shows the number of generated configurations, whether p-cycle or FIPP p-cycle ones, or physical paths mapping intra-domain virtual links. We observe that only a very small number of configurations are generated while there are millions of possible configurations, thanks to the column generation technique which allows reaching an optimal solution of the linear relaxation without the requirement of an explicit enumeration of all the configurations. The number of selected configurations, which are part of the near optimal ILP solutions, is even smaller as can be observed in Table 6.II.

6.5.1.3 Performance evaluation : protection characteristics

In Table 6.III, we provide the number of unit p-cycles selected in the optimal integer solution along with the overall number of p-cycle occurrences (overall number of p-cycle copies as given by $\sum_{c \in C} z^c$) which are required in order to guarantee the protection of all the inter-domain links.

	# configurations		
Instances	generated	selected	occurrences
1	40	9	92
2	35	8	58
3	30	6	66
4	36	8	101
5	63	9	154
6	42	8	151
7	36	7	180
8	47	8	272
9	35	7	153
10	39	10	381
11	27	7	415
12	57	9	533

Table 6.III: Inter-domain link protection.

For the protection of the intra-domain segments, we provide the details of the results for domain EON in Table 6.IV. It contains the number of unit FIPP p-cycles and unit paths used for mapping the virtual intra-domain links. Furthermore, the overall number of FIPP p-cycle and physical path occurrences are reported in the

Instances	# configurations					
	generated		selected		occurrences	
	FIPP	Path	FIPP	Path	FIPP	Path
1	23	16	17	3	69	134
2	20	16	13	2	38	101
3	27	16	17	4	59	133
4	32	16	23	2	98	75
5	91	16	38	3	164	197
6	45	16	32	2	97	82
7	71	16	40	3	219	158
8	75	16	50	3	264	190
9	62	16	44	3	293	231
10	138	16	85	3	331	477
11	118	16	86	2	406	377
12	258	16	165	2	613	640

Table 6.IV: Intra-domain segment protection

two last columns of the table.

6.5.2 Results of the distributed scheme

This section presents the results of distributed scheme. The network and data instances are described in Section 6.5.2.1, and then performances of the proposed model are discussed in Section 6.5.2.2 and Section 6.5.2.3.

The transport capacity values were set as follows. Let CAP_e^W be the bandwidth requirements on link e for the primary paths (working routing of the requests). Then, the spare capacity values for the protection requirements were set as follows:

$$\text{Inter Links} : \text{CAP}_e^P = 1.5 \times \text{ALEA}\{\text{CAP}_e^W - 20\%, \text{CAP}_e^W + 20\%\}$$
$$\text{Intra Links} : \text{CAP}_e^P = 2 \times \text{ALEA}\{\text{CAP}_e^W - 20\%, \text{CAP}_e^W + 20\%\}$$

where $\text{ALEA}\{a, b\}$ randomly generates either a or b.

In order to compare the solutions between centralized and distributed model, we adapt the optimization ILP centralized model proposed in Section 6.3 to the problem *"Full protected dimensioning"* (see Section 6.7).

6.5.2.1 Network and data instances

We use the multi-domain network as Section 6.5.1.1.

(a) Initial inter/intra domain request distribution

(b) Inter/Intra domain sub-request distribution after primary routing completion

Figure 6.7: Traffic characteristics before/after primary routing

Experiments are conducted on sets of 100 up to 1,000 requests, which are generated between randomly selected pairs of nodes with bandwidth requirement varying in OC-1, 3, 6, 9, 12. We used a shortest path routing for the primary routes. Once primary routing is completed, we are left with a set of inter-link sub-requests (see Section 6.2 for the definitions) that will be protected by p-cycles and a set of intra-domain sub-requests that will be protected by FIPP p-cycles in each domain. This distribution of the links are described in Figure 6.7 for each of the 12 traffic instances we generated. Instances 1 to 4 contain 100 requests, instances 5 to 9: 200 requests, instances 10 and 11: 500 requests, instance 12: 1,000 requests.

6.5.2.2 Performance evaluation : quality and comparison of the solutions between centralized and distributed model

Accuracy of the solutions can be measured by the optimality gap, as defined in Section 2.6.1. As shown in Table 6.V, the obtained optimality gaps are very small for all benchmark instances, meaning our solutions are all nearly optimal. In Tables 6.VI and 6.VII, we can see that the column generation solution scheme is quite efficient for both the centralized and the distributed schemes: not only very

Traffic Instances	Centralized Scheme					Distributed Scheme					Comparison
	z_C^{LP}	z_C^{ILP}	Gap (%)	ADD (%)	CPU times (sec.)	z_D^{LP}	z_D^{ILP}	Gap (%)	ADD (%)	CPU times (sec.)	$\frac{z_D^{\mathrm{ILP}} - z_C^{\mathrm{ILP}}}{z_C^{\mathrm{ILP}}}(\%)$
1	6,492.3	6,577	1.30	4.8	1,193	7,023.0	7,094	1.01	8.7	583	7.8
2	7,243.2	7,303	0.83	6.1	1,214	8,466.8	8,603	1.61	13.5	997	17.8
3	5,534.5	5,602	1.22	4.3	815	5,727.5	5,795	1.18	7.1	294	3.4
4	6,377.0	6,499	1.91	3.5	576	7,100.3	7,197	1.36	6.2	258	10.7
5	13,143.0	13,282	1.06	5.9	7,246	14,324.5	14,470	1.02	9.8	2,003	8.9
6	11,141.3	11,306	1.48	6.3	4,689	11,791.5	11,911	1.01	9.6	723	5.3
7	12,716.3	12,843	1.00	7.3	3,711	14,175.5	14,314	0.98	13.0	602	11.4
8	14,559.5	14,701	0.97	6.9	2,439	15,902.0	16,055	0.96	12.9	1,465	7.8
9	12,831.8	12,989	1.23	5.4	5,710	13,869.1	14,038	1.22	11.6	1,254	8.1
10	30,222.7	30,581	1.19	8.3	22,572	32,814.5	33,174	1.10	13.0	3,041	8.5
11	33,274.9	33,597	0.97	8.5	17,321	35,204.0	35,493	0.82	13.4	4,231	5.6
12	54,877.6	55,313	0.79	8.6	72,554	57,110.1	58,732	2.84	13.7	12,340	6.2

Table 6.V: Comparison of the centralized/distributed scheme solutions

few configurations need to be generated (see column entitled "G") in comparison with the overall number of potential configurations (an exponential number), but very few are selected (see column entitled "S") in comparison with the number of generated ones. Moreover, the overall computing times (column entitled CPU) are all very reasonable for a network planning tool.

Differences between centralized and distributed solutions are of the order of 8.4 %, on average, ranging from 17.8 % (a bit an outlier) down to 3.4 %. It shows that distributed solutions are therefore quite good, in comparison with centralized ones. In terms of bandwidth requirements, differences between the two schemes can be seen throughout the supplementary bandwidth requirements (column entitled ADD, where ADD represents the average required supplementary bandwidth requirement per link) in addition to the initial transport capacities which are required in order to protect all demand requests. While for the centralized scheme, the average percentage over the 12 instances is 6.3 % per link on average (ranging between 3.5 and 8.6 %), it is 11.0 % on average for the distributed scheme (ranging between 6.2 and 13.7 %).

6.5.2.3 Performance evaluation: protection characteristics

Table 6.VI and 6.VII display the overall number of protection structures in the column entitled "C". Each selected configuration (i.e., a p-cycle or a FIPP p-cycle together with the set of unit (sub-)requests it protects) can be re-used for several wavelengths, depending on the demand values. Note that while the numbers reported in the columns entitled "S" correspond to the number of distinct selected configurations, the numbers reported in the columns entitled "C" correspond to the sum of the number of copies of each configuration.

Columns entitled "L" contain the average lengths (number of hops or links) of the p-cycles or of the FIPP p-cycles, while columns entitled 'D" contain the average numbers of domain traversals for a p-cycle, i.e., the average number of inter-domain links protected by a single p-cycle. As usual, as we did not restrict the lengths of the p-cycles and of the FIPP p-cycles in this study, protection cycles tend to be

Traffic Instances	# Configurations G ≡ generated, S ≡ selected, C ≡ overall # of configuration copies L ≡ (FIPP) p-cycle length, D ≡ # domain traversals per p-cycle										
	p-Cycles				FIPP p-Cycles				Paths		
	G	S	C	D	G	S	C	L	G	S	C
1	54	8	85	4.2	252	120	507	9.4	85	21	627
2	41	6	83	4.7	220	118	524	8.5	83	24	726
5	49	8	166	4.7	500	233	1,019	8.5	81	23	1,283
6	55	6	151	4.5	454	210	921	8.7	81	17	926
10	65	10	373	4.6	1,248	510	2,311	8.5	85	22	2,677
11	62	8	402	4.3	1,295	567	2,565	8.5	152	31	3,730
12	37	8	541	4.9	2,715	956	4,239	8.5	86	22	4,764

Table 6.VI: Protection characteristics of centralized model

Traffic Instances	# Configurations G ≡ generated, S ≡ selected C ≡ overall # of configuration copies L ≡ (FIPP) p-cycle length D ≡ # domain traversals per p-cycle								
	p-Cycles					FIPP p-cycles			
	G	S	C	L	D	G	S	C	L
1	20	10	85	21.0	4.5	251	116	459	9.4
2	19	8	121	17.0	3.5	259	120	527	8.4
5	19	13	243	21.9	4.5	502	233	969	8.7
6	19	8	151	18.0	4.5	439	197	873	8.9
10	18	9	448	19.8	4.2	1,157	494	2,192	8.6
11	15	7	410	19.7	4.0	1,256	523	2,333	8.5
12	14	8	530	21.1	4.7	1,896	854	3,797	8.8

Table 6.VII: Protection characteristics of distributed model

quite long on average, but could easily be restricted to shorter ones if required for, e.g., delay requirements. Note that the lengths of the p-cycles include the number of protected inter domain links (indeed, equal to the number of domain traversals) plus the number of intra-domain links (i.e., the physical support of the virtual links). As p-cycles take care of the protection of inter-domain links, they tend to be rather long, as virtual links are only between two border nodes in each domain, and as the number of traversed domains need to be at least three in practice (it is

unlikely to be two due to the sparsity of the inter-domain links).

6.6 Conclusion

We have proposed an original two-level protection scheme for multi-domain optical networks, with the combination of p-cycles and FIPP p-cycles. First, we designed a large scale optimization ILP centralized model which allows the definition of a minimum cost 2-level protection scheme in reasonable computing times. While the model relies on a decomposition into subproblems, where at least one class of subproblems is associated with the design of a protection scheme in a singe domain, and another class with the mappings of some intra-domain virtual links onto physical paths in order to establish p-cycles for the protection of inter-domain links.

Next, we have proposed a first fully distributed scheme for protection in multi-domain optical networks, where the different optimization problems are solved exactly thanks to a mathematical models relying on large scale optimization tools for their solution. While the solutions of the distributed scheme require more bandwidth than the solutions of a centralized scheme, the differences are around 10%, meaning that they remain bandwidth efficient solutions, while corresponding to realistic solutions with respect to the protocols in use in single and multi-domain optical networks.

6.7 Appendix

Herein, we propose the optimization ILP centralized model to the problem *"Full protected dimensioning"*.

In the centralized model, we assume that the network management is aware of all the details of the physical topologies of the domains. The objective function, i.e., the minimization of the overall capacity cost (bandwidth requirements) for protection corresponds to the sum of the p-cycle bandwidth requirements for the protection of the inter-link, of the FIPP p-cycle bandwidth requirements for the

protection of the intra-domain requests (or sub-requests), and of the mappings of the intra virtual links. It can be written as follows:

$$\min z_{\text{OBJ}} = \sum_{c \in C} \sum_{e \in E^{\text{INTER}}} \overline{\alpha}_e^c \, \text{COST}_e \, z^c + \sum_{d \in D} \sum_{f \in F_d} \text{COST}_f \, z^f + \sum_{e' \in E^{\text{VIRTUAL}}} \sum_{p \in P_{e'}} \text{COST}_p z^p + \text{PENAL} \sum_{e \in E^{\text{INTER}}} \text{ADD}_e + \text{PENAL} \sum_{d \in D} \sum_{e \in E_d} \text{ADD}_e, \quad (6.23)$$

where COST_e designates the unit spare capacity cost of link e, $\text{COST}_f = \sum_{e \in E_d} \text{COST}_e \overline{\beta}_e^f$, $\text{COST}_p = \sum_{e \in E_d} \text{COST}_e \gamma_e^p$, and PENAL is a penalty coefficient in order to discourage the addition of bandwidth in order to ensure the protection of all requests, i.e., favour the use of the available transport capacity even if it means longer cycles/paths.

Constraints can be written as follows:

$$\sum_{c \in C} \alpha_e^c z^c \geq b_{e'^i}^{\text{REQ}} \qquad e \in E^{\text{INTER}} \quad (6.24)$$

$$\sum_{c \in C} \overline{\alpha}_e^c z^c \leq \text{CAP}_e^P + \text{ADD}_e \qquad e \in E^{\text{INTER}} \quad (6.25)$$

$$\sum_{f \in F_d} \beta_\kappa^f z^f \geq b_\kappa \qquad \kappa \in K_d, d \in D \quad (6.26)$$

$$\sum_{e \in E_d^{\text{VIRTUAL}}} \sum_{p \in P} \gamma_e^p z^p + \sum_{f \in F_d} \overline{\beta}_e^f z^f \leq \text{CAP}_e^P + \text{ADD}_e \qquad e \in E_d, d \in D \quad (6.27)$$

$$\sum_{p \in P} z^p - \sum_{c \in C} \overline{\alpha}_e^c z^c \geq 0 \qquad e \in E_d^{\text{VIRTUAL}}, d \in D \quad (6.28)$$

$$z^c \in \mathbb{Z}^+ \qquad c \in C \quad (6.29)$$

$$z^f \in \mathbb{Z}^+ \qquad f \in F = \bigcup_{d \in D} F_d \quad (6.30)$$

$$z^p \in \mathbb{Z}^+ \qquad p \in P, e \in E_d^{\text{VIRTUAL}}. \quad (6.31)$$

Constraints (6.24) ensure that the working traffic on each inter-domain link is fully protected by p-cycles. Constraints (6.25) ensure that the bandwidth required by p-cycles on an inter-domain link is smaller than the sum of available

spare capacity for protection and added capacity on that edge. Constraint (6.26) guarantee a FIPP p-cycle protection for each intra-domain segment. Constraints (6.27) ensure that the amount of bandwidth requested from an intra-domain link e by the mapping of virtual links to physical paths and for the protection provided by FIPP p-cycles does not exceed the available spare capacity for protection and the possibly added capacity on link e. Constraints (6.28) check that enough spare capacity is available for the mapping of virtual link e to one or more physical paths in order to carry the traffic of the p-cycles using link e'. In order to guarantee the protection of all demand requests, we allow the increase of the link transport capacities in constraints (6.25) and (6.27).

CHAPTER 7

ENHANCED DIMENSIONING AND PROVISIONING OF SURVIVABLE MULTI-DOMAIN OPTICAL NETWORKS

7.1 Chapter presentation

In the following, we present the article entitled "A p-cycle protection scheme in multi-domain optical network". The article was submitted for publication in *Optical Switching and Networking*. A preliminary version of this article was published under title of "Distributed design and provisioning of survivable multi-domain optical networks" in *Proceeding of the International Conference on Optical Network Design and Modeling (ONDM)*, April 2013.

Herein, we propose enhancements of protection schemes against single failure through bandwidth sharing, the application of these enhancements to the dimensioning problem in multi-domain optical networks. We investigate two methods to construct a virtual aggregated network. We also consider the impact of the number of inter-domain links to bandwidth requirement while still keeping a survivable multi-domain network. Experiments were successfully conducted on a multi-domain network with 10 domains.

7.2 Bandwidth sharing

We consider the same type of protection as in Chapter 6, where FIPP p-cycles protect intra-domain segments while p-cycles protect inter-domain links. In the single link failure case, a failed link is either part of an intra-domain segment or an inter-domain link, cannot be both. Thus, backup bandwidth for FIPP p-cycles and for the physical paths of p-cycles can be shared on intra-domain links. Hence, we propose a bandwidth sharing scheme on intra-domain links between the FIPP p-cycles and the physical paths mapped on virtual links in the p-cycles in order to save backup bandwidth.

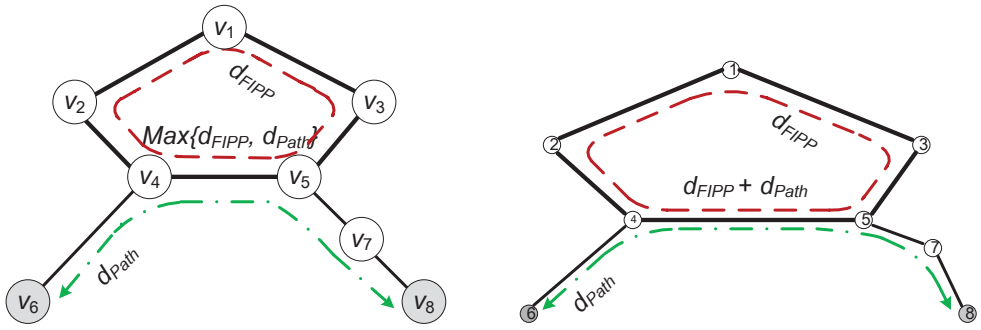

Figure 7.1: Examples of backups that share (a) and do not share (b) bandwidth

The sharing is depicted in Figure 7.1. In both cases, it comprises the FIPP p-cycle with requested bandwidth d_{FIPP} and the physical path connecting border nodes (v_6, v_8) with requested bandwidth d_{Path}. These backup paths can share bandwidth over the common link (v_4, v_5). In this case, the needed bandwidth on link (v_4, v_5) is $max\{d_{FIPP}, d_{Path}\}$ in order to ensure protection for both inter-domain and intra-domain (see case 7.1(a)). In case 7.1(b) without bandwidth sharing, the needed backup bandwidth on link (v_4, v_5) is $d_{FIPP} + d_{Path}$ which is greater than in case 7.1(a).

7.3 Virtual aggregated network

We use the same notations and definitions of multi-domain networks as in Section 6.2 of Chapter 6. Herein, we focus on concepts of virtual aggregated network and protection scheme taking acount bandwidth sharing before discussing about the mathematical models.

Both the centralized and the distributed models that are proposed in Section 7.4 relies on an aggregated network, called virtual network, and denoted by $G^{\text{VIRTUAL}} = (V^{\text{BORDER}}, E^{\text{INTER}} \cup E^{\text{VIRTUAL}})$, derived from the multi-domain network topology, where V^{BORDER} is the set of border nodes, E^{INTER} is the set of inter-domain links and E^{VIRTUAL} is the set of so-called virtual edges. For each domain, all pairs of border nodes are connected in G^{VIRTUAL}. Those node connections correspond to virtual edges, where

each virtual edge e' must be mapped onto a physical path $p_{e'}$.

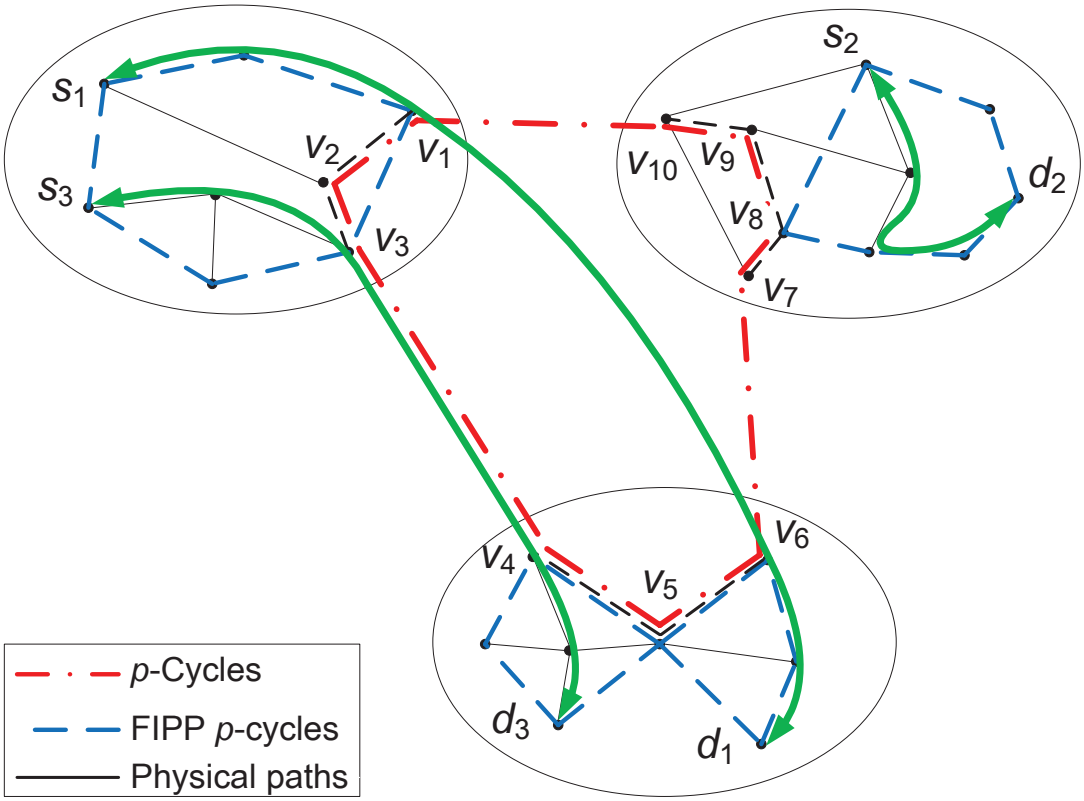

Figure 7.2: An illustration of the 2-level protection scheme

The union of these complete single-domain networks, together with the set of inter links, define a multi-graph as depicted in Figure 7.2. Therein, we can observe that the multi-domain protection problem can be decomposed into a two-level protection scheme, where p-cycles are generated on the virtual network for protecting the inter-domain links, and FIPP p-cycles are generated on each original domain to protect the intra-domain paths or segments. The (dash followed by dot) red cycle connecting border nodes $v_1, v_2, \ldots, v_{10}$ in Figure 7.2 represents a p-cycle which protects inter-domain physical links $\{v_3, v_4\}$ and $\{v_1, v_6\}$ while FIPP p-cycles are represented by dash blue cycles. Note that each inter-domain edge in a p-cycle has an one-to-one mapping relation with an inter-domain physical link.

Each pair of border nodes, within a domain, is connected by one or more virtual edges, where each virtual edge is mapped onto a specific physical path, and different virtual edges correspond to different physical paths. In our two-level protection scheme, bandwidth requirement of FIPP p-cycles and p-cycles are independent in the context of single link failure, i.e., failures can not occur at the same time. Based on these characteristics, we calculate parameters for virtual edges.

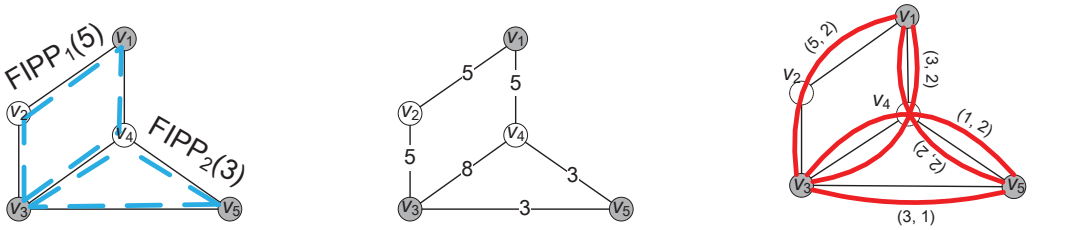

(a) FIPP p-cycles

(b) Available Protection Bandwidth

(c) Virtual Aggregated Domain Network

Figure 7.3: An illustration of virtual aggregated topology

Figure 7.3 illustrates the construction of a virtual network for one domain. The physical network comprises 5 nodes, of which three (v_1, v_3, v_5) are border nodes, and 6 physical links. There are two FIPP p-cycles (dash blue lines), depicted in Figure 7.3(a), the first FIPP p-cycle requires 5 bandwidth units while the second one requires 3 bandwidth units. In Figure 7.3(b), each physical link is associated with an integer indicating its available protection bandwidth, i.e., bandwidth requirement of FIPP p-cycles that can be shared with p-cycles. We use the mapping phase (Section 7.4.3.3) to calculate parameters of each virtual edge. Here, each virtual edge e' is denoted by a pair $\{\text{CAP}_{e'}, \text{LENG}_{e'}\}$, where $\text{CAP}_{e'}$ denotes the available bandwidth of virtual edge e' and $\text{LENG}_{e'}$ indicates the length of physical path $p_{e'}$, i.e., the mapping of virtual edge e'. The resulting virtual topology is described in Figure 7.3(c), with the mapping of the virtual edges onto the physical links, where the virtual edges are represented by bold red lines and the physical links by plain lines. For example, from the path $\{\{v_3, v_2\}, \{v_2, v_1\}\}$ associated with virtual edge connecting $\{v_3, v_1\}$ we deduce the available capacity $\text{CAP}_{\{v_3,v_1\}} = 5$ and

$\text{LENG}_{\{v_3,v_1\}} = 2$.

Last, virtual edges have to be mapped to physical paths inside each domain. In both the centralized and the distributed models, we use a k-shortest path algorithm to compute physical paths on which the virtual links are mapped. Weights or lengths of the edges, to be used in the k-shortest path algorithm, correspond to the (residual) spare transport capacities available for protection. The difference between the centralized and the distributed models lie in the order in which the mappings are computed. In the centralized model, mapping of virtual/physical paths is computed prior to the computation of p-cycles as it is assumed that central management has detailed network information about all domains. In the distributed model, the mappings are independently computed both before and after p-cycles have been computed.

7.4 Mathematical models

In this section, we propose two mathematical models, one for the centralized framework one for the distributed one, for the p-cycle-based protection with bandwidth sharing to tackle the dimensioning problem in multi-domain optical networks. Optimization models rely on the concept of configurations and variables.

7.4.1 Configurations and variables

There are three types of configurations.

p-Cycle configurations: Each such configuration associates a p-cycle with the subset of inter-domain links covered (and therefore protected) by that p-cycle. Let C be the overall set of potential p-cycles in a virtual network G^{VIRTUAL}. For each cycle c and each inter-domain edge $e \in G^{\text{VIRTUAL}}$, we define $\alpha_e^c \in \{0, 1, 2\}$ which represents the protection provided by p-cycle c for link e: $\alpha_e^c = 1$ if e lies on cycle c, $\alpha_e^c = 2$ if e straddles cycle c, and $\alpha_e^c = 0$ otherwise. Similarly, parameter $\overline{\alpha}_e^c \in \{0, 1\}$ is such that $\overline{\alpha}_e^c = 1$ if link e lies on cycle c, and 0 otherwise.

FIPP p-cycle configurations: Each such configuration associates a FIPP p-cycle

with the traffic (intra-domain requests and sub-requests) it protects in a given domain. Let F_d be the overall set of potential FIPP p-cycle configurations in domain d. Any $f \in F_d$ is characterized by vector $\beta^f = (\beta^f_\kappa)_{\kappa \in K_d}$ where $\beta^f_\kappa \in \{0, 1, 2\}$ defines the level of protection (the number of protection paths) provided by the FIPP p-cycle associated with f for intra-domain segment κ. Similarly parameter $\overline{\beta}^f_e \in \{0, 1\}$ is such that $\overline{\beta}^f_e = 1$ if link e lies on the cycle associated with configuration f, and 0 otherwise.

Path configurations: They are only defined in the centralized scheme. Each such configuration associates a physical path with the virtual edge which is mapped to this path. A path configuration is characterized by: $\gamma^p_e \in \{0, 1\}$ such that $\gamma^p_e = 1$ if virtual edge e' is mapped to path p, 0 otherwise.

Variables: For both centralized and distributed models, we use three sets of variables to keep track of how many units of each resource (configuration) is used: variables z^c stand for the number of unit-capacity copies of p-cycle configuration c, variables z^f stand for the number of unit copies of FIPP p-cycle configuration f, and variables z^p stand for the amount of bandwidth associated with the mapping of virtual link e' onto the physical path $p \in P$.

7.4.2 Centralized model

In the centralized model, it is assumed that the network management is aware of all the details of the physical topologies of the domains.

The objective function aims at minimizing capacity requirements to protect all the requests. Such capacity corresponds to the sum of the required bandwidth on inter-domain links for p-cycles and on intra-domain links for FIPP p-cycles and for the physical paths of p-cycles while taking acount sharing bandwidth. The objective function is given by $z^{\text{CEN}}_{\text{OBJ}}(z^c, z^f, z^p, \text{CAP}^P_e)$, and is written as follows:

$$\min z^{\text{CEN}}_{\text{OBJ}} \quad = \quad \sum_{c \in C} \sum_{e \in E^{\text{INTER}}} \overline{\alpha}^c_e \quad z^c \quad + \quad \sum_{d \in D} \sum_{e \in E_d} \quad \text{CAP}^P_e. \quad (7.1)$$

The set of constraints can be next described.

$$\sum_{c \in C} \alpha_e^c z^c \geq \text{CAP}_e^W \qquad e \in E^{\text{INTER}} \tag{7.2}$$

$$\sum_{f \in F_d} \beta_\kappa^f z^f \geq \text{CAP}_\kappa^{\text{W}} \qquad \kappa \in K_d, d \in D \tag{7.3}$$

$$\sum_{p \in P_{e'}} z^p - \sum_{c \in C} \overline{\alpha}_{e'}^c z^c \geq 0 \qquad e' \in E^{\text{VIRTUAL}} \tag{7.4}$$

$$\sum_{f \in F_d} \overline{\beta}_e^f z^f \leq \text{CAP}_e^P \qquad e \in E_d, d \in D \tag{7.5}$$

$$\sum_{e' \in E_d^{\text{VIRTUAL}}} \sum_{p \in P_{e'}} \gamma_e^p z^p \leq \text{CAP}_e^P \qquad e \in E_d, d \in D \tag{7.6}$$

$$z^c \in \mathbb{Z}^+ \qquad c \in C \tag{7.7}$$

$$z^f \in \mathbb{Z}^+ \qquad f \in F = \bigcup_{d \in D} F_d \tag{7.8}$$

$$z^p \in \mathbb{Z}^+ \qquad p \in P_{e'}, e' \in E_d^{\text{VIRTUAL}} \tag{7.9}$$

$$\text{CAP}_e^P \in \mathbb{Z}^+ \qquad e \in \bigcup_{d \in D} E_d. \tag{7.10}$$

Constraints (7.2) ensure that the working traffic on each inter-domain link is protected by p-cycles against any single inter-link failure. Constraints (7.3) guarantee a FIPP p-cycle protection for each intra-domain sub-request. Constraints (7.5) ensure the bandwidth required by FIPP p-cycles on a intra-domain link. Constraints (7.4) ensure that each virtual link e belonging to p-cycles is mapped onto one or more physical paths in order to protect the inter-link traffic (see Figure 7.4(a)). Constraints (7.6) ensure that the amount of bandwidth requested from an intra-domain link e by the mapping of virtual links to physical paths does not exceed the provided spare capacity.

This model assumes that the bandwidth on intra-domain link e is shared among FIPP p-cycles and physical paths mapping of the virtual links. The sharing is depicted in Figure 7.4(b). It comprises 2 (FIPP_1, FIPP_2) FIPP p-cycles and 2 (P_1, P_2) physical paths, each associated with an integer indicating its capacity

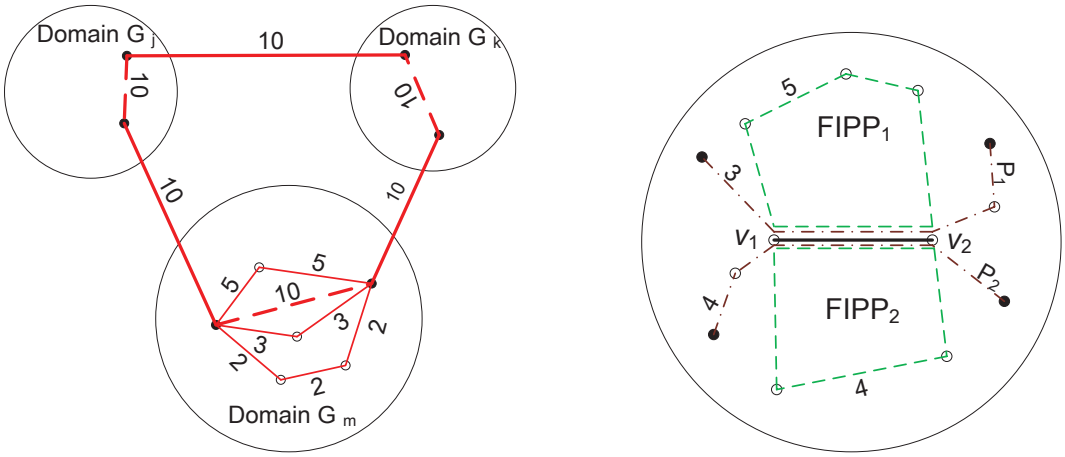

(a) Mapping of Virtual Link (b) Sharing of Bandwidth

Figure 7.4: Sharing of bandwidth in centralized model

requirement, and all go thought link e connecting nodes v_1 and v_2. FIPP p-cycles require 9 capacity units while virtual links need 7 capacity units for mapping link e to physical paths. So, capacity requirement on link connecting (v_1, v_2) is 9 capacity units.

7.4.3 Distributed model

7.4.3.1 Outline

The distributed model is depicted in Figure 7.5. Initially, FIPP p-cycles solutions are independently generated in each domain, in order to protect intra-domain (sub-)requests while minimizing the total capacity usage. We next map the virtual links onto intra-domain physical paths, using as much as possible the bandwidth already reserved for the FIPP p-cycles. The iterative process then starts, where at each iteration, a p-cycle protection scheme is computed in order to protect the inter-domain working traffic, for given intra-domain capacities allocated to the virtual links. p-Cycles are constructed using as much as possible the available bandwidth of the virtual links, i.e., the bandwidth that can be shared with the FIPP p-cycles, and with additional bandwidth on those virtual links if the incumbent bandwidth is not sufficient. And then, we perform a mapping of bandwidth requirement of the

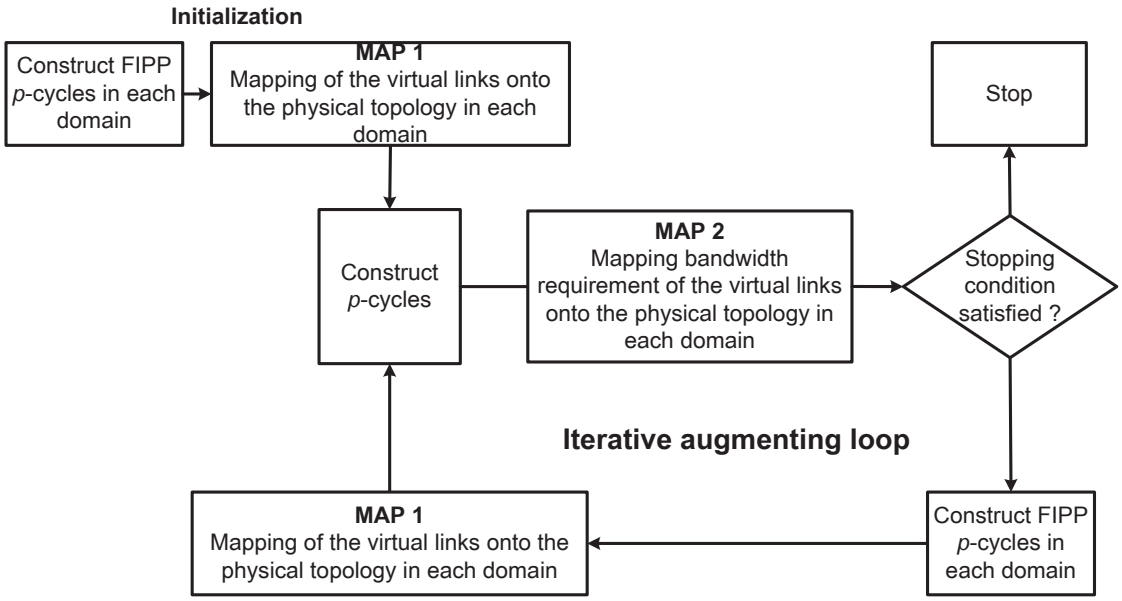

Figure 7.5: Flowchart of the distributed solution process

virtual links onto the physical topology in each domain, using as less as possible additional bandwidth on each physical link. At the end of each iteration, if an overall protection scheme with a smaller bandwidth requirement has been found, a new iteration is initiated. Here, FIPP p-cycles are then possibly updated in order to take advantage of the added bandwidth, i.e., maximize the shared bandwidth in order to minimize the bandwidth requirements. Last, the mapping of the virtual links onto the physical domain topologies are revised. It leads to new spare bandwidth availability for each virtual link. The value of the objective function (overall bandwidth requirements for the p-cycle and FIPP p-cycle protection structures), z^t_{DIS} (see Section (7.4.3.6)) where t is the iteration index, is re-evaluated.

The computation of p-cycles requires the knowledge of the capacity and length of the virtual links. These latter values are computed in the mapping phase, which takes care of mapping the virtual links onto physical paths. The computation of the FIPP p-cycles requires the knowledge of how much bandwidth is used by the p-cycles in a given domain. These values are obtained directly from the computation of the p-cycles. Therefore, the proposed distributed scheme satisfies the multi-

domain network assumptions regarding the limitations on inter-domain sharing of operational information, i.e., do not assume any inter-domain information sharing.

7.4.3.2 An illustration of the distributed model

Let us consider an illutration of the process of the distributed model in Figure 7.6. Figure 7.6(a) describes three (bold green lines) requests connecting $\{s_1, d_1\}$, $\{s_2, d_2\}$ and $\{s_3, d_3\}$ with traffic demand 10, 5 and 10 bandwidth units respectively. These requests are subdivided into two inter-domain link sub-requests $\{e_1, e_2\}$ and five intra-domain (sub-)requests $\{\kappa_1, \kappa_2, \kappa_3, \kappa_4, \kappa_5\}$. Figure 7.6(b) describes the initial step of the process. Indeed, the dashed green cycles represent FIPP p-cycles which are independently generated in each domain to protect intra-domain (sub-)requests. Each FIPP p-cycle is associated with an integer indicating its banwidth requirement. From these values, we know available protection bandwidth on each intra-domain link that is reused as much as possible for the protection of inter-domain links, i.e., for p-cycles. Then, MAP 1 (see Section 7.4.3.3) caculates parameters of each virtual edge that connects a pair of border nodes within a domain, i.e., the mapping of the virtual edges onto the physical paths. The resulting virtual topology is described in Figure 7.6(c), where the virtual edges are represented by dotted violet lines with its parameters. For example, virtual edge $e'_{v_1v_4v_5}(5, 2)$ connectting two border nodes $\{v_1, v_5\}$ is mapped on the physical path $\{v_1, v_4, v_5\}$, with the available capacity $\text{CAP}_{e'} = 5$ and the length $\text{LENG}_{e'} = 2$. These virtual edges with inter-domain links creat a virtual network that is used for the computation of p-cycles. The (dash followed by dot) red cycle describes p-cycle to protect inter-domain link sub-requests $\{e_1, e_2\}$ and associated with an integer indicating its banwidth requirement. This cycle requires 10 bandwidth units, hence, we need to add 5 bandwidth units for each chosen virtual edge. Now, we can see that the overall bandwidth requirement for the protection, i.e., the sum of the bandwidth requirements of FIPP p-cycles, the capacity requirement of p-cycles on the inter-domain links and the added bandwidth requirement in all domains to supply for p-cycles, is 220. However, we can improve this result by using MAP 2 (see Section

7.4.3.3) to re-map virtual edges on other physical paths. This process is depicted in Figure 7.6(d). For example, the virtual edge connecting two border nodes $\{v_1, v_5\}$ now maps on two physical paths (arrowed red lines). We can observe that we do not need now add any bandwidth units for each chosen virtual edge. Hence, the the overall bandwidth requirement is more effective and only equals 195. From MAP 2, we know bandwidth requirement on each intra-domain links that can be reused for the computation of FIPP p-cycles in the next step (at the initial step, these values equal 0).

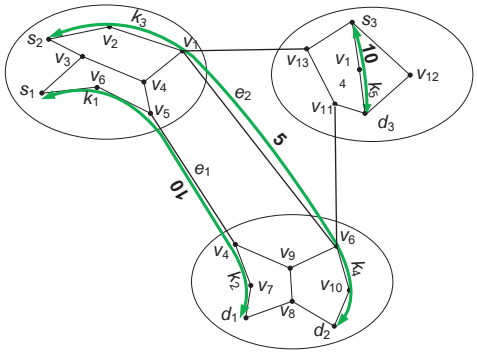

(a) Three working paths, with their respective amount of traffic

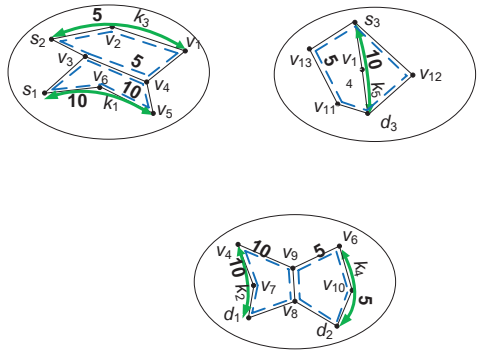

(b) FIPP p-cycles to protect intra-domain sub-requests

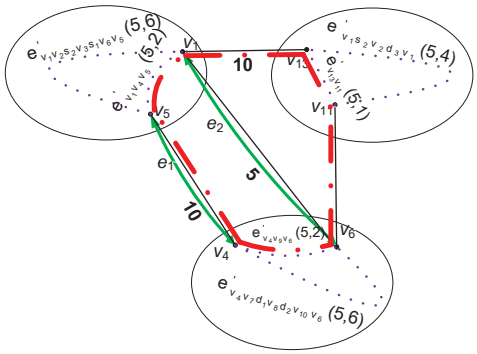

(c) Virtual edges and p-cycles to protect inter-domain sub-requests

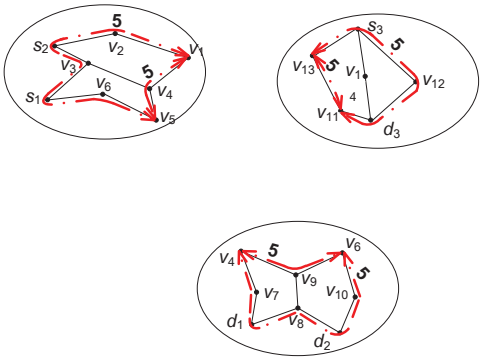

(d) Re-mapping of virtual edges

Figure 7.6: An illustration of the distributed model

7.4.3.3 Mapping problems

There are two types of mapping problems: one (called MAP 1 in Figure 7.5) is implemented before generating a new p-cycle protection scheme and another (called MAP 2 in Figure 7.5) is implemented after getting a new p-cycle protection scheme.

MAP 1: The objective of this mapping phase is to construct a mapping of the virtual links (denoted by e') onto a set of physical paths (denoted by p), in each domain. Indeed, we construct a virtual network for caculating a new p-cycle protection scheme.

Input : Available spare bandwidth, i.e., bandwidth used by the FIPP p-cycles on each physical link e, denoted by $\text{CAP}_e^{\text{FIPP}}$ for $e \in E_d, d \in D$.
Output : Parameters of the virtual edge e', denoted by $\{\text{CAP}_{e'}, \text{LENG}_{e'}\}$.

In this mapping problem, we do not know the bandwidth requirement on virtual edges. The objective function aims at maximizing the number of bandwidth provisioned physical paths with the FIPP p-cycle bandwidth. Let P_d be the potential set of physical paths associated with the pairs of border nodes. Denote by x_p the bandwidth capacity of physical path $p \in P = \bigcup_{d \in D} P_d$. Here, p is choosen as the shortest path between the border nodes.

MAP1_ILP(d)

$$\max \quad \sum_{p \in P_d} x_p \tag{7.11}$$

$$\text{subject to:} \quad \sum_{p \in P_d} \delta_e^p x_p \leq \text{CAP}_e^{\text{FIPP}} \qquad e \in E_d \tag{7.12}$$

$$x_p \in \mathbb{Z}^+ \qquad p \in P_d. \tag{7.13}$$

where $\delta_e^p = 1$ if physical link e lies on path p. Constraints (7.12) ensure that bandwidth capacity of physical paths thought link e does not exceed the available spare capacity (i.e., the capacity reserved for the FIPP p-cycles).

After solving MAP1_ILP(d), set $\text{CAP}_{e'} = x_p^\star$ for virtual edge e' mapped onto physical path p, where $x_p^\star$ denotes the optimal value of x_p. And $\text{LENG}_{e'}$ equal length of physical path p.

MAP 2: The objective of this mapping phase is also to construct a mapping of the virtual links onto a set of physical paths, in each domain. However, this mapping phase is implemented after caculating p-cycles, i.e., we now know the bandwidth requirement on virtual edges.

The objective function, $z_{\text{ADD}}^{\text{INTRA}}(d)$, aims at minimizing the added bandwidth in order to fulfill the bandwidth requirement $\text{CAP}_{e'}^{\text{REQ}}$ on virtual edge e',

$$\min \quad z_{\text{ADD}}^{\text{INTRA}}(d) = \sum_{e \in E_d} \text{ADD}_e \tag{7.14}$$

subject to:

$$\sum_{p \in P_d(e')} z_p \geq \text{CAP}_{e'}^{\text{REQ}} \qquad e' \in E^{\text{VIRTUAL}} \tag{7.15}$$

$$\sum_{p \in P_d} \delta_e^p z_p \leq \text{CAP}_e^{\text{FIPP}} + \text{ADD}_e \qquad e \in E_d \tag{7.16}$$

$$x_\ell^{v_1 v_2} \in \mathbb{Z}^+ \qquad \ell \in L_d \tag{7.17}$$

$$\text{ADD}_e \in \mathbb{Z}^+ \qquad e \in E_d \tag{7.18}$$

where $P_d(e')$ is the potential set of physical paths used for the mapping of virtual edge e', and $P_d = \bigcup_{e' \in E^{\text{VIRTUAL}}} P_d(e')$.

Constraints (7.15) ensure that each virtual edge e' belonging to p-cycles is mapped onto one or more physical paths. Constraints (7.16) ensure that the amount of bandwidth requested from virtual edges is smaller than the available spare capacity and of the possibly added capacity.

We propose and analysis two methods to construct the set $P_d(e')$ that lies in *Distributed scheme 1* and *Distributed scheme 2*, respectively. Indeed, $P_d(e')$ is 2-shortest physical paths mapping of virtual edge $e^{'}$ in *Distributed scheme 1*, while

this set is constructed by column generation in *Distributed scheme 2*.

After solving in all domains, the added bandwidth requirement in order to provision properly all p-cycles is: $\text{CAP}_{\text{ADD}}^{\text{INTRA}} = \sum_{d \in D} z_{\text{ADD}}^{\text{INTRA}}(d)$

7.4.3.4 *p*-Cycle model

p-Cycles are computed on the virtual network where virtual links connect the protected inter-domain links.

The objective function aims at minimizing the bandwidth requirements, i.e., the required added capacity on the physical paths on which the virtual edges are mapped, in order to protect the inter-domain links. Maximizing the bandwidth sharing with the FIPP p-cycles amounts to maximize the re-use of the $\text{CAP}_e^{\text{FIPP}}$ bandwidth, under a single link failure assumption (whether the link is an inter or an intra domain link). The p-cycle model can be written as follows:

$$\min \quad \underbrace{\sum_{c \in C} \left(\sum_{e \in E^{\text{INTER}}} \overline{\alpha}_e^c \right) z_c}_{\substack{\text{Bandwidth requirements} \\ \text{for the inter-domain links}}} + \sum_{e' \in E^{\text{VIRTUAL}}} \text{LENG}_{e'} \text{ADD}_{e'}, \tag{7.19}$$

where $\text{ADD}_{e'}$ estimates the amount of required additional bandwidth, if any, on virtual edge e', in order to protect all inter-domain link requests. Constraints can be written as follows :

$$\sum_{c \in C} \alpha_e^c z^c \geq \text{CAP}_e^{\text{W}} \qquad e \in E^{\text{INTER}} \tag{7.20}$$

$$\sum_{c \in C} \overline{\alpha}_{e'}^c z^c \leq \text{CAP}_{e'} + \text{ADD}_{e'} \qquad e' \in E^{\text{VIRTUAL}} \tag{7.21}$$

$$z^c \in \mathbb{Z}^+ \qquad c \in C \tag{7.22}$$

$$\text{ADD}_{e'} \in \mathbb{Z}^+ \qquad e' \in E^{\text{VIRTUAL}}. \tag{7.23}$$

Constraints (7.20) ensure that the working traffic on each inter-domain link is fully protected by p-cycles. Constraints (7.21) ensure that the amount of bandwidth

requested from virtual edge e' does not exceed the available spare capacity and the possibly added capacity.

The capacity requirement of p-cycles on the inter-domain links is: $\text{CAP}_{\text{INTER}}^{\text{PCYCLE}} = \sum_{c \in C} \left(\sum_{e \in E^{\text{INTER}}} \overline{\alpha}_e^c \right) z_c^\star$, where $z_c^\star$ denotes the optimal value of z_c. And The capacity requirement of p-cycles on the virtual links e' is: $\text{CAP}_{e'}^{\text{REQ}} = \sum_{c \in C} \overline{\alpha}_{e'}^c z_c^\star$ for $e' \in E^{\text{VIRTUAL}}$

7.4.3.5 FIPP *p*-cycle model

FIPP p-cycles are constructed in each domain to protect intra-domain sub-requests and requests.

Input: $\text{CAP}_e^{\text{P\_CYCLE}} = \sum_{e' \in E_d^{\text{VIRTUAL}}} \delta_e^{p(e')} z_{p(e')}^\star$ is the bandwidth used by the p-cycles on intra-domain link e. It will be re-used as much as possible in order to construct FIPP p-cycles. At the outset, (i.e, $t = 0$), $\text{CAP}_e^{\text{P\_CYCLE}} = 0$.

Output: Bandwidth requirements of FIPP p-cycles.

The FIPP p-cycle objective function aims at minimizing the capacity requirement and added capacity, ADD_e, induced by FIPP p-cycle protection. It is written as follows:

$$\min \quad \sum_{e \in E_d} \text{ADD}_e, \tag{7.24}$$

Constraints for FIPP p-cycles are written as follows:

$$\sum_{f \in F_d} \beta_\kappa^f z_f \geq \text{CAP}_\kappa^{\text{W}} \qquad \kappa \in K_d \tag{7.25}$$

$$\sum_{f \in F_d} \overline{\beta}_e^f z_f \leq \text{CAP}_e^{\text{P\_CYCLE}} + \text{ADD}_e \qquad e \in E_d \tag{7.26}$$

$$z_f \in \mathbb{Z}^+ \qquad f \in F_d. \tag{7.27}$$

Constraints (7.25) guarantee a FIPP p-cycle protection for each intra-domain segment. Constraints (7.26) ensure that the required bandwidth by FIPP p-cycles on an intra-domain link is smaller than its available spare capacity (i.e., the capacity of the physical paths mapping of the virtual edge on the p-cycles) and added

capacity. The FIPP p-cycle bandwidth requirements on link $e \in E_d$, $d \in D$, are: $\text{CAP}_e^{\text{FIPP}} = \sum_{f \in F} \overline{\beta}_e^f \, z_f^\star$,, where $z_f^\star$ denotes the optimal value of z_f in model (7.24) - (7.27). Bandwidth requirements of FIPP p-cycles are as follows: $\text{CAP}^{\text{FIPP}} = \sum_{e \in E^{\text{INTRA}}} \text{CAP}_e^{\text{FIPP}}$.

7.4.3.6 Overall bandwidth requirements

At a current iteration, before the stopping condition, see the flowchart in Figure 7.5, the overall bandwidth requirements are as follows:

$$z_{\text{DIS}} = \text{CAP}^{\text{FIPP}} + \text{CAP}_{\text{INTER}}^{\text{PCYCLE}} + \text{CAP}_{\text{ADD}}^{\text{INTRA}}. \quad (7.28)$$

Indeed, it is the sum of the bandwidth requirements of FIPP p-cycles, the capacity requirement of p-cycles on the inter-domain links and the added bandwidth requirement in all domains to supply for p-cycles.

7.5 Solution of the ILP model

We use the same technique as in Chapter 6 to solve the ILP models of the previous, i.e., column generation technique (see Section 2.6.1 for the "*base*" framework of ILP & column generation algorithm). Indeed, the optimization model of the centralized scheme (see Section 7.4.2) corresponds to a master problem with three different pricing problems. The model associated with the distribution scheme involves two column generation models, one for p-cycle generation, another for FIPP p-cycle generation. Formulations of the all pricing problems can be constructed as follows.

7.5.1 Pricing problems

Here, we construct pricing problems in the centralized scheme. These problems are defined similarly in distributed scheme.

7.5.1.1 *p*-cycle generation pricing problem

It is denoted by PP(c) for $c \in C$. Its reduced cost objective, REDCOST_c, depends on dual variables u_e^{CYCLE} and $u_{e'}^{\text{VIRTUAL}}$ associated with constraints (7.2) and (7.4) respectively:

$$\text{REDCOST}_c = \sum_{e \in E^{\text{INTER}}} x_e - \sum_{e \in E^{\text{INTER}}} (2s_e - x_e) u_e^{\text{CYCLE}} + \sum_{e' \in E^{\text{VIRTUAL}}} x_{e'} u_{e'}^{\text{VIRTUAL}}, \quad (7.29)$$

where $x_{e'} = 1$ if link e supports the sought cycle in configuration c, 0 otherwise; $s_{e'} = 1$ if link e is protected by configuration c, and 0 otherwise. Column coefficients associated with c are then deduced as follows: $\alpha_e^c = 2s_e - x_e, \overline{\alpha}_e^c = x_e$.

For the set of constraints, refer to [66].

7.5.1.2 FIPP *p*-cycle generation pricing problem

It is denoted by PP(f, d) for $f \in F_d, d \in D$. Its reduced cost objective, REDCOST_{fd}, can be expressed using $u_{\kappa d}^{\text{FIPP}}$ and u_{ed}^{FIPP}, the dual variables associated with constraints (7.3) and (7.5):

$$\text{REDCOST}_{fd} = -\sum_{\kappa \in K_d} (s_\kappa + w_\kappa) u_{\kappa d}^{\text{FIPP}} + \sum_{e \in E_d} x_e u_{ed}^{\text{FIPP}}, \quad (7.30)$$

where $x_e = 1$ if and only if link e belongs to the FIPP p-cycle associated with configuration f, $s_\kappa = 1$ if and only if working sub-path κ is protected, and $w_\kappa = 1$ if and only if working sub-path κ is protected and straddles cycle associated with f. Column coefficients associated with f, d are then deduced as follows: $\beta_\kappa^f = s_\kappa + w_\kappa, \overline{\beta}_e^f = x_e$.

For the set of constraints, refer to [67].

7.5.1.3 Path generation pricing problem

It is denoted by PP(p, e', d) for $p \in P_{e'}, e' \in E_d^{\text{VIRTUAL}}, d \in D$. Its reduced cost objective, $\text{REDCOST}_{e'pd}$, can be expressed using dual variables $u_{e'}^{\text{VIRTUAL}}$ and u_{ed}^{PATH}

from constraints (7.4) and (7.6):

$$\text{REDCOST}_{epd} = -u_{e'}^{\text{VIRTUAL}} + \sum_{e \in E_d} \gamma_e u_{ed}^{\text{PATH}} \tag{7.31}$$

subject to:

$$\sum_{e \in \omega(v)} \gamma_e = 2d_v \qquad v \in V_d \diagdown \{o_e, d_e\} \tag{7.32}$$

$$\sum_{e \in \omega(o_e)} \gamma_e = \sum_{e \in \omega(d_e)} \gamma_e = 1 \tag{7.33}$$

$$\gamma_e \in \{0, 1\} \qquad e \in E_d \tag{7.34}$$

$$d_v \in \{0, 1\} \qquad v \in V_d. \tag{7.35}$$

where $\gamma_e = 1$ if physical link e lies on path p, $d_v = 1$ if path p goes through node v.

All nodes which are on the physical path p are required to have two incident links, which is ensured by constraints (7.32). Constraints (7.33) take care of the generation of at most one physical path in order to map virtual link e'.

7.6 Computational results

We implemented the model developed in Section 7.4 and solved it using the solution process described in Section 7.5. Algorithms were implemented using the OPL programming language, C++ and solved using CPLEX 12. Programs were run on a 2.2 GHz AMD Opteron 64-bit processor with 24GB of RAM. The network and data instances are described in Section 7.6.1, and then performances of the proposed model are discussed in Section 7.6.2 and Section 7.6.3.

7.6.1 Network and data instances

We firstly examined the protection schemes on network MD-10, which is built using real optical networks: EON [56], RedIrid [3], Garr [2], Renater [4], Surfnet [5], Atlanta, PDH, Nobel-germany, Abilence [58]. The numbers of nodes and links of

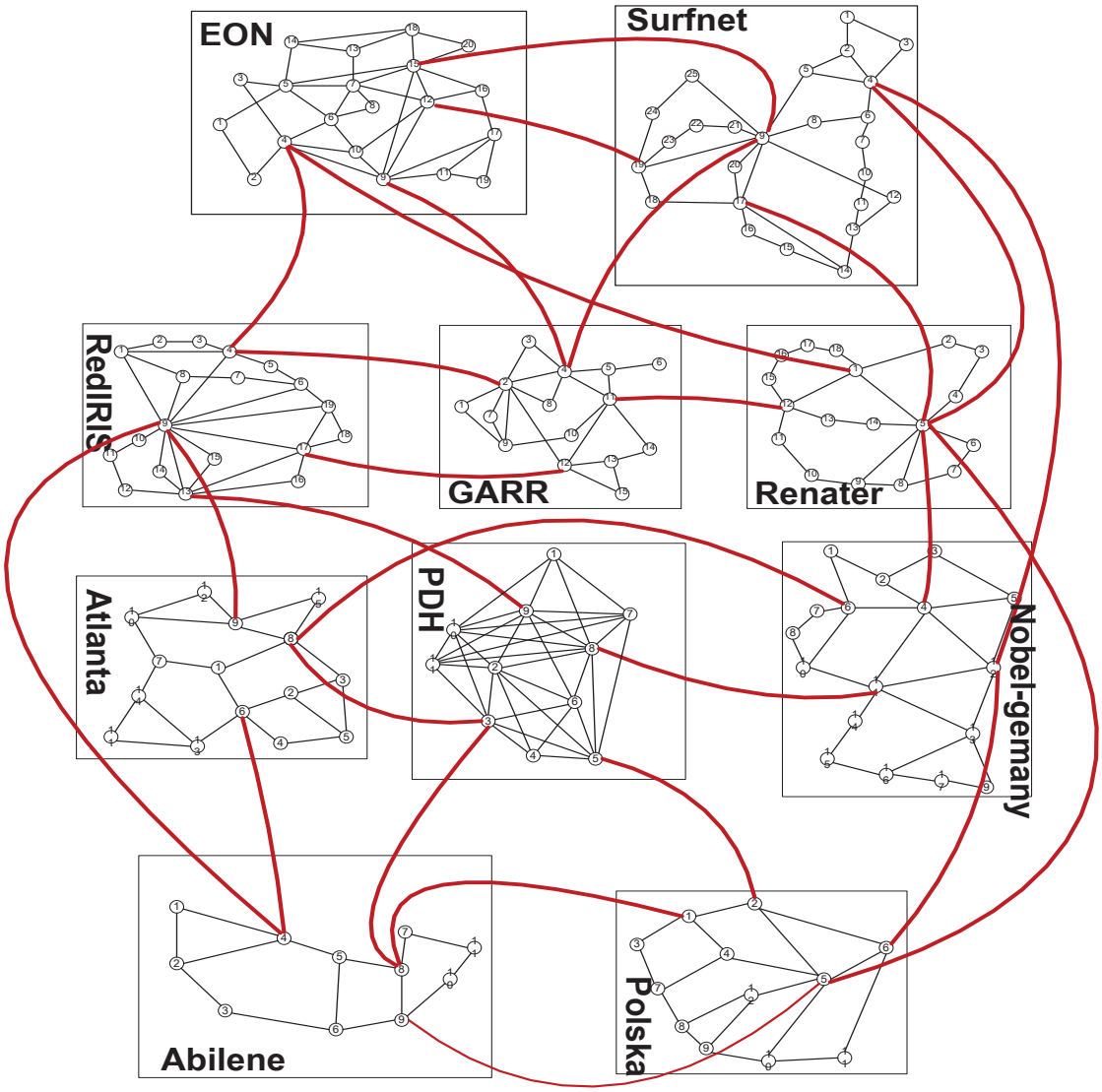

Figure 7.7: Topology of the MD-10

each network are: EON (20, 39), RedIrid (19, 31), Garr (15, 24), Renater (18, 23), Surfnet (25, 34), Atlanta (15, 22), PDH (11, 34), Nobel-germany(17, 26), Abilence (11, 14). For each optical network, we identify up to 4 border nodes. Some inter-links are added to connect the border nodes of the domains such that the degree of each border node is 1, 2 or 3. The topologies of the network is depicted in Fig 7.7.

Experiments are conducted on sets of 100 up to 1,000 requests, which are generated between randomly for selected pairs of nodes with bandwidth requirement

Instances	removed border nodes	# removed inter-domain links
MD-10-1	(1,12) (5, 19)	1
MD-10-2	(2,17) (3, 12)	1
MD-10-3	(3,11) (4, 12)	1
MD-10-4	(7,8) (8, 11)	1

Table 7.I: Characteristics of the request sets

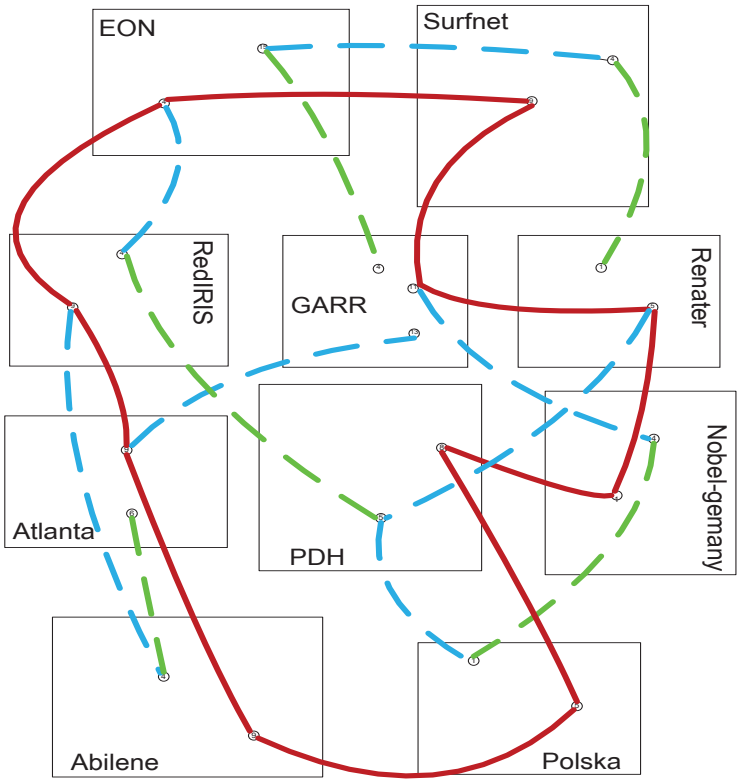

Figure 7.8: Topology of the MD-10-reduced

varying in {OC-1, 3, 6, 9, 12}. We used a shortest path routing for the primary routes. Once primary routing is completed, we are left with a set of inter-link sub-requests (see Section 6.2 for the definitions) that will be protected by p-cycles and a set of intra-domain sub-requests that will be protected by FIPP p-cycles in each domain.

7.6.2 Performance evaluation : quality and comparison of the solutions between centralized and distributed model

We compare the solutions of the centralized and the distributed protection scheme in Table 7.II where p-cycles are limited to go through no more than 3, 5, 7 and 9 domains as well as no limit is imposed on the number of domain traversals. We first observe that solutions ($z_{\text{CEN}}^{\text{ILP}}$ and $z_{\text{CEN}}^{\text{LP}}$ for the ILP and LP values, respectively) of the centralized scheme are obtained with a high accuracy as attested by the GAP values (see Section 2.6.1 for definitions), between 2.44% and 5.37%. Comparison of the distributed and centralized bandwidth requirements is done on two schemes proposed in Section 7.4.3, and through the relative differences of their solution values ($\text{Comp} = \frac{z_{\text{DIS}}^{\text{ILP}} - z_{\text{CEN}}^{\text{ILP}}}{z_{\text{CEN}}^{\text{ILP}}}(\%)$). For *Distributed scheme 1*, these differences are of the order of 5.61 %, on average, ranging from 4.16 % up to 6.96 %. It shows that distributed solutions are therefore quite good, in comparison with centralized ones. Moreover, if we use the set of 2-shortest paths in column generation technique for the mapping of virtual edges, solutions in *Distributed scheme 2* are not much better. Indeed, these differences are only 2.95 %, on average. In addition, observe that 2 to 7 rounds are necessary before reaching a stable bandwidth requirement for both of the distributed schemes.

7.6.3 Bandwidth requirement vs. number of inter-domain links

With the purpose of evaluating the impact of the number of inter-domain links to bandwidth requirement while still keeping a survivable multi-domain network, additional experriments were performed on *Distributed Scheme 1* that uses column generation technique to construct a virtual network. To do this, we remove some border nodes and some inter-domain links in the network MD-10. This modification is described in Table 7.I. The obtained results are illustrated in Table 7.III. We can observe that bandwidth requirement increase slightly when the number of inter-domain links reduce. In other words, we investigated the bandwidth requirements of a the multi-domain network where each domain has only two border nodes and

Instances			Centralized Scheme				Distributed Scheme 1				Distributed Scheme 2			
Instance number	# Requests	Bounds on the # of domain traversals	z^{LP}_{CEN}	z^{ILP}_{CEN}	Gap (%)	CPU times (sec.)	z^{ILP}_{DIS}	CPU times (sec.)	# Rounds	Comp(%)	z^{ILP}_{DIS}	CPU times (sec.)	# Rounds	Comp(%)
1	100	3	4,864.55	5,005	2.88	4,185	5,214	24,103	5	4.18	5,035	8,936	3	0.60
2		5	3,989.50	4,119	3.24	28,631	4,367	278,597	5	6.02	4,188	137,393	4	1.68
3		7	3,670.47	3,853	4.97	106,502	4,043	379,715	4	4.93	4,133	508,776	3	7.27
4		9	3,657.33	3,809	4.14	17,230	4,022	57,147	3	5.59	3,950	104,633	7	3.70
5		10	3,637.26	3,774	3.75	9,024	4,011	13,594	2	6.28	3,924	16,668	4	3.97
6	500	3	20,204.45	20,699	2.44	20,209	21,842	109,958	7	5.52	21,023	131,719	7	1.57
7		5	16,240.85	16,867	3.85	171,984	17,853	341,971	4	5.85	17,403	135,301	3	3.18
8		7	15,176.36	15,804	4.13	267,515	16,893	390,861	2	6.89	16,468	336,970	3	4.20
9		9	14,770.17	15,378	4.11	188,267	16,448	262,404	3	6.96	16,115	100,732	3	4.79
10		10	14,749.92	15,385	4.30	154,930	16,398	460,175	7	6.58	15,968	224,917	7	3.79
11	1000	3	40,436.75	41,526	2.69	91,792	43,485	219,702	4	4.72	41,922	270,143	3	0.95
12		5	32,918.26	34,470	4.71	236,068	36,190	370,325	3	4.99	35,026	409,629	4	1.61
13		7	30,638.66	32,220	5.16	287,450	33,561	460,293	2	4.16	33,305	354,797	2	3.37
14		9	29,750.60	31,185	4.82	123,632	32,532	179,275	2	4.32	32,222	289,754	3	3.33
15		10	29,540.21	31,127	5.37	153,568	32,615	215,109	3	4.78	31,945	400,747	5	2.63

Table 7.II: Comparison of the centralized/distributed scheme solutions

# Requests	Bounds on the # of domain traversals	MD-10-1	MD-10-2	MD-10-3	MD-10-4
100	5	5,295	5,328	5,351	5,376
	10	4,886	4,899	4,965	5,068
500	5	22,402	22,427	22,779	23,009
	10	20,689	20,712	20,898	21,118
1000	5	44,029	44,161	44,982	45,091
	10	40,021	40,315	41,610	41,847

Table 7.III: Comparison of the distributed scheme solutions (remove 1, 2, 3, 4 inter-domain links)

Instances	Scenario 1 (Red)			Scenario 2 (Red+ Green + Blue)		
# Requests	$z_{\text{DIS}}^{\text{ILP}}$	CPU times (sec.)	# Rounds	$z_{\text{DIS}}^{\text{ILP}}$	CPU times (sec.)	# Rounds
100	4,375	217	2	4,175	2,469	5
500	19,913	7,269	2	19,215	50,982	8
1000	38,218	42,247	2	36,536	97,453	3

Table 7.IV: Comparison of distributed scheme solutions

number of inter-domain links is very small. Indeed, we consider two scenarios of multi-domain networks: *Scenario 1* only contains one (solid red lines) cycle in the multi-domain network (see Figure 7.8) while *Scenario 2* is added several (dashed blue and green lines) inter-links. Results in Table 7.IV show that *Scenario 1* reaches a stable bandwidth requirement after 2 rounds, resulting from only one p-cycle and without sharing bandwidth between p-cycle and FIPP p-cycles while *Scenario 2* takes from 3 to 8 rounds. Because of small number of border nodes and inter-domain links, the different between two scenarios is not much. However, *Scenario 2* can provide shorter p-cycles than *Scenario 1*, that is meaningful in realistic.

7.7 Conclusion

We proposed the enhancement of the protection schemes that presented in Chapter 6. We improved the value of the objective function of previous CG-ILP models with bandwidth sharing. We also investigated two methods to construct a virtual aggregated network where physical paths mapping virtual edges are computed by column generation techique or by k-shortest paths. Experiments were successfully conducted on a multi-domain network with 10 domains. Results showed

that the proposed distributed scheme provided bandwidth efficient solutions. Indeed, the differences between solutions of the distributed scheme and the solutions of a centralized scheme, that computes an ideal exact solution, are around 7%.

CHAPTER 8

RESILIENT DESIGN OF VERY LARGE MULTI-DOMAIN OPTICAL NETWORKS

8.1 Chapter presentation

This chapter presents an article whose title is the same as this chapter. It will very shortly be submitted for publication in *JOCN - Journal of Optical Communications and Networking*. A shorter version of this paper with preliminary results was accepted in the *Proceedings of the International Telecommunications Network Strategy and Planning Symposium (Networks 2014)* under the title of "Distributed Resilient Design of Very Large Multi-Domain Optical Networks".

Herein, we investigate a two-level protection scheme for the design of survivable very large multi-domain optical networks. In this scheme, the shared link protection model is used to protect the inter-domain links, while the shared path protection model is used for the protection of paths or subpaths in each individual domain. First, we propose optimization models for both a centralized and a distributed scheme. In order to obtain solutions for very large multi-domain optical networks, up to 45 domains, we then propose a parallelization strategy for each of these schemes.

8.2 Virtual aggregated network and protection scheme

We use the same notations and definitions of multi-domain networks as in Section 6.2 of Chapter 6. Herein, we focus on concepts of virtual aggregated network and protection scheme before discussing about the mathematical models.

The optimization models that are proposed in Section 8.3 relies on an aggregated network, called virtual network, and denoted by $G^{\text{VIRTUAL}} = (V^{\text{BORDER}}, E^{\text{INTER}} \cup E^{\text{VIRTUAL}})$, derived from the multi-domain network topology, where V^{BORDER} is the set of border nodes, E^{INTER} is the set of inter-domain links and E^{VIRTUAL} is the set of

so-called virtual edges. In each domain, all pairs of border nodes are connected in G^{VIRTUAL} throughout virtual edges, where each virtual edge e' must be mapped onto one physical path $p_{e'}$. Note that each pair of border nodes, within a domain, can be connected by one or more virtual edges, where different virtual edges correspond to different physical paths.

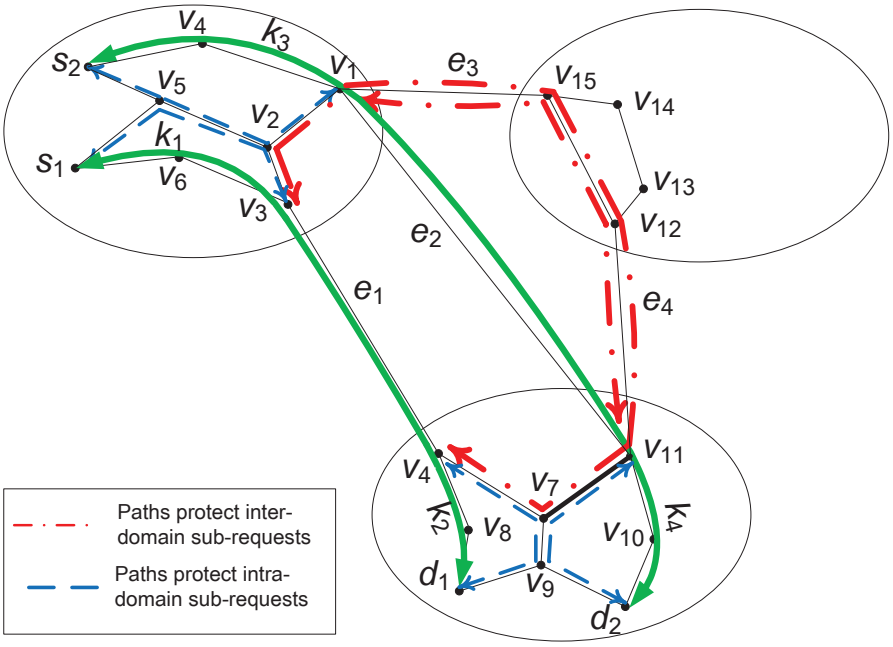

Figure 8.1: An illustration of the 2-level protection scheme

The union of these complete single-domain networks, together with the set of inter links, define a multi-graph as depicted in Figure 8.1. Therein, the multi-domain protection problem is decomposed into a two-level protection scheme, where the shared link protection model is generated on the virtual network for protecting the inter-domain links, and the shared path protection model is generated on each original domain to protect the intra-domain paths or segments. The bold green lines connecting $\{s_1, d_1\}$ and $\{s_2, d_2\}$ represent inter-domain requests that need to be protected. These requests are subdivided into two inter-domain link sub-requests $\{e_1, e_2\}$ and four intra-domain sub-requests $\{\kappa_1, \kappa_2, \kappa_3, \kappa_4\}$. The (dash followed by dot) red lines connecting border nodes $v_1, v_{15}, v_{12}, v_{11}$ and $v_3, v_2, v_1, v_{15}, v_{12}, v_{11}, v_7, v_4$

in Figure 8.1 represent shared paths to protect inter-domain physical links $\{e_1, e_2\}$ while shared paths protecting intra-domain sub-requests are represented by dashed blue lines. Note that each inter-domain edge in a path has a one-to-one mapping relation with an inter-domain physical link.

Each pair of border nodes, within a domain, is connected by one or more virtual edges, where each virtual edge is mapped onto a specific physical path, and different virtual edges correspond to different physical paths. In our two-level protection scheme, bandwidth requirement of intra protection level and inter protection level are independent in the context of single link failure, i.e., failures can not occur at the same time, and we assume we have the time to fix a first failure before a second one occurs. Indeed, the (dash followed by dot) red lines can reuse bandwidth of the dashed blue lines in Figure 8.1, and vice-versa. Based on these characteristics, we calculate parameters for virtual edges.

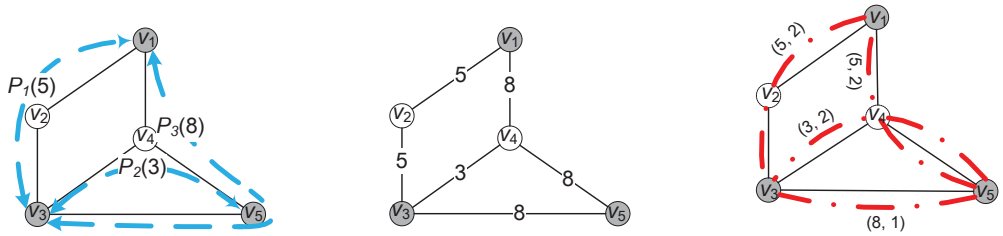

(a) Paths protect intra domain

(b) Available protection bandwidth

(c) Virtual network

Figure 8.2: Illustration of a virtual aggregated topology

Figure 8.2 illustrates the construction of a virtual network for one domain. The physical network comprises 5 nodes, of which three $\{v_1, v_3, v_5\}$ are border nodes, and 6 physical links. Figure 8.2(a) describes three paths, denoted by p_1, p_2 and p_3, to protect intra domain. These paths require 5, 3 and 8 bandwidth units respectively. In Figure 8.2(b), each physical link is associated with an integer indicating its available protection bandwidth, i.e., bandwidth requirement to protect intra domain which can be shared to protect inter-domain links. We use the mapping phase (Section 8.3.3.2) to calculate the spare capacity on each virtual edge. Here,

each virtual edge e' is denoted by a pair $\{\text{CAP}_{e'}, \text{LENG}_{e'}\}$, where $\text{CAP}_{e'}$ denotes the available bandwidth of virtual edge e' and $\text{LENG}_{e'}$ indicates the length of physical path $p_{e'}$, i.e., the mapping of virtual edge e'. The resulting virtual topology is described in Figure 8.2(c), with the mapping of the virtual edges onto the physical links, where the virtual edges are represented by (dash followed by dot) red lines and the physical links by plain lines. For example, from the path connecting nodes $\{v_3, v_2, v_1\}$ associated with virtual edge $\{v_3, v_1\}$ we deduce the available capacity $\text{CAP}_{\{v_3,v_1\}} = 5$ and $\text{LENG}_{\{v_3,v_1\}} = 2$.

8.3 Mathematical models

We propose here mathematical models for shared protection in multi-domain optical networks, the first one assuming a centralized management scheme, the second one a distributed scheme. The aim is to find the centralized/distributed protection scheme with the minimum bandwidth requirements. Both models rely on the concept of configurations, which we define below, before detailing the models.

8.3.1 Configurations and variables

There are three types of path configurations in our models.

In the inter level, each configuration is defined in the virtual network G^{VIRTUAL}, by a potential path together with the inter-domain link it protects. Let P_e be the overall set of potential path configurations for protecting the inter-link e, indexed by p. For each path p, we also define parameter $\alpha_e^p \in \{0, 1\}$ such that $\alpha_e^p = 1$ if e lies on path p, and 0 otherwise.

In the intra level, each configuration associates a path with the traffic (intra-domain request and sub-request) it protects in a given domain. Let P_κ be the overall set of potential path configurations for protecting the intra-domain sub-request κ. Similarly parameter $\beta_e^p \in \{0, 1\}$ is such that $\beta_e^p = 1$ if e lies on path p, and 0 otherwise.

The third path configuration is defined for virtual edges. Let $P_{e'}$ be the set

of potential path configurations for the mapping of a virtual intra-domain edge e' onto an intra physical path. Any $p \in P_{e'}$ is characterized by vector $\gamma_e^p \in \{0,1\}$ such that $\gamma_e^p = 1$ if physical link e lies on path p, 0 otherwise.

We use set of variables to keep track of how many bandwidth units of each resource (configuration) are used. Indeed, variables z_p^{INTER} stand for the number of unit-capacity copies of path configuration p to protect the inter-link e, variables z_p^{INTRA} stand for the number of unit-capacity copies of path configuration p to protect the intra-domain sub-request κ, and z_p^{VIR} for the amount of bandwidth associated with the mapping of virtual link e' onto the physical path $p \in P_{e'}$.

8.3.2 Centralized model

In the centralized model, it is assumed that the network management is aware of all the details of the physical topologies of the domains.

The objective function aims at minimizing capacity requirements to protect all the requests. Such capacity corresponds to the sum of the bandwidth requirements of the shared link protection model, of the shared path protection, and of the mappings of the intra virtual links while taking acount sharing bandwidth. The objective function is given by $z_{\text{OBJ}}^{\text{CEN}}(z_p^{\text{INTER}}, z_p^{\text{INTRA}}, z_p^{\text{VIR}}, \text{CAP}_e^P)$, and is written as follows:

$$\min z_{\text{OBJ}}^{\text{CEN}} \quad = \quad \sum_{e \in E^{\text{INTER}}} \text{CAP}_e^P \quad + \quad \sum_{d \in D} \quad \sum_{e \in E_d} \text{CAP}_e^P \quad (8.1)$$

subject to:

$$\sum_{p \in P_e} z_p^{\text{INTER}} \geq \text{CAP}_e^W \qquad e \in E^{\text{INTER}} \tag{8.2}$$

$$\sum_{p \in P_\kappa} z_p^{\text{INTRA}} \geq \text{CAP}_\kappa^{\text{W}} \qquad \kappa \in K_d, d \in D \tag{8.3}$$

$$\sum_{p \in P_e} \alpha_{e'}^p z_p^{\text{INTER}} \leq \text{CAP}_{e'} \qquad e' \in E^{\text{INTER}}, e \in E^{\text{INTER}} \setminus \{e'\} \tag{8.4}$$

$$\sum_{p \in P_{e'}} z_p^{\text{VIR}} - \sum_{p \in P_e} \alpha_{e'}^p z_p^{\text{INTER}} \geq 0 \qquad e' \in E^{\text{VIRTUAL}}, e \in E^{\text{INTER}} \tag{8.5}$$

$$\sum_{\kappa \in K_d : f \in \text{WP}_\kappa} \sum_{p \in P_\kappa} \beta_e^p z_p^{\text{INTRA}} \leq \text{CAP}_e^P \qquad e \in E_d, f \in E_d \setminus \{e\}, d \in D \tag{8.6}$$

$$\sum_{e' \in E_d^{\text{VIRTUAL}}} \sum_{p \in P_{e'}} \gamma_e^p z_p^{\text{VIR}} \leq \text{CAP}_e^P \qquad e \in E_d, d \in D \tag{8.7}$$

$$z_p^{\text{INTER}} \in \mathbb{Z}^+ \qquad p \in P_e \tag{8.8}$$

$$z_p^{\text{INTRA}} \in \mathbb{Z}^+ \qquad p \in P = \bigcup_{d \in D} P_d \tag{8.9}$$

$$z_p^{\text{VIR}} \in \mathbb{Z}^+ \qquad p \in P_{e'}, e' \in E_d^{\text{VIRTUAL}} \tag{8.10}$$

$$\text{CAP}_e^P \in \mathbb{Z}^+ \qquad e \in \bigcup_{d \in D} E_d. \tag{8.11}$$

Constraints (8.2) ensure that the working traffic on each inter-domain link is protected by a set of physical paths against any single inter-link failure. Constraints (8.3) guarantee a shared path protection for each intra-domain sub-request. Constraints (8.4) ensure that the required bandwidth by protetion paths on an inter-domain link is smaller than its available spare capacity. Constraints (8.5) ensure that each virtual link e' belonging to shared link protetion model is mapped onto one or more physical paths in order to protect the inter-link traffic. Constraints (8.6) ensure the bandwidth required by shared path proltection model on a intra-domain link. Constraints (8.7) ensure that the amount of bandwidth requested from an intra-domain link e by the mapping of virtual links to physical paths does not exceed the provided spare capacity.

8.3.3 Distributed models

We propose here a distributed protection model in multi-domain optical networks.

8.3.3.1 Outline

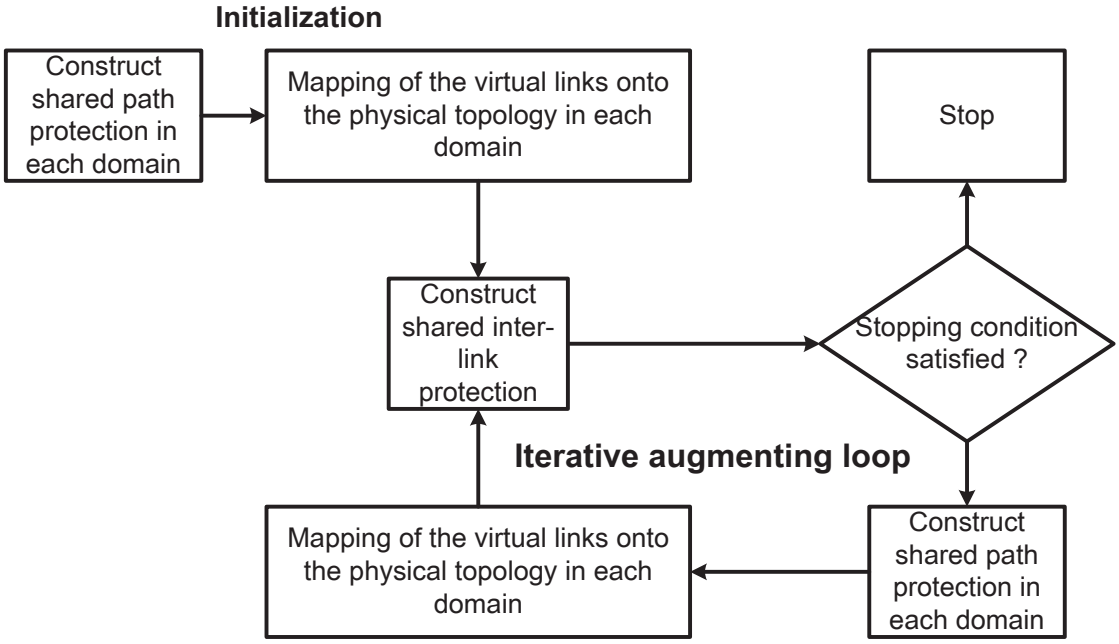

Figure 8.3: Flowchart of the distributed solution process (sequential version)

The distributed model is depicted in Figure 8.3. Initially, shared path protection scheme is independently generated in each domain, in order to protect intra-domain (sub-)requests while minimizing the total capacity usage. We then map the virtual links onto intra-domain physical paths, using as much as possible the bandwidth already reserved for the intra-domain protection. The iterative process then starts, where each iteration ends with the computation of a shared link protection scheme that protects the inter-domain working traffic given intra-domain capacities allocated to the virtual links. If an overall protection scheme with a smaller bandwidth requirement has been found, a new iteration is initiated. Shared link protection scheme is constructed using as much as possible the available bandwidth of the

virtual links, i.e., the bandwidth that can be shared with the protection paths in the intra level, and with additional bandwidth on those virtual links if the incumbent bandwidth is not sufficient. Shared path protection schemes are then possibly updated in order to take advantage of the added bandwidth (i.e., maximize the shared bandwidth in order to minimize the bandwidth requirements). Last, the mapping of the virtual links onto the physical domain topologies are revised. It leads to new spare bandwidth availability for each virtual link. The value of the objective function (overall bandwidth requirements for the shared link and path protection structures), z_{OBJ} (see Section 8.3.3.5) where t is the iteration index, is re-evaluated.

The computation of shared link protection scheme requires the knowledge of the capacity and length of the virtual links. These latter values are computed in the mapping phase, which takes care of mapping the virtual links onto physical paths. The computation of the shared path protection schemes require the knowledge of how much bandwidth is used in the inter level in a given domain. These values are obtained directly from the bandwidth computation of the shared link protection scheme. Therefore, the proposed distributed scheme satisfies the multi-domain network assumptions regarding the limitations on inter-domain sharing of operational information, i.e., do not assume any inter-domain information sharing. We propose then the models for these computations.

8.3.3.2 Model for constructing a virtual network

We propose an algorithm to construct a mapping of the virtual links onto a set of physical paths in each domain.

Input : Available spare bandwidth, i.e., bandwidth used for protecting intra domain on each physical link e, denoted by $\text{CAP}_e^{\text{INTRA}}$ for $e \in E_d, d \in D$.

Output : Information of the mapped virtual edges, denoted by $(\text{CAP}_{e'}, \text{LENG}_{e'})$ where $\text{CAP}_{e'}$ be the bandwidth capacity of virtual edge e' and $\text{LENG}_{e'}$ be the length of physical path p mapping of the virtual edge e'

The mapping phase is as follows:

1. Find the k-shortest paths [1] for each pair of border nodes

2. Solve the integer linear program MAP_ILP that determines the bandwidth capacity of the paths computed in Step 1, while re-using the bandwidth reserved for protecting inter-domain links

3. Map as many virtual links e', each onto a bandwidth provisioned physical path p using the source and destinations of e' and p. $\text{CAP}_{e'} = 0$ if e' is not mapped onto a physical path.

MAP_ILP: The objective function aims at maximizing the number of bandwidth provisioned physical paths for protecting intra domain. Let P_d be the potential set of physical paths (calculated in Step 1) between the pairs of border nodes. Denote by x_p the bandwidth capacity of virtual edge e' and mapped on physical path $p \in P = \bigcup_{d \in D} P_d$.

MAP_ILP

$$\max \quad \sum_{p \in P_d} x_p \tag{8.12}$$

$$\text{subject to:} \quad \sum_{p \in P_d} \delta_e^p x_p \leq \text{CAP}_e^{\text{INTRA}} \qquad e \in E_d, d \in D \tag{8.13}$$

$$x_p \in \mathbb{Z}^+ \qquad p \in P_d. \tag{8.14}$$

where $\delta_e^p = 1$ if physical link e lies on path p.

$\text{CAP}_{e'} = x_p^\star$ for virtual link e' belonging to $d \in D$, and mapped onto p, $\text{LENG}_{e'}$ equal length of physical path p,where $x_p^\star$ denotes the optimal value of x_p, after solving MAP_ILP.

1. $k = 2$ in our numerical experiments

8.3.3.3 Shared link protection model

Paths for protecting inter-domain links are computed on the virtual network where virtual links connect the protected inter-domain links.

The objective function aims at minimizing the bandwidth requirements, i.e., the sum of the bandwidth requirements for the inter-domain links and the required added capacity on the physical paths on which the virtual edges are mapped, in order to protect the inter-domain links. Maximizing the bandwidth sharing with the intra-domain protection amounts to maximize the re-use of the $\text{CAP}_e^{\text{INTRA}}$ bandwidth, under a single link failure assumption (whether the link is an inter or an intra domain link). Moreover, bandwidth is also shared among paths for protecting inter-domain links. The objective function is given by $z_{\text{PROTECT}}^{\text{INTER}}(z_p^{\text{INTER}}, \text{ADD}_{e'})$, and is written as follows:

$$\min z_{\text{PROTECT}}^{\text{INTER}} = \underbrace{\sum_{e \in E^{\text{INTER}}} \text{ADD}_e}_{\substack{\text{Bandwidth requirements} \\ \text{for the inter-domain links}}} + \underbrace{\sum_{e' \in E^{\text{VIRTUAL}}} \text{LENG}_{e'} \text{ADD}_{e'}}_{\substack{\text{Additional bandwidth} \\ \text{in the intra domains}}}, \quad (8.15)$$

where $\text{ADD}_{e'}$ (or ADD_e) estimates the amount of required additional bandwidth, if any, on virtual edge e' (or inter-domain link e), in order to protect all inter-domain link requests. Constraints can be written as follows :

$$\sum_{p \in P_e} z_p^{\text{INTER}} \geq \text{CAP}_e^W \qquad e \in E^{\text{INTER}} \quad (8.16)$$

$$\sum_{p \in P_e} \alpha_{e'}^p z_p^{\text{INTER}} \leq \text{ADD}_e \qquad e' \in E^{\text{INTER}}, e \in E^{\text{INTER}} \setminus \{e'\} \quad (8.17)$$

$$\sum_{p \in P_e} \alpha_{e'}^p z_p^{\text{INTER}} \leq \text{CAP}_{e'} + \text{ADD}_{e'} \qquad e' \in E^{\text{VIRTUAL}}, e \in E^{\text{INTER}} \quad (8.18)$$

$$z_p^{\text{INTER}} \in \mathbb{Z}^+ \qquad p \in P \quad (8.19)$$

$$\text{ADD}_{e'} \in \mathbb{Z}^+ \qquad e' \in E^{\text{VIRTUAL}} \quad (8.20)$$

$$\text{ADD}_e \in \mathbb{Z}^+ \qquad e \in E^{\text{INTER}}. \quad (8.21)$$

Constraints (8.16) ensure that the working traffic on each inter-domain link is fully protected by paths. Constraints (8.17) ensure that the required bandwidth by protetion paths on an inter-domain link is smaller than its available spare capacity. Constraints (8.18) ensure that the amount of bandwidth requested from an virtual edge e' does not exceed the available spare capacity and the possibly added capacity.

The bandwidth requirements for protecting inter-domain links on virtual link $e' \in E_d^{\text{VIRTUAL}}, d \in D$, are $\text{CAP}_{e'}^{\text{REQ}} = \text{Max}_{e \in E^{\text{INTER}}} \left(\sum_{p \in P_e} \alpha_{e'}^{p} z_p^{\text{INTER}(\star)} \right)$, where $z_p^{\text{INTER}(\star)}$ denotes the optimal value of z_p^{INTER} in model (8.15) - (8.21).

8.3.3.4 Shared path protection model

Paths are also constructed in each domain to protect intra-domain sub-requests and requests.

Input: $\text{CAP}_e^{\text{INTER}} = \sum_{e' \in E_d^{\text{VIRTUAL}}} \delta_e^{p(e')} \text{CAP}_{e'}^{\text{REQ}}$ is the bandwidth used for protecting inter-domain links on intra-domain link e, where $p(e')$ denotes the physical path mapping of the virtual link e', $\delta_e^{p(e')} = 1$ if physical link e lies on the path $p(e')$. $\text{CAP}_e^{\text{INTER}}$ will be re-used as much as possible in order to construct paths for protecting intra-domains. At the outset, (i.e, $t = 0$), $\text{CAP}_e^{\text{INTER}} = 0$.

Output: Bandwidth requirements on the intra-domain links, $\text{CAP}_e^{\text{INTRA}}$ for $e \in E_d, d \in D$.

The objective function aims at minimizing the added capacity, ADD_e, induced by protection paths. It is written as follows:

$$\min \quad \sum_{e \in E_d} \text{ADD}_e \tag{8.22}$$

Constraints are written as follows:

$$\sum_{p \in P_\kappa} z_p^{\text{INTRA}} \geq \text{CAP}_\kappa^{\text{W}} \qquad \kappa \in K_d \tag{8.23}$$

$$\sum_{\kappa \in K_d : f \in \text{WP}_\kappa} \sum_{p \in P_\kappa} \beta_e^p z_p^{\text{INTRA}} \leq \text{CAP}_e^{\text{INTER}} + \text{ADD}_e \qquad e \in E_d, f \in E_d \diagdown \{e\} \tag{8.24}$$

$$z_p^{\text{INTRA}} \in \mathbb{Z}^+ \qquad p \in P_\kappa, \kappa \in K_d \tag{8.25}$$

$$\text{ADD}_e \in \mathbb{Z}^+ \qquad e \in E_d. \tag{8.26}$$

Constraints (8.23) guarantee a protection for each intra-domain segment. Constraints (8.24) ensure that the required bandwidth by protetion paths on an intra-domain link is smaller than its available spare capacity (i.e., the capacity is used to protect inter-domain links)and added capacity.

The bandwidth requirements for protecting intra-domain level on link $e \in E_d$, $d \in D$, are: $\text{CAP}_e^{\text{INTRA}} = \text{Max}_{f \in E_d \diagdown \{e\}} \left(\sum_{\kappa \in K_d : f \in \text{WP}_\kappa} \sum_{p \in P_\kappa} \beta_e^p z_p^{\text{INTRA}(\star)} \right)$, where $z_p^{\text{INTRA}(\star)}$ denotes the optimal value of z_p^{INTRA} in model (8.22) - (8.26). And the bandwidth requirements for protecting intra-domain level in domain d is: $z_{\text{PROTECT}}^{\text{INTRA}(d)} = \sum_{e \in E_d} \text{CAP}_e^{\text{INTRA}}$.

8.3.3.5 Overall bandwidth requirements

At a current iteration t, before the stopping condition, see the flowchart in Figure 8.3, the overall bandwidth requirements are as follows:

$$z_{\text{OBJ}} = z_{\text{PROTECT}}^{\text{INTER}} + \sum_{d \in D} z_{\text{PROTECT}}^{\text{INTRA}(d)}. \tag{8.27}$$

8.4 Solution of the ILP model

A straightforward way to solve the ILP models of the previous would be to enumerate all potential path configurations. Although easy, it will not be scalable. Indeed, the ILP models of Section 8.3 have each a natural decomposition which

allows their linear relaxation to be solved by column generation techniques (see Section 2.6.1 for the "*base*" framework of ILP & column generation algorithm), and therefore ensure a scalable solution scheme.

The optimization model of the centralized scheme corresponds to a master problem with three different pricing problem. Formulations of the pricing problems can be constructed as follows.

The pricing problem, denoted by $\mathrm{PP}^{\mathrm{CEN}}_{\mathrm{INTER}}(e)$ for $e \in E^{\mathrm{INTER}}$, is set and and solved for each inter-domain link e. The reduced cost objective, $\mathrm{REDCOST}_{pe}$, depends on dual variables $u_e^{(8.2)}$ and $u_{e'}^{(8.5)}$ associated with constraints (8.2) and (8.5) respectively.

$$\mathrm{REDCOST}_{pe} = \sum_{e \in E^{\mathrm{INTER}}} s_e - u_e^{(8.2)} + \sum_{e' \in E^{\mathrm{VIRTUAL}}} s_{e'} u_{e'}^{(8.5)} \tag{8.28}$$

where $s_e = 1$ if link e lies on path configuration p, 0 otherwise.

The pricing problem, denoted by $\mathrm{PP}^{\mathrm{CEN}}_{\mathrm{INTRA}}(\kappa, d)$ for $\kappa \in K_d, d \in D$, is set and and solved for each intra-domain sub-request κ in domain d. The reduced cost objective, $\mathrm{REDCOST}^{d}_{p\kappa}$, depends on dual variables $u_{\kappa d}^{(8.3)}$ and $u_{efd}^{(8.6)}$ associated with constraints (8.3) and (8.6) respectively.

$$\mathrm{REDCOST}^{d}_{p\kappa} = -u_{\kappa d}^{(8.3)} + \sum_{e \in E_d} \sum_{f \in E_d \setminus \{e\}} s_e u_{efd}^{(8.6)} \tag{8.29}$$

The pricing problem, denoted by $\mathrm{PP}^{\mathrm{CEN}}_{\mathrm{VIR}}(e', d)$ for $e' \in E_d^{\mathrm{VIRTUAL}}, d \in D$, is set and and solved for each virtual link e' in domain d. The reduced cost objective, $\mathrm{REDCOST}_{e'd}$, depends on dual variables $u_{e'}^{(8.5)}$ and $u_{ed}^{(8.7)}$ associated with constraints (8.3) and (8.6) respectively.

$$\mathrm{REDCOST}_{e'd} = -u_{e'}^{(8.5)} + \sum_{e \in E_d} s_e u_{ed}^{(8.7)} \tag{8.30}$$

where $s_e = 1$ if link e lies on path configuration p, 0 otherwise.

Constraints of pricing problems can be determined by constructing a path in

the modified graph $G' = (V, E')$, where $E' = E^{\text{VIRTUAL}} \setminus \{e\}$ for the pricing problem $\text{PP}^{\text{CEN}}_{\text{INTER}}(e)$, or $E' = E_d \setminus \{e : e \in \text{WP}_\kappa\}$ for the pricing problem $\text{PP}^{\text{CEN}}_{\text{INTRA}}(\kappa, d)$, or $E' = E_d$ for the pricing problem $\text{PP}^{\text{CEN}}_{\text{VIR}}(e', d)$.

The model associated with the distribution scheme involves two column generation models, one for the inter level, another for the intra level. Formulations of their pricing problems can be determined as follows.

In the inter level, for each inter-domain link e, the reduced cost objective of the pricing problem, denoted byREDCOST_{pe}, depends on dual variables $u_e^{(8.16)}$, $u_{e'e}^{(8.17)}$ and $u_{e'e}^{(8.18)}$ associated with constraints (8.16) and (8.18) respectively.

$$\text{REDCOST}_{pe} = -u_e^{(8.16)} + \sum_{e' \in E^{\text{INTER}} \setminus \{e\}} s_{e'} u_{e'e}^{(8.17)} + \sum_{e' \in E^{\text{VIRTUAL}}} s_{e'} u_{ee'}^{(8.18)} \tag{8.31}$$

where $s_e = 1$ if link e lies on path configuration p, 0 otherwise.

In the intra level, for each intra-domain sub-request κ, the reduced cost objective, $\text{REDCOST}^d_{p\kappa}$, depends on dual variables $u_\kappa^{(8.23)}$ and $u_{ef}^{(8.24)}$ associated with constraints (8.23) and (8.24) respectively.

$$\text{REDCOST}^d_{p\kappa} = -u_\kappa^{(8.23)} + \sum_{e \in E_d} \sum_{f \in E_d \setminus \{e\}} s_e u_{ef}^{(8.24)} \tag{8.32}$$

Constraints of pricing problems can be determined by constructing a path in the modified graph $G' = (V, E')$, where $E' = E^{\text{VIRTUAL}} \setminus \{e\}$ in the inter level or $E' = E_d \setminus \{e : e \in \text{WP}_\kappa\}$ in the intra level.

8.5 Parallel implementations

In this section, we describe parallelization strategies for both proposed centralized and distributed scheme in order to find a solution for very large multi-domain networks.

8.5.1 Centralized scheme in parallel

As described in Section 8.4, an iteration of the column generation in the centralized scheme is defined as a solution of the restricted master problem (RMP) and the pricing problems (PPs). There is no data or control dependencies among the PPs, therefore the computation of the PPs can be performed independently. We will use this particularity of the pricing problems to parallelize the centralized scheme. To clarify this aspect of column generation, an example is presented in Figures 8.4 and 8.5.

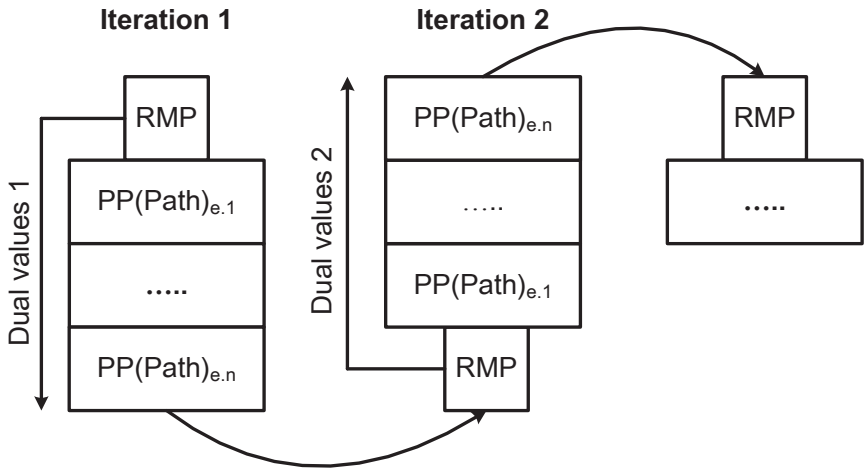

Figure 8.4: Sequential version of centralized scheme

The sequential implementation is described in Figure 8.4. In this figure, *"Dual values 1"* represents the vector of dual variables obtained after the first solution of the RMP. Once (PPs) are solved, a new set of columns is produced which triggers the second column generation iteration. This new iteration consists of solving the RMP with the new columns and, sequentially, solving PPs with the new vectors of dual variables *"Dual values 2"*.

In the parallel implementation, the computation of the restricted master problem and of each pricing problem is assigned to different processors. The restricted master problem is always solved first on the host machine, next the pricing problems are be solved in parallel. The iterations are thus performed synchronously.

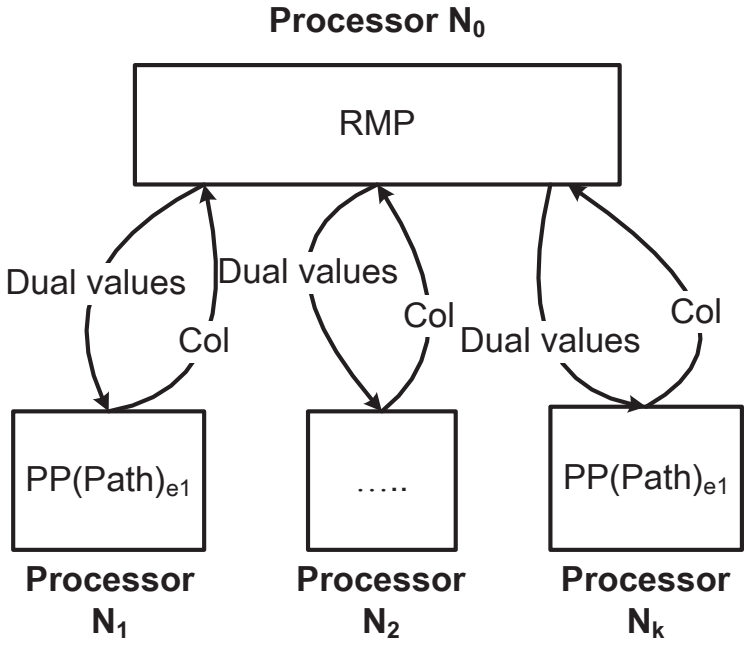

Figure 8.5: Parallel version of centralized scheme

This implementation is depicted in more details in Figure 8.5. Initially, processor N_0 solves the restricted master problem. As soon as the RMP is solved, N_0 sends the vector of dual variables to each of the processors computing the solution of the pricing problems. All those processors receive the dual variables, solve the pricing problems and send back the columns to processor N_0 for a new iteration. The process is repeated until the optimal linear programming solution is found, i.e., no new column can be found. Algorithm 2 describes the process in detail.

8.5.2 Distributed scheme in parallel

We also investigate a parallel strategy for the proposed distributed scheme. We have the advantage that this scheme can be implemented directly in parallel. This implementation is depicted in more details in Figure 8.6. Processor N_0 is used to find a new shared inter-link protection solution. Then, N_0 sends the capacity requirement on the virtual links to each processor allocated in each domain of the multi-domain network. Those processors in parallel re-optimize the shared path

Algorithm 2 Parallel Centralized Scheme

Step 1: Initiate the parallel computing environment by creating n processes with N_0 as the master process and N_1 to N_{n-1} as the slave processes.
Step 2: The master process solves the current RMP, i.e., (8.1)-(8.7), and determines the dual values associated with constraints.
Step 3: The master process broadcasts the dual values to each slave master and assign i^{th} slave to solve the i^{th} pricing problem.
Step 4: Once i^{th} slave finishes to solve the i^{th} pricing problem, it sends a feedback (a new column with a negative reduced cost or a message to said that no such a column is found) to the master.
Step 5: After all of the slaves return their feedbacks, if all said that no column is found, then the optimal linear programming solution is found, the master solves the ILP model resulting from set of columns of the last solved RMP in order to output an ILP solution, and the algorithm teminates. Otherwise, go to Step 2

protection solutions, map the virtual links (construct an aggregated topology) and send back this information to processor N_0. The process is repeated until a feasible solution is found. Algorithm 3 describes the process in detail.

8.6 Computational results

We implemented the model developed in Section 8.3 and solved it using the solution process described in Section 8.4 and 8.5. Algorithms were implemented using the OPL programming language, C++ and solved using CPLEX 12. We used the message passing interface (MPI) library routines to develop the message-passing environment for distributed computing. Programs were run on a group of 4 computer nodes. Each node has two Intel Westmere EP X5650 six-core processors running at 2.667 GHz [1].

We examined the protection schemes on a very large multi-domain network, with 45 domains built from real optical networks EON [56], RedIrid [3], Garr [2], Renater [4], Surfnet [5], Atlanta, PDH, Nobel-germany, Abilence [58]. The numbers of nodes and links of each network are: EON (20, 39), RedIrid (19, 31), Garr (15, 24), Renater (18, 23), Surfnet (25, 34), Atlanta (15, 22), PDH (11, 34), Nobel-germany(17, 26), Abilence (11, 14). For each optical network, we identify 3 or

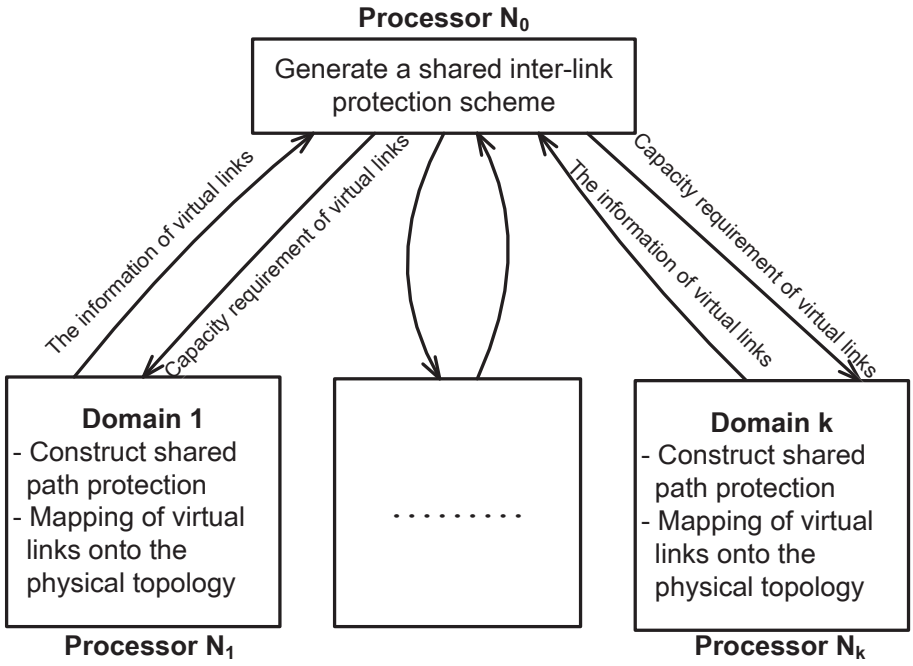

Figure 8.6: Flowchart of the distributed solution process (sequential version)

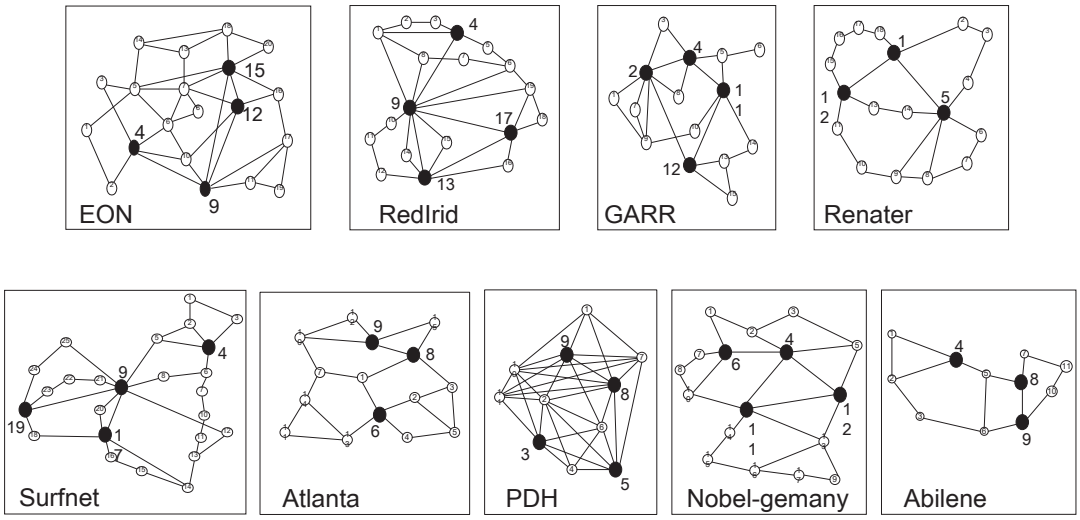

Figure 8.7: Network topologies and border nodes

4 border nodes. Fig 8.7 describes the topologies of the networks as well as their border nodes (black nodes).

In order to built a multi-domain network with 45 domains, we use 5 copies of

Algorithm 3 Parallel Distributed Scheme

Step 1: Initiate the parallel computing environment by creating n processes with N_0 as the master process and N_1 to N_{n-1} as the slave processes.

Step 2: The i^d slave process caculates bandwidth requerements, $z_{\text{PROTECT}}^{\text{INTRA}(d)}$, for protecting intra-domain subrequests in domain d, using the CG-ILP model proposed in Section 8.3.3.4. The slave then calculates the information, $(\text{CAP}_{e'}, \text{LENG}_{e'})$, of the virtual edge $e' \in E^{\text{VIRTUAL}}$, using the ILP model in Section 8.3.3.2 and send them with $z_{\text{PROTECT}}^{\text{INTRA}(d)}$ to the master process.

Step 3: After receiving the information of virtual edges from all slaves, the master process solves the CG-ILP model described in Section 8.3.3.3 and determines $z_{\text{PROTECT}}^{\text{INTER}}$ which is the bandwidth requirements for the inter-domain links and the required added capacity on virtual edges in order to protect the inter-domain links.

Step 4: The master checks an overall bandwidth requirement, z_{OBJ}. If the ε-optimal distributed solution is found, i.e., $(z_{\text{OBJ}} - z_{\text{OBJ}}^{\star}) / z_{\text{OBJ}}^{\star} \leq \varepsilon$ where $z_{\text{OBJ}}^{\star}$ is the overall bandwidth requirement of the current best solution, then the algorithm teminates. Otherwise, the master broadcasts the information of all virtual edges to slaves and go to step 2.

each given network with the same way to choose the border nodes. Then, some inter-links are added to connect the border nodes of the domains such that each domain has 4 neighboring domains and the multi-domain network is a grid one. The topology of this multi-domain network is depicted in Fig 8.8.

Experiments are conducted on sets of 100 up to 1,000 inter requests, which are generated between randomly selected pairs of nodes with bandwidth requirement varying in {OC-1, 3, 6, 9, 12}. We used a shortest path routing for the primary routes. Once primary routing is completed, we are left with a set of inter-link sub-requests (see Section 6.2 for the definitions) that will be protected by shared link protection model and a set of intra-domain sub-requests that will be protected by shared path protection model in each domain.

The results are summarized in Table 8.I. For both schemes, we limit paths for the protection of the inter-link sub-requests to go through no more than 3 domains or 7 domains. For centralized scheme, we provide the solutions that are output by the solution process: $z_{\text{CEN}}^{\text{LP}}$ is the optimal solution of the LP relaxation, hence a lower bound on the optimal ILP solution, $z_{\text{CEN}}^{\text{ILP}}$ is the integer solution. Quality of solutions

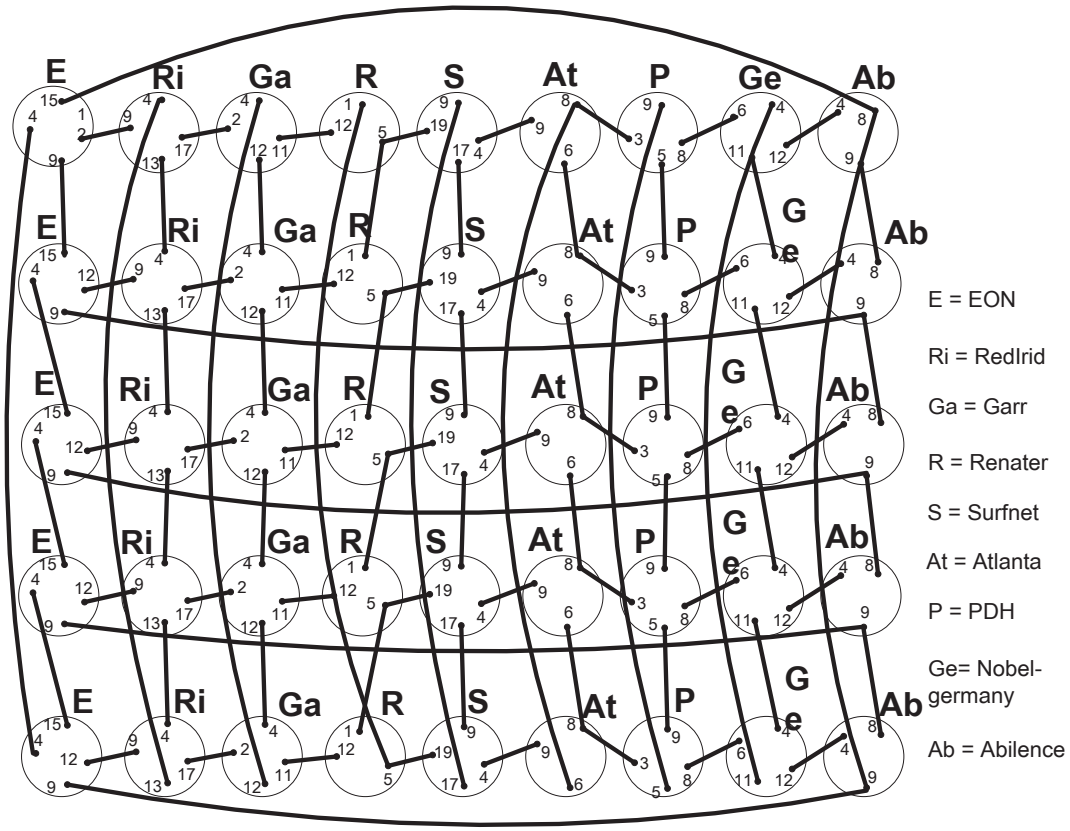

Figure 8.8: Topology of multi-domain network

can be measured by the optimality gap, as defined in Section 2.6.1. As shown in Table II, the obtained optimality gaps are very small for all benchmark instances, meaning our solutions are all nearly optimal. For distributed scheme, observe that 4 to 11 rounds are necessary before reaching a stable bandwidth requirement for the distributed scheme. Comparison of the distributed and centralized bandwidth requirements is done in the last column through the relative differences of their solution values. Indeed, this value is about 30% on average. However, note that the results corresponds to the largest multi-domain network solved so far with 45 domains. Computation times are very reasonable for both schemes thanks to proposed parallel stratergies.

Instances			Centralized Scheme Solutions				Distributed Scheme Solutions			Comparision
Instance number	# Requests	Bounds on the # of domain traversals	$z^{\text{LP}}_{\text{CEN}}$	$z^{\text{ILP}}_{\text{CEN}}$	Gap (%)	CPU times (sec.)	$z^{\text{ILP}}_{\text{DIS}}$	CPU times (sec.)	# Rounds	$\frac{z^{\text{ILP}}_D - z^{\text{ILP}}_C}{z^{\text{ILP}}_C}(\%)$
1	100	3	8,918.9	8,985	0.7	10,537	11,426	3,106	4	27.17
2		7	8,559.4	8,705	1.7	10,994	11,265	6,364	9	29.41
3	200	3	18,113.4	18,152	0.2	23,487	23,055	9,694	10	27.01
4		7	17,300.8	17,335	0.2	23,862	22,308	4,788	5	28.69
5	500	3	42,381.6	42,455	0.2	59,709	54,835	7,924	9	29.16
6		7	40,926.5	40,970	0.1	62,840	53,043	9,341	11	29.47
7	1000	3	80,287.2	80,335	0.1	96,491	104,310	12,392	4	29.84
8		7	76,263.0	76,308	0.1	110,435	100,444	29,484	10	31.63

Table 8.I: Performance of the centralized/distributed scheme solutions

8.7 Conclusion

In this chapter we have presented new developments for protection in multi-domain optical networks. The method relies on a two-level protection scheme in which inter-domain working traffic is protected by a shared link protection scheme and intra-domain working traffic is protected by a shared path protection scheme. The different optimization problems are solved exactly thanks to mathematical models relying on large scale optimization tools for their solution. Parallel strategies are also proposed in order to solve the large instances. The result of this study allows the efficent design of a protection scheme for very large multi-domain networks (45 domains) both with a centralized and distributed scheme.

CHAPTER 9

CONCLUSIONS AND FUTURE WORKS

9.1 Conclusions

As a core problem in optical networks, the RWA problem has been extensively studied in many existing approaches. However, conventional formulations are challenged with scalability issues due to the large network size and the large number of wavelengths supported on a single fiber nowadays. Moreover, the existing algorithms do not consider asymmetric switching property which is a key property of the WSS based ROADM network. In order to solve these problems, we have proposed two CG-ILP models: (*i*) a CG-ILP model for the RWA problem in network with pre-configured asymmetric nodes; (*ii*) a CG-ILP for the RWA problem with the objective of finding the best switching connectivity matrix for a given number of ports and a given number of switching connections.

Protection against single failure is a particular case of the overall survivability issue in communication networks. To make our approach more general, we have addressed protection against multiple failures. As protection against multiple failures has not been widely addressed for single domain networks, we have first considered protection against multiple failures in a single domain. We proposed a new flow formulation for FIPP p-cycles subject to multiple failures, derived from a generic flow formulation for shared path protection, which resembles the model of Orlowsky and Pioro [57]. Although it is a column generation formulation, the pricing problem may have many constraints, making it difficult to design an efficient exact algorithm to solve it. Therefore, we have proposed two heuristics in order to efficiently solve the pricing problems.

Multi-domain networks are characterized by the autonomy of different domain components and scalability requirements. The autonomy implies that no external element has direct control over the internal domain resources. The scalability

requirement leads to a situation where no network node has a complete view of the entire network. Such characteristics make the protection of multi-domain lightpaths more difficult than single-domain ones.

The existing protection approaches either limit themselves to single-domain networks, or are using heuristics to solve the multi-domain lightpath protection problem in an inefficient way in terms of recovery quality and resource utilization. In this study, we have proposed a protection strategy to address the issue of recovery quality and we have developed a large scale optimization model, with the additional feature of parallel and distributed schemes, to address the issue of efficient resource utilization in quite large instances.

We have proposed an original 2-level decomposition scheme of the protection problem in multi-domain optical networks. This decomposition allows representing the protection problem into two subproblems: one is the protection of inter-domain links using p-cycles or a shared link protection model which scale at the level of the multi-domain network; another is the protection of intra-domain working paths which can be performed at the level of each domain using FIPP p-cycles or a shared path protection model. Moreover, our large scale optimization model formally addresses this minimum cost 2-level protection problem.

We have proposed a centralized model that obtains an exact solution for the protection problem, using parallel column generation, which can tackle quite large instances. The problem of optimizing resource utilization for protection in multi-domain optical networks is inherently a distributed optimization problem. Consequently, we have proposed a distributed optimization model to provide realistic solutions to protection in multi-domain. For each data network instance, the distributed scheme yields several independent optimization problems that are solved in parallel. Extensive experiments were successfully conducted on very large multi-domain optical networks, up to 45 domains.

9.2 Future Works

With respect to the provisioning problem in optical networks with asymmetric nodes, we plan to adapt the proposed models to dynamic traffic, in order to take advantage of the flexibility of ROADMs.

With respect to protection problems, we firstly need to further study how to improve the proposed solutions for the protection against multiple failures in single domain networks. Indeed, future work will include further investigations of the heuristic strategies in order to reach a better accuracy without increasing the computing times, and ultimately with multiple failure sets not limited to dual failure sets. Then, we will extend the protection in multi-domain networks against multiple failures, e.g., with dual failures in multi-domain for a selection of critical pairs.

In other words, we plan to improve the quality as well as the computing times of the proposed parallel solutions. For the centralized scheme, we plan to investigate different solution strategies for the pricing problem, e.g., we do not need to solve all pricing problems at each round of the column generation solution algorithm. For the distributed scheme, we will focus on improving sharing bandwidth between inter level and intra level in order to reduce the accuracy, e.g., using CG-ILP for calculating a virtual network.

BIBLIOGRAPHY

[1] *Calcul Quebec*. `http://http://calculquebec.ca/en/`.

[2] *Consortium GARR*. `http://www.garr.it`.

[3] *Redirid*. `http://www.rediris.es/rediris/index.html.en`.

[4] *RENATER-4 network*. `http://www.renater.fr`.

[5] *Surfnet*. `http://www.surfnet.nl`.

[6] J. Akpuh and J. Doucette. Enhanced failure-specific p-cycle network dual-failure restorability design and optimization. *J. Opt. Netw*, 8:1–13, 2009.

[7] D.L. Applegate, R.E. Bixby, V. Chvatal, and W.J. Cook. *The Traveling Salesman Problem: A Computational Study*. Princeton University Press, 2007.

[8] R. Asthana, Y. Singh, and W. Grover. p-cycles: An overview. *Communication Surveys Tutorials*, 12(1):97–111, 2010.

[9] C. Barnhart, E.L. Johnson, G.L. Nemhauser, M.W.P. Savelsbergh, and P.H. Vance. Branch-and-price: Column generation for solving huge integer programs. *Operations Research*, 46:316–329, 1998.

[10] C. Barnhart, E.L. Johnson, G.L. Nemhauser, M.W.P. Savelsbergh, and P.H. Vance. Branch-and-price: Column generation for solving huge integer programs. *Operations Research*, 46(3):316–329, 1998.

[11] R. Barry and O. Humblet. Models of blocking probability in all-optical networks with and without wavelength changers. *IEEE Journal of Selected Areas in Communications*, 14(5):858–867, 1996.

[12] G.M. Bernstein, Y. Lee, A. Gavler, and J. Martensson. Modeling WDM wavelength switching systems for use in GMPLS and automated path computation. *Journal of Optical Communications and Networking*, 1(1):187–195, June 2009.

[13] R. Bhandari, editor. *Survivable Networks: Algorithms for Diverse Routing*. Kluwer Academic Publishers, Massachusetts, USA, 1999.

[14] Y. Chen, N. Hua, X. Wan, H. Zhang, and X. Zheng. Dynamic lightpath provisioning in optical WDM mesh networks with asymmetric nodes. *Photonic Network Communications*, 25:166–177, 2013.

[15] I. Chlamtac, A. Ganz, and G. Karmi. Lightpath communications: An approach to high bandwidth optical wans. *IEEE Transactions on Communications*, 40: 1171–1182, 1992.

[16] H. Choi, S. Subramaniam, and H.A. Choi. On double-link failure recovery in WDM optical networks. In *IEEE Annual Joint Conference of the IEEE Computer and Communications Societies - INFOCOM*, volume 2, 2002.

[17] V. Chvatal. *Linear Programming*. Freeman, 1983.

[18] M. Clouqueur and W. D. Grover. Mesh-restorable networks with complete dual failure restorability and with selectively enhanced dualfailure restorability properties. *Optical Network and Communications*, 4874(1):1–12, 2002.

[19] M. Clouqueur and W.D. Grover. Mesh-restorable networks with enhanced dual-failure restorability properties. *Photonic Network Communications*, 9(1): 7–18, January 2005.

[20] G. Desaulniers, J. Desrosiers, and M. M. Solomon, editors. *Column Generation*, GERAD 25th Anniversary Series, 2005. Spring.

[21] J. Doucette, W. Li, and M. Zuo. Failure-specific p-cycle network dualfailure restorability design. In *Workshop on Design of Reliable Communication Networks - DRCN*, pages 1–9, 2007.

[22] H. Drid, B. Cousin, S. Lahoud, and M. Molnar. Multi-criteria p-cycle network design. In *IEEE conference on local computer networks (LCN)*, pages 361–366, 2008.

[23] H. Drid, B. Cousin, M. Molnar, and N. Ghani. Graph partitioning for survivability in multidomain optical networks. In *IEEE international conference on communications (ICC)*, pages 1–5, 2010.

[24] H. Drid, S. Lahoud, B. Cousin, and M. Molnar. Survivability in multi-domain optical networks using p-cycles. *Photonic Network Communications*, 19(1): 81–89, 2010.

[25] M. Eiger, H. Luss, and D. Shallcross. Optical path restoration for up to two failures using preconfigured cycles. *Telecommunication Systems*, 2011.

[26] M.I. Eiger, H. Luss, and D.F. Shallcross. Network restoration under a single link or node failure using preconfigured virtual cycles. *Telecommunication Systems*, 46(1):17–30, 2011.

[27] O. Gerstel, G. Sasaki, S. Kutten, and R. Ramaswami. Worst-case analysis of dynamic wavelength allocation in optical networks. *IEEE/ACM Transactions on Networking*, 7(6):833–845, 1999.

[28] N. Ghani, Q. Liu, A. Gumaste, D. Benhaddou, N. Rao, and T. Lehman. Control plane design in multidomain/multilayer optical networks. *IEEE Communications Magazine*, 2008.

[29] P.C. Gilmore and R.E. Gomory. A linear programming approach to the cutting-stock problem. *Operations Research*, 9:849–859, December 1961.

[30] P.C. Gilmore and R.E. Gomory. A linear programming approach to the cutting-stock problem-part ii. *Operations Research*, 11:863–888, December 1963.

[31] J. Gondzio, P.G. Brevis, and P. Munari. New developments in the primal–dual column generation technique. *Journal of Optical Communications and Networking*, pages 41–51, 2013.

[32] W. D. Grover and D. Stamatelakis. Cycle-oriented distributed preconfiguration: Ring-like speed with mesh-like capacity for self-planning network restoration. In *IEEE International Conference on Communications - ICC*, pages 537–543, June 1998.

[33] W.D. Grover and D. Stamatelakis. Bridging the ring-mesh dichotomy with p-cycles. In *Proceedings of IEEE/VDE Workshop on Design of Reliable Communication Networks - DRCN*, pages 92–104, Munich, Germany, April 2000.

[34] W.D. Grover, J. Doucette, A. Kodian, D. Leung, A. Sack, M. Clouqueur, and G. Shen. *Design of survivable networks based on p-cycles*. 2006.

[35] M.F. Habiba, M. Tornatoreb, F. Dikbiyikc, and B. Mukherjeea. Disaster survivability in optical communication networks. *Computer Communications*, 36: 630–644, 2013.

[36] T. Hashiguchi, Y. Zhu, K. Tajima, Y. Takita, T. Naito, and J. P Jue. Iteration-free node-disjoint paths search in WDM networks with asymmetric nodes. In *International Conference on Optical Networking Design and Modeling - ONDM*, pages 1–6, 2012.

[37] P.H. Ho, J. Yapolcai, and T. Cinkler. Shared segment protection in mesh communication networks with bandwidth guaranteed tunnels. *IEEE/ACM Transactions on Networking*, 2004.

[38] H.A. Hoang and B. Jaumard. A new flow formulation for FIPP p-cycle protection subject to multiple link failures. In *IEEE International Workshop on Reliable Networks Design and Modeling - RNDM*, pages 1–7, 2011.

[39] C.C. Huang, M.Z. Li, and A. Srinivasan. A scalable path protection mechanism for guaranteed network reliability under multiple failures. *IEEE Transactions on Reliability*, 56:254–267, June 2007.

[40] B. Jaumard and H. Li. A survey on p-cycle based scheme design and solution methods for WDM mesh networks. *Telecommunication Systems*, 2012. to appear.

[41] B. Jaumard, C. Meyer, and B. Thiongane. *ILP formulations for the RWA problem - symmetric systems*. Handbook of Optimization in Telecommunications, 2006.

[42] B. Jaumard, C. Meyer, and X. Yu. How much wavelength conversion allows a reduction in the blocking rate? *Journal of Optical Networking*, 5(12):881–900, 2006.

[43] B. Jaumard, C. Meyer, and B. Thiongane. Comparison of ilp formulations for the rwa problem. *Optical Switching and Networking*, 4:157–172, 2007.

[44] B. Jaumard, C. Meyer, and B. Thiongane. Comparison of ILP formulations for the RWA problem. *Optical Switching and Networking*, 4(3-4):157–172, November 2007.

[45] B. Jaumard, C. Rocha, D. Baloukov, and W. D. Grover. A column generation approach for design of networks using path-protecting p-cycles. In *Proceedings of IEEE/VDE Workshop on Design of Reliable Communication Networks - DRCN*, pages 1–8, October 2007.

[46] B. Jaumard, C. Meyer, and B. Thiongane. On column generation formulations for the RWA problem. *Discrete Applied Mathematics*, pages 1291–1308, 2009.

[47] B. Jaumard, H.A. Hoang, and D.T. Kien. Robust FIPP p-Cycles against dual link failures. *Telecommunications Systems*, pages 1–12, 2013.

[48] M. Kiaei, C. Assi, and B. Jaumard. A survey on the p-cycle protection method. *Communication Surveys Tutorials*, 11(3):53–70, 2009.

[49] A. Kodian and W.D. Grover. Failure-independent path-protecting p-cycles efficient and simple fully preconnected optical-path protection. *Journal of Lightwave Technology*, 23(10):3241–3259, October 2005.

[50] A. Kodian, W.D. Grover, and J. Doucette. A disjoint route sets approach to design of failure-independent path-protection p-cycle networks. In *Proceedings of IEEE/VDE Workshop on Design of Reliable Communication Networks - DRCN*, October 2005. 8pp.

[51] W. Li, J. Doucette, and M. Zuo. p-cycle network design for specified minimum dual-failure restorability. In *IEEE International Conference on Communications - ICC*, pages 2204–2210, 2007.

[52] C. Liu and L. Ruan. p-Cycle design in survivable WDM networks with shared risk link groups (SRLGs). *Photonic Network Communications*, 11(3):301–311, 2006.

[53] J.P. Madhavarapu, P.K. Gummadi, and C.S.R. Murthy. A segment backup scheme for dependable real time communication in multihop networks. In *15th Workshop on Parallel and Distributed Processing*, pages 678–684, 2000.

[54] M. Minoux. A class of combinatorial problems with polynomially solvable large scale set covering/partitioning relaxations. *RAIRO Operations Research*, 21: 105–136, 1987.

[55] D. S. Mukherjee, C. Assi, and A. Agarwal. An alternative approach for enhanced availability analysis and design methods in p-cycle based networks. *IEEE Journal of Selected Areas in Communications*, 24:23–34, 2006.

[56] M. OMahony, D. Simeonidu, A. Yu, and J. Zhou. The design of the european optical network. *Journal of Lightwave Technology*, 13(5):817–828, 1995.

[57] S. Orlowski and M. Pioro. On the complexity of column generation in survivable network design with path-based survivability mechanisms. *Networks*, 2011. to appear.

[58] S. Orlowski, M. Pioro, A. Tomaszewski, and R. Wessaly. Sndlib 1.0 survivable network design library. In *the 3rd International Network Optimization Conference (INOC 2007)*, Spa, Belgium, 2007.

[59] C. Ou, J. Zhang, H. Zang, L.H. Sahasrabuddhe, and B. Mukherjee. New and improved approaches for shared-path protection in WDM networks. *Journal of Lightwave Technology*, 22:1223–1232, May 2004.

[60] S. Ramamurthy and B. Mukherjee. Survivable wdm mesh networks. part i-protection. *Annual Joint Conference of the IEEE Computer and Communications Societies - INFOCOM*, 2:744–751, 1999.

[61] S. Ramasubramanian and A. Chandak. Dual-link failure resiliency through backup link mutual exclusion. *IEEE/ACM Transactions on Networking*, 16 (1):539–548, 2008.

[62] R. Ramaswami and G. Sasaki. Multiwavelength optical networks with limited wavelength conversion. *IEEE/ACM Transactions on Networking*, 6(6):744–754, 1998.

[63] R. Ramaswami and K.N. Sivarajan. Routing and wavelength assignment in all-optical networks. *IEEE/ACM Transactions on Networking*, 3(5):489–500, 1995.

[64] R. Ramaswami, K.N. Sivarajan, and G.H. Sasaki. *Optical Networks - A Practical Perspective*. Morgan Kaufmann, 3nd edition edition, 2010.

[65] C. Rocha. *Optimization of p-cycle protection schemes in optical networks*. PhD thesis, DIRO, Université de Montréal, 2009.

[66] C. Rocha and B. Jaumard. Revisiting *p*-cycles / FIPP *p*-cycles vs. shared link / path protection. In *International Conference on Computer Communications and Networks - ICCCN*, pages 1–6, 2008.

[67] C. Rocha and B. Jaumard. Efficient computation of FIPP p-cycles. *to appear in Telecommunications Systems*, 2012.

[68] E. Ronnberg and T. Larsson. All-integer column generation for set partitioning: Basic principles and extensions. *Journal of Optical Communications and Networking*, pages 529–538, 2014.

[69] G.N. Rouskas. *Wiley Encyclopedia of Telecommunications*. John Wiley and Sons, 2001.

[70] T. Sakano, Z.M. Fadlullah, T. Ngo, H. Nishiyama, M. Nakazawa, F. Adachi, N. Kato, A. Takahara, T. Kumagai, H. Kasahara, and S. Kurihara. Disaster-resilient networking: A new vision based on movable and deployable resource units. *IEEE Network*, page 40–46, 2013.

[71] C.V. Saradhi, E. Salvadori, A. Zanardi, G.M. Galimberti, G. Martinelli, R. Pastorelli, E.S. Vercelli, A. Tanzi, and D. La Fauci. Novel signaling based approach for handling linear and non-linear impairments in transparent optical networks. In *Proceeding of Broadnets*, 2009.

[72] D.A. Schupke. An ILP for optimal p-cycle selection without cycle enumeration. In *Proceedings of the 8th Working Conference on Optical Network Design and Modelling (ONDM)*, Ghent, Belgium, February 2004.

[73] D.A. Schupke, W.D. Grover, and M. Clouqueur. Strategies for enhanced dual failure restorability with static or reconfigurable p-cycle networks. In *IEEE International Conference on Communications - ICC*, volume 3, pages 1628–1633, June 2004.

[74] S. Sebbah and B. Jaumard. Dual failure recovery in WDM networks based on p-cycles. In *International Conference on Optical Networking Design and Modeling - ONDM*, pages 1–9, 2009.

[75] S. Sebbah and B. Jaumard. Dual failure recovery in WDM networks based on p-cycles. In *International Conference on Optical Networking Design and Modeling - ONDM*, Braunschweig, Germany, 2009.

[76] S. Sebbah and B. Jaumard. A Global Approach to Fully Pre-cross Connected Protection Schemes Design using p-structures. In *IEEE RNDM*, St Petersburg, Russia, 2009.

[77] G. Shen and Wayne D. Grover. Sparse placement of electronic switching nodes for low-blocking in translucent optical networks. *Journal of Optical Networking*, page 424–444, 2002.

[78] L. Shen, X. Yang, and B. Ramamurthy. Shared risk link group (srlg)-diverse path provisioning under hybrid service level agreements in wavelength-routed optical mesh networks. *IEEE/ACM Transactions on Networking*, 13:918 – 931, August 2005.

[79] S. Subramaniam, M. Azizoglu, and A.K. Somani. All-optical networks with sparse wavelength conversion. *IEEE/ACM Transactions on Networking*, 4(4): 544–557, 1996.

[80] C.-C. Sue and J.-Y. Du. Capacity-efficient strategy for 100% dual-failure restorability in optical mesh networks utilising reconfigurable p-cycles and a forcer filling concept. *IET Communications*, 3:198 – 208, 2009.

[81] J. Suurballe and R. Tarjan. A quick method for finding shortest pairs of disjoint paths. *Neyworks*, 14:325–336, 1984.

[82] J. Szigeti, R. Romeral, T. Cinkler, and D. Larrabeiti. p-cycle protection in multi-domain optical networks. *Photonic Network Communications*, 17(1): 35–47, 2009.

[83] D. Truong and B. Jaumard. Using topology aggregation for efficient shared segment protection solutions in multi-domain networks. *IEEE Journal of Selected Areas in Communications*, 25(9):96–107, 2007.

[84] D. Truong and B. Thiongane. Dynamic routing for shared path protection in multidomain optical mesh networks. *Journal of Optical Networking*, 5(1): 58–74, 2006.

[85] F. Vanderbeck. Branching in branch-and-price: A generic scheme. *Mathematical Programming*, 130:249–294, 2011.

[86] H. Wang and H. Mouftah. p-cycles in multi-failure network survivability. In *7th International Conference on Transparent Optical Networks (ICTON)*, pages 381–384, 2005.

[87] X. Xie, W. Sun, W. Hu, , and J. Wang. A shared sub-path protection strategy in multi-domain optical networks. In *Optical Fiber Communication and Optoelectronics Conference*, pages 418–420, Shanghai, China, 2007.

[88] H. Zang, J. P. Jue, and B. Mukherjee. A review of routing and wavelength assignment approaches for wavelength-routed optical WDM networks. *Optical Networks Magazine*, pages 47–60, January 2000.

[89] J. Zyskind and A. Srivastava, editors. *Optically Amplified WDM Networks*. Elsevier, San Diego, USA, 2011.